

Electromagnetic Scattering by a Perfectly Conducting Patch
Array on a Dielectric Slab

Jian-Ming Jin and John L. Volakis

Radiation Laboratory
Department of Electrical Engineering
and Computer Science
The University of Michigan
Ann Arbor, MI 48109

March 22, 1989

Prepared for:

General Dynamics – Fort Worth Div.
P.O. Box 748
Ft. Worth, Texas 76101

REPORT SUMMARY

This report describes the theoretical development and numerical implementation of a methodology for the electromagnetic characterization of an infinite and truncated periodic array of perfectly conducting patches on a dielectric slab. More specifically, it contains the following:

- Derivation of the dyadic Green's functions for an infinite dielectric slab
- Development of the equation for computing the currents on an infinite periodic patch array supported by an infinite slab
- Application of a Conjugate Gradient (CG) – FFT method for the solution of the equation
- Exact solution of the reflection by and transmission through an infinite periodic patch array on a dielectric slab
- Approximate solution of the scattering by a truncated patch array on an infinite dielectric slab
- Approximate solution of the scattering by a truncated patch array on a finite slab.

Of particular interest is the application of the CG-FFT method and the approximate solution for the truncated array scattering. Unlike traditional matrix inversion techniques, the CG-FFT solution method allows a substantial computer

storage economy and is thus suitable for practical size geometries. The approximate solution for the truncated array scattering is compared with available exact data and is found to be reasonably accurate.

Table of Contents

1. INTRODUCTION	1
2. DYADIC GREEN'S FUNCTIONS	4
Geometry	4
Maxwell's Equations in Spatial Form	6
Maxwell's Equations in Spectral Form	7
Solutions in Spectral Form	7
Dyadic Green's Functions	9
3. FORMULATION FOR PATCH CURRENTS	12
Geometry of an Infinite Array	12
Floquet's Theorem	15
Scattered Field	16
Equation for Patch Currents	17
4. NUMERICAL IMPLEMENTATION	19
Discretization of Geometry	19
Discretization of Currents	19
Application of Galerkin's Technique	22
CG-FFT Technique	24
5. REFLECTION, TRANSMISSION AND DIFFRACTION OF A PERIODIC ARRAY	26
Reflection and Transmission Coefficients	26
Bragg Diffractions	27
Numerical Results	28

6. SCATTERING BY A TRUNCATED ARRAY	37
Bidirectionally Truncated Array	37
Unidirectionally Truncated Array	42
Numerical Results	43
7. TRUNCATION EFFECT OF DIELECTRIC SLAB	51
Physical Optics Approximation	51
Numerical Results	56
8. CONCLUSION	61
9. REFERENCES	63
10. APPENDIX	65

Index to Figures

2.1	Geometry of a dielectric slab.	5
3.1	Geometry of a periodic patch array on a dielectric slab. (a) Top view. (b) Side view.	13
4.1	Discretization of a square, circular, and triangular patch.	20
5.1	Three types of cell geometries. (a) A square patch cell. (b) A circular patch cell. (c) A cross-shaped patch cell.	29
5.2	(a) Reflection and (b) transmission coefficients vs frequency for an array of square patches with various dielectric slab thicknesses.	30
5.3	(a) Reflection and (b) transmission coefficients vs frequency for an array of square patches for three incident angles for TM incidence.	32
5.4	(a) Reflection and (b) transmission coefficients vs frequency for an array of square patches for three incident angles for TE incidence.	33
5.5	(a) Reflection and (b) transmission coefficients vs angle of incidence for an array of circular patches.	34
5.6	(a) Reflected, (b) transmitted and (c) dissipated power vs frequency for an array of cross-shaped patches with various lossy dielectric slabs.	35-36
6.1	Far field patterns in the $\phi = 180^\circ$ half-plane for a unidirectionally truncated array having nine patches in the x direction.	44-45
6.2	Bistatic radar cross section for a unidirectionally truncated array having seven patches in the x direction.	46
6.3	Bistatic radar cross section patterns for a 9×9 cross-shaped patch array at $f = 5$ GHz.	48

6.4	Bistatic radar cross section patterns for a 9×9 cross-shaped patch array at $f = 9$ GHz.	49
6.5	Bistatic radar cross section patterns for a 9×9 cross-shaped patch array at $f = 20$ GHz.	50
7.1	Bistatic radar cross section patterns for a $26 \text{ cm} \times 26 \text{ cm}$ dielectric slab at 9 GHz.	57
7.2	Bistatic radar cross section patterns for a $26 \text{ cm} \times 26 \text{ cm}$ dielectric slab at 20 GHz.	58
7.3	Bistatic radar cross section patterns for a 9×9 cross-shaped patch array on a $26 \text{ cm} \times 26 \text{ cm}$ dielectric slab at 9 GHz.	59
7.4	Bistatic radar cross section patterns for a 9×9 cross-shaped patch array on a $26 \text{ cm} \times 26 \text{ cm}$ dielectric slab at 20 GHz.	60

Chapter 1

Introduction

The subject of electromagnetic characterization of periodic structures has been of continuing interest over the recent years. The problem that has received most attention is that of free-standing arrays. In typical applications, however, dielectric slabs are used to support patch arrays and modify their characteristic spectral response [1]-[3]. One approach for the treatment of such arrays is to first pursue individual studies of the free-standing array and dielectric slab in isolation. The composite structure can then be analyzed by cascading the generalized scattering matrix parameters found for each problem [4], [5]. Alternatively, one can treat the composite structure directly by including the effect of the dielectric slab through the use of the dyadic Green's function associated with the slab and this approach is adopted in this study.

The formulation for scattering by periodic structures usually invokes Floquet's theorem leading to an equation for the patch currents upon enforcement of the required boundary condition on the array elements. Among various numerical methods for solving the resulting system of equations, the method of moments has

been widely used [1]-[3], [6], [7]. The major drawback of this method, however, is a need to explicitly generate and store a square impedance matrix whose size could exceed the memory capacity of modern computing facilities. On the other hand, an iterative approach such as the conjugate gradient method when combined with the fast Fourier transform [8] avoids the explicit generation of the square matrix, allowing the study of practical size geometries.

In the first part of this report, after a derivation of the pertinent dyadic Green's functions (Chapter 2), an equation is formulated for the patch currents on an infinite periodic array of perfectly conducting patches residing on a dielectric slab (Chapter 3). The Galerkin's procedure is then employed using subdomain roof-top basis functions to develop a system of equations for the patch currents. The system is subsequently solved via the conjugate gradient method in conjunction with the fast Fourier transform technique (Chapter 4). A computation of the radiation by the patch currents provides a solution for the reflection and transmission of the infinite periodic array and this is discussed in Chapter 5.

In practice, an array is always of finite extent and the second part of the report deals with the characterization of the truncated array. An exact analysis of the finite array, however, is time consuming, costly and sometimes impractical to achieve for engineering design purposes. As a result, the scattering by the truncated array is considered here approximately (Chapter 6). In particular, the infinite array currents are integrated over the extent of the truncated array to evaluate the scattering pattern. The accuracy of this approximation is examined

and discussed in relation to some available exact data.

In actual applications, both the patch array and the supporting dielectric slab are of finite extent. A method to characterize the scattering by the truncated array on a finite slab is developed in Chapter 7. In particular, a physical optics approximation is employed to compute the field diffracted by the slab edge which is then added to that contributed by the truncated patch array.

Chapter 2

Dyadic Green's Functions

This chapter describes the derivation of the Green's functions associated with a dielectric slab. Though there are such Green's functions available in the literature, they are usually presented in an incomplete form and often contain typographical errors. It is, therefore, instructive to derive them here since their use is crucial in our study.

2.1 Geometry

The geometry we consider here is illustrated in Figure 2.1 where a unit infinitesimal electric current source oriented in the \hat{x} direction is located on the upper surface of a dielectric slab. The coordinate system is chosen so that the x - y plane is coincident with the lower surface of the slab. The slab is assumed to have a thickness d , a permittivity $\epsilon_r \epsilon_0$, and a permeability of the free-space. The current source is then located at (x', y', d) . In the following, we begin with Maxwell's equations to find the resulting E_x , E_y , and E_z fields.

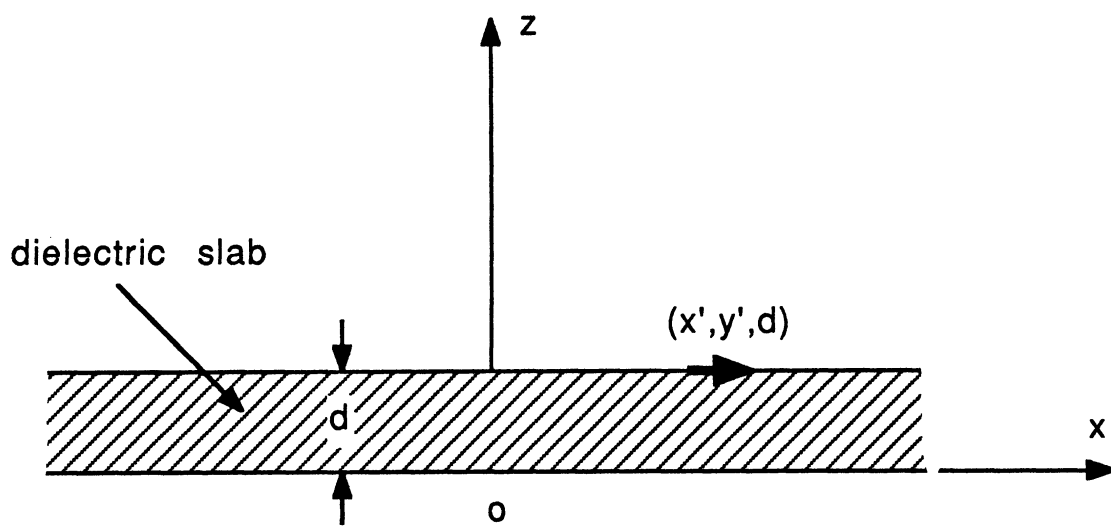


Figure 2.1: Geometry of a dielectric slab.

2.2 Maxwell's Equations in Spatial Form

The source-free Maxwell's equations are

$$\nabla \times \bar{E} = -j\omega\mu_0\bar{H} \quad (2.1)$$

$$\nabla \times \bar{H} = j\omega\epsilon_i\epsilon_0\bar{E} \quad (2.2)$$

where an $e^{j\omega t}$ time convention is employed and ω is the angular frequency. In the above, $\epsilon_i = \epsilon_1 = \epsilon_r$ inside the dielectric slab and $\epsilon_i = \epsilon_2 = 1$ in air. Equations (2.1) and (2.2) can be easily transformed to the two vector wave equations

$$\nabla \times \nabla \times \bar{E} - k_0^2\epsilon_i\bar{E} = 0 \quad (2.3)$$

$$\nabla \times \nabla \times \bar{H} - k_0^2\epsilon_i\bar{H} = 0 \quad (2.4)$$

and since $\nabla \cdot (\epsilon_i\bar{E}) = 0$ and $\nabla \cdot \bar{H} = 0$, they can be further reduced into six scalar wave equations. They are

$$\nabla^2 E_z + k_0^2\epsilon_i E_z = 0 \quad (2.5)$$

$$\nabla^2 H_z + k_0^2\epsilon_i H_z = 0 \quad (2.6)$$

for the z components and

$$\left(\epsilon_i k_0^2 + \frac{\partial^2}{\partial z^2} \right) E_x = \frac{\partial^2}{\partial x \partial z} E_z - j\omega\mu_0 \frac{\partial}{\partial y} H_z \quad (2.7)$$

$$\left(\epsilon_i k_0^2 + \frac{\partial^2}{\partial z^2} \right) E_y = \frac{\partial^2}{\partial y \partial z} E_z + j\omega\mu_0 \frac{\partial}{\partial x} H_z \quad (2.8)$$

$$\left(\epsilon_i k_0^2 + \frac{\partial^2}{\partial z^2} \right) H_x = \frac{\partial^2}{\partial x \partial z} H_z + j\omega\epsilon_i\epsilon_0 \frac{\partial}{\partial y} E_z \quad (2.9)$$

$$\left(\epsilon_i k_0^2 + \frac{\partial^2}{\partial z^2} \right) H_y = \frac{\partial^2}{\partial y \partial z} H_z - j\omega\epsilon_i\epsilon_0 \frac{\partial}{\partial x} E_z \quad (2.10)$$

for the other components.

2.3 Maxwell's Equations in Spectral Form

To solve (2.5) and (2.6), we introduce the Fourier transform pair

$$\tilde{F}(k_x, k_y, z) = \int_{-\infty}^{\infty} \int_{-\infty}^{\infty} F(x, y, z) e^{-jk_x x} e^{-jk_y y} dk_x dk_y \quad (2.11)$$

$$F(x, y, z) = \frac{1}{4\pi^2} \int_{-\infty}^{\infty} \int_{-\infty}^{\infty} \tilde{F}(k_x, k_y, z) e^{jk_x x} e^{jk_y y} dx dy \quad (2.12)$$

where F represents any component of electric and magnetic fields. In the transform domain, equations (2.5) and (2.6) can be written as

$$\frac{\partial^2 \tilde{E}_z}{\partial z^2} + k_i^2 \tilde{E}_z = 0 \quad (2.13)$$

$$\frac{\partial^2 \tilde{H}_z}{\partial z^2} + k_i^2 \tilde{H}_z = 0 \quad (2.14)$$

where $k_i^2 = k_1^2 = \epsilon_r k_0^2 - \beta^2$ within the slab, $k_i^2 = k_2^2 = k_0^2 - \beta^2$ in air and $\beta^2 = k_x^2 + k_y^2$.

Similarly (2.7)-(2.10) become

$$\tilde{E}_x = \frac{jk_x}{\beta^2} \frac{\partial}{\partial z} \tilde{E}_z + \frac{\omega \mu_0 k_y}{\beta^2} \tilde{H}_z \quad (2.15)$$

$$\tilde{E}_y = \frac{jk_y}{\beta^2} \frac{\partial}{\partial z} \tilde{E}_z - \frac{\omega \mu_0 k_x}{\beta^2} \tilde{H}_z \quad (2.16)$$

$$\tilde{H}_x = \frac{jk_x}{\beta^2} \frac{\partial}{\partial z} \tilde{H}_z - \frac{\omega \epsilon_i \epsilon_0 k_y}{\beta^2} \tilde{E}_z \quad (2.17)$$

$$\tilde{H}_y = \frac{jk_y}{\beta^2} \frac{\partial}{\partial z} \tilde{H}_z + \frac{\omega \epsilon_i \epsilon_0 k_x}{\beta^2} \tilde{E}_z. \quad (2.18)$$

2.4 Solutions in Spectral Form

The solution of (2.13) and (2.14) must satisfy the radiation condition and as a result the spectral field components take the form

$$\tilde{E}_z = A e^{-jk_2 z}, \quad \text{Im} k_2 < 0, \quad \text{for } z > d \quad (2.19)$$

$$\widetilde{H}_z = B e^{-jk_2 z}, \quad \text{Im}k_2 < 0, \quad \text{for } z > d \quad (2.20)$$

$$\widetilde{E}_z = C \cos k_1 z + D \sin k_1 z, \quad \text{for } d > z > 0 \quad (2.21)$$

$$\widetilde{H}_z = E \sin k_1 z + F \cos k_1 z, \quad \text{for } d > z > 0 \quad (2.22)$$

$$\widetilde{E}_z = G e^{jk_2 z}, \quad \text{Im}k_2 < 0, \quad \text{for } z < 0 \quad (2.23)$$

$$\widetilde{H}_z = H e^{jk_2 z}, \quad \text{Im}k_2 < 0, \quad \text{for } z < 0 \quad (2.24)$$

where A, B, C, D, E, F, G and H are the unknown constants to be determined by applying the boundary conditions.

The boundary conditions for this problem are

$$E_x^+ - E_x^- = 0, \quad \text{for } z = 0 \text{ and } z = d \quad (2.25)$$

$$E_y^+ - E_y^- = 0, \quad \text{for } z = 0 \text{ and } z = d \quad (2.26)$$

$$H_x^+ - H_x^- = 0, \quad \text{for } z = 0 \text{ and } z = d \quad (2.27)$$

$$H_y^+ - H_y^- = 0, \quad \text{for } z = 0 \text{ and } \quad (2.28)$$

$$H_y^+ - H_y^- = -\delta(x - x')\delta(y - y'), \quad \text{for } z = d \quad (2.29)$$

where the superscript “+” denotes the associated quantities on the plane $z = 0 + \sigma$ or $z = d + \sigma$ and “-” denotes the corresponding quantities on the plane $z = 0 - \sigma$ or $z = d - \sigma$, in which σ is an infinitesimal number. Upon application of (2.25)-(2.29) we find

$$A = \frac{jk_1 k_x Z_0}{k_0(\epsilon_r k_2 \Gamma_1 - jk_1)} e^{-jk_x x'} e^{-jk_y y'} e^{jk_2 d} \quad (2.30)$$

$$B = \frac{k_y}{jk_1 \Gamma_2 - k_2} e^{-jk_x x'} e^{-jk_y y'} e^{jk_2 d} \quad (2.31)$$

$$C = -\frac{k_2 e^{-jk_2 d}}{jk_1 \sin k_1 d + \epsilon_r k_2 \cos k_1 d} A \quad (2.32)$$

$$D = j \frac{\epsilon_r k_2}{k_1} C \quad (2.33)$$

$$E = \frac{k_2 e^{-jk_2 d}}{k_2 \sin k_1 d - j k_1 \cos k_1 d} B \quad (2.34)$$

$$F = -j \frac{k_1}{k_2} E \quad (2.35)$$

$$G = \epsilon_r C \quad (2.36)$$

$$H = F \quad (2.37)$$

where

$$\Gamma_1 = \frac{\epsilon_r k_2 \sin k_1 d - j k_1 \cos k_1 d}{\epsilon_r k_2 \cos k_1 d + j k_1 \sin k_1 d} \quad (2.38)$$

$$\Gamma_2 = \frac{k_2 \cos k_1 d + j k_1 \sin k_1 d}{k_2 \sin k_1 d - j k_1 \cos k_1 d} \quad (2.39)$$

Substituting now the constants into (2.19)-(2.20), we find, from (2.15)-(2.16), that for $z > d$

$$\tilde{E}_x = \frac{Z_0}{k_0 \beta^2} \left(\frac{j k_1 k_2 k_x^2}{\epsilon_r k_2 \Gamma_1 - j k_1} + \frac{k_0^2 k_y^2}{j k_1 \Gamma_2 - k_2} \right) e^{-jk_x x'} e^{-jk_y y'} e^{-jk_2(z-d)} \quad (2.40)$$

$$\tilde{E}_y = \frac{Z_0}{k_0 \beta^2} \left(\frac{j k_1 k_2 k_x k_y}{\epsilon_r k_2 \Gamma_1 - j k_1} - \frac{k_0^2 k_x k_y}{j k_1 \Gamma_2 - k_2} \right) e^{-jk_x x'} e^{-jk_y y'} e^{-jk_2(z-d)}. \quad (2.41)$$

The fields E_x and E_y for $z > d$ can then be found via inverse Fourier transformation as described in (2.12).

2.5 Dyadic Green's Functions

The component of the total radiated field transverse to z can be written as

$$\bar{E}_T(x, y, z) = \iint \bar{G}(x, y, z|x', y') \cdot \bar{J}_s(x', y') dx' dy' \quad (2.42)$$

where $\bar{\bar{G}} = \hat{x}\hat{x}G_{xx} + \hat{y}\hat{x}G_{yx} + \hat{y}\hat{y}G_{yy} + \hat{x}\hat{y}G_{xy}$ is the pertinent dyadic Green's function and $\bar{J}_s = J_x\hat{x} + J_y\hat{y}$ is a two-dimensional radiating surface current residing on the surface $z = d$. In accordance with the development in the previous section,

$$G_{xx} = \frac{Z_0}{4\pi^2 k_0} \int_{-\infty}^{\infty} \int_{-\infty}^{\infty} \frac{1}{\beta^2} \left(\frac{jk_1 k_2 k_x^2}{\epsilon_r k_2 \Gamma_1 - jk_1} + \frac{k_0^2 k_y^2}{jk_1 \Gamma_2 - k_2} \right) \cdot e^{-jk_2(z-d)} e^{jk_x(x-x')} e^{jk_y(y-y')} dk_x dk_y \quad (2.43)$$

$$G_{yx} = \frac{Z_0}{4\pi^2 k_0} \int_{-\infty}^{\infty} \int_{-\infty}^{\infty} \frac{1}{\beta^2} \left(\frac{jk_1 k_2 k_x k_y}{\epsilon_r k_2 \Gamma_1 - jk_1} - \frac{k_0^2 k_x k_y}{jk_1 \Gamma_2 - k_2} \right) \cdot e^{-jk_2(z-d)} e^{jk_x(x-x')} e^{jk_y(y-y')} dk_x dk_y \quad (2.44)$$

valid for $z > d$. Introducing now the definitions

$$\tilde{G}_{xx} = \frac{Z_0}{k_0 \beta^2} \left(\frac{jk_1 k_2 k_x^2}{\epsilon_r k_2 \Gamma_1 - jk_1} + \frac{k_0^2 k_y^2}{jk_1 \Gamma_2 - k_2} \right) \quad (2.45)$$

$$\tilde{G}_{yx} = \frac{Z_0}{k_0 \beta^2} \left(\frac{jk_1 k_2 k_x k_y}{\epsilon_r k_2 \Gamma_1 - jk_1} - \frac{k_0^2 k_x k_y}{jk_1 \Gamma_2 - k_2} \right) \quad (2.46)$$

we may rewrite (2.43)-(2.44) as

$$G_{xx} = \frac{1}{4\pi^2} \int_{-\infty}^{\infty} \int_{-\infty}^{\infty} \tilde{G}_{xx} e^{-jk_2(z-d)} e^{jk_x(x-x')} e^{jk_y(y-y')} dk_x dk_y \quad (2.47)$$

$$G_{yx} = \frac{1}{4\pi^2} \int_{-\infty}^{\infty} \int_{-\infty}^{\infty} \tilde{G}_{yx} e^{-jk_2(z-d)} e^{jk_x(x-x')} e^{jk_y(y-y')} dk_x dk_y \quad (2.48)$$

where we observe that \tilde{G}_{xx} and \tilde{G}_{yx} are not transforms of G_{xx} and G_{yx} but simply functionals introduced for convenience. The other two components of $\bar{\bar{G}}$, namely G_{yy} and G_{xy} , can be found by a simple interchange in coordinates. They are

$$G_{yy} = \frac{1}{4\pi^2} \int_{-\infty}^{\infty} \int_{-\infty}^{\infty} \tilde{G}_{yy} e^{-jk_2(z-d)} e^{jk_x(x-x')} e^{jk_y(y-y')} dk_x dk_y \quad (2.49)$$

$$G_{xy} = \frac{1}{4\pi^2} \int_{-\infty}^{\infty} \int_{-\infty}^{\infty} \tilde{G}_{xy} e^{-jk_2(z-d)} e^{jk_x(x-x')} e^{jk_y(y-y')} dk_x dk_y \quad (2.50)$$

where

$$\tilde{G}_{yy} = \frac{Z_0}{k_0\beta^2} \left(\frac{jk_1k_2k_y^2}{\epsilon_r k_2 \Gamma_1 - jk_1} + \frac{k_0^2 k_x^2}{jk_1 \Gamma_2 - k_2} \right) \quad (2.51)$$

$$\tilde{G}_{xy} = \tilde{G}_{yx}. \quad (2.52)$$

Equations (2.47)-(2.50) can be written in a compact form as

$$\bar{\bar{G}} = \frac{1}{4\pi^2} \int_{-\infty}^{\infty} \int_{-\infty}^{\infty} \tilde{\tilde{G}}(k_x, k_y) e^{-jk_2(z-d)} e^{jk_x(x-x')} e^{jk_y(y-y')} dk_x dk_y \quad (2.53)$$

in which

$$\tilde{\tilde{G}} = \hat{x}\hat{x}\tilde{G}_{xx} + \hat{y}\hat{x}\tilde{G}_{yx} + \hat{y}\hat{y}\tilde{G}_{yy} + \hat{x}\hat{y}\tilde{G}_{xy}. \quad (2.54)$$

The above is the Green's function valid in the region $z > d$. The Green's function for $z < 0$ can also be derived in similar manner and is given by

$$\bar{\bar{G}} = \frac{1}{4\pi^2} \int_{-\infty}^{\infty} \int_{-\infty}^{\infty} \tilde{\tilde{G}}(k_x, k_y) e^{jk_2z} e^{jk_x(x-x')} e^{jk_y(y-y')} dk_x dk_y \quad (2.55)$$

where

$$\tilde{G}'_{xx} = \frac{Z_0}{k_0\beta^2} \left[\frac{j\epsilon_r k_1 k_2^2 k_x^2}{\gamma_1(\epsilon_r k_2 \Gamma_1 - jk_1)} - \frac{jk_0^2 k_1 k_y^2}{\gamma_2(jk_1 \Gamma_2 - k_2)} \right] \quad (2.56)$$

$$\tilde{G}'_{yx} = \frac{Z_0}{k_0\beta^2} \left[\frac{j\epsilon_r k_1 k_2^2 k_x k_y}{\gamma_1(\epsilon_r k_2 \Gamma_1 - jk_1)} + \frac{jk_0^2 k_1 k_x k_y}{\gamma_2(jk_1 \Gamma_2 - k_2)} \right] \quad (2.57)$$

$$\tilde{G}'_{yy} = \frac{Z_0}{k_0\beta^2} \left[\frac{j\epsilon_r k_1 k_2^2 k_y^2}{\gamma_1(\epsilon_r k_2 \Gamma_1 - jk_1)} - \frac{jk_0^2 k_1 k_x^2}{\gamma_2(jk_1 \Gamma_2 - k_2)} \right] \quad (2.58)$$

$$\tilde{G}'_{xy} = \tilde{G}'_{yx} \quad (2.59)$$

with

$$\gamma_1 = jk_1 \sin k_1 d + \epsilon_r k_2 \cos k_1 d \quad (2.60)$$

$$\gamma_2 = k_2 \sin k_1 d - jk_1 \cos k_1 d. \quad (2.61)$$

Chapter 3

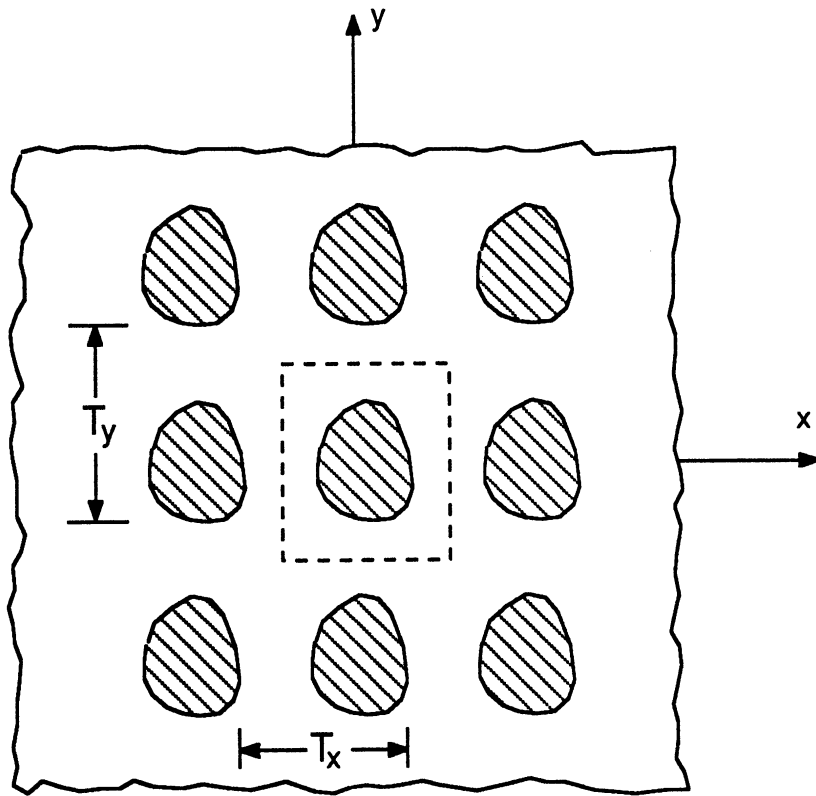
Formulation for Patch Currents

In this chapter, Floquet's theorem is employed in conjunction with the Green's functions derived earlier to develop an equation for the electric currents generated on an infinite periodic patch array due to a plane wave excitation.

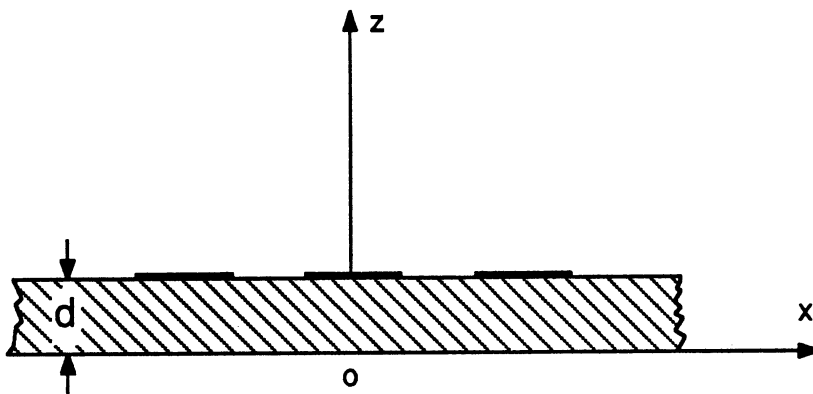
3.1 Geometry of an Infinite Array

The geometry of an infinite periodic patch array is shown in Figure 3.1, where a periodic array of conducting patches with periodicities T_x and T_y in the x and y directions, respectively, is residing on the surface of a dielectric slab. To be consistent with the notation used in the last chapter, the thickness of the slab is assumed to be d and the chosen coordinate system is shown in Figure 3.1.

The excitation field to be considered is a plane wave, but other excitation can be employed if expressed as a superposition of plane waves through the use of the Fourier integral. Further, although the formulation to be presented is in general valid for arbitrary polarizations, particular attention is concentrated in the case of transverse electric (TE) and transverse magnetic (TM) incidences. For the TE



(a)



(b)

Figure 3.1: Geometry of a periodic patch array on a dielectric slab. (a) Top view.
(b) Side view.

case, the incident electric field can be written as

$$\overline{E}^i(\bar{\rho}, z) = (-\hat{x} \sin \phi^i + \hat{y} \cos \phi^i) E_0 e^{j\bar{k}_T^i \cdot \bar{\rho}} e^{jk_0 z \cos \theta^i} \quad (3.1)$$

while for the TM case, it is given by

$$\overline{E}^i(\bar{\rho}, z) = (\hat{x} \cos \theta^i \cos \phi^i + \hat{y} \cos \theta^i \sin \phi^i - \hat{z} \sin \theta^i) E_0 e^{j\bar{k}_T^i \cdot \bar{\rho}} e^{jk_0 z \cos \theta^i} \quad (3.2)$$

where $\bar{\rho} = \hat{x}x + \hat{y}y$ and $\bar{k}_T^i = \hat{x}k_x^i + \hat{y}k_y^i$ in which $k_x^i = k_0 \sin \theta^i \cos \phi^i$ and $k_y^i = k_0 \sin \theta^i \sin \phi^i$.

If the conducting patches are absent, a reflected and transmitted plane wave will result. Since these fields are required later in the formulation, we proceed to derive them for the TE and TM cases.

For the TE case, the reflected field can be expressed as

$$\overline{E}^r(\bar{\rho}, z) = (-\hat{x} \sin \phi^i + \hat{y} \cos \phi^i) E_0 R^{TE} e^{j2k_0 d \cos \theta^i} e^{j\bar{k}_T^i \cdot \bar{\rho}} e^{-jk_0 z \cos \theta^i} \quad (3.3)$$

in which R^{TE} is the corresponding reflection coefficient given by

$$R^{TE} = \frac{\cos \theta^i - j\sqrt{\epsilon_r - \sin^2 \theta^i} C_0}{\cos \theta^i + j\sqrt{\epsilon_r - \sin^2 \theta^i} C_0} \quad (3.4)$$

where

$$C_0 = \frac{j\sqrt{\epsilon_r - \sin^2 \theta^i} \sin(k_0 d \sqrt{\epsilon_r - \sin^2 \theta^i}) + \cos \theta^i \cos(k_0 d \sqrt{\epsilon_r - \sin^2 \theta^i})}{j\sqrt{\epsilon_r - \sin^2 \theta^i} \cos(k_0 d \sqrt{\epsilon_r - \sin^2 \theta^i}) - \cos \theta^i \sin(k_0 d \sqrt{\epsilon_r - \sin^2 \theta^i})}$$

The transmitted field is found as

$$\overline{E}^t(\bar{\rho}, z) = (-\hat{x} \sin \phi^i + \hat{y} \cos \phi^i) E_0 T^{TE} e^{jk_0 d \cos \theta^i} e^{j\bar{k}_T^i \cdot \bar{\rho}} e^{jk_0 z \cos \theta^i} \quad (3.5)$$

in which T^{TE} is the corresponding transmission coefficient given by

$$T^{TE} = \frac{j\sqrt{\epsilon_r - \sin^2 \theta^i}(1 + R^{TE})}{j\sqrt{\epsilon_r - \sin^2 \theta^i} \cos(k_0 d \sqrt{\epsilon_r - \sin^2 \theta^i}) - \cos \theta^i \sin(k_0 d \sqrt{\epsilon_r - \sin^2 \theta^i})}. \quad (3.6)$$

Similarly, for the TM case the reflected field is

$$\begin{aligned} \bar{E}^r(\bar{\rho}, z) = & -(\hat{x} \cos \theta^i \cos \phi^i + \hat{y} \cos \theta^i \sin \phi^i + \hat{z} \sin \theta^i) \\ & \cdot E_0 R^{TM} e^{j2k_0 d \cos \theta^i} e^{j\bar{k}_T^i \cdot \bar{\rho}} e^{-jk_0 z \cos \theta^i} \end{aligned} \quad (3.7)$$

where again R^{TM} is the reflection coefficient given by

$$R^{TM} = \frac{\epsilon_r \cos \theta^i - j\sqrt{\epsilon_r - \sin^2 \theta^i} C_1}{\epsilon_r \cos \theta^i + j\sqrt{\epsilon_r - \sin^2 \theta^i} C_1} \quad (3.8)$$

with

$$C_1 = \frac{j\sqrt{\epsilon_r - \sin^2 \theta^i} \sin(k_0 d \sqrt{\epsilon_r - \sin^2 \theta^i}) + \epsilon_r \cos \theta^i \cos(k_0 d \sqrt{\epsilon_r - \sin^2 \theta^i})}{j\sqrt{\epsilon_r - \sin^2 \theta^i} \cos(k_0 d \sqrt{\epsilon_r - \sin^2 \theta^i}) - \epsilon_r \cos \theta^i \sin(k_0 d \sqrt{\epsilon_r - \sin^2 \theta^i})}.$$

The transmitted field is found as

$$\begin{aligned} \bar{E}^t(\bar{\rho}, z) = & (\hat{x} \cos \theta^i \cos \phi^i + \hat{y} \cos \theta^i \sin \phi^i - \hat{z} \sin \theta^i) \\ & \cdot E_0 T^{TM} e^{jk_0 d \cos \theta^i} e^{j\bar{k}_T^i \cdot \bar{\rho}} e^{jk_0 z \cos \theta^i} \end{aligned} \quad (3.9)$$

in which T^{TM} is the corresponding transmission coefficient given by

$$T^{TM} = \frac{j\sqrt{\epsilon_r - \sin^2 \theta^i}(1 + R^{TM})}{j\sqrt{\epsilon_r - \sin^2 \theta^i} \cos(k_0 d \sqrt{\epsilon_r - \sin^2 \theta^i}) - \epsilon_r \cos \theta^i \sin(k_0 d \sqrt{\epsilon_r - \sin^2 \theta^i})} \quad (3.10)$$

3.2 Floquet's Theorem

In accordance with Floquet's theorem, the electric current supported by the array residing on the plane $z = d$ may be deduced by that on a single patch.

Namely, the array current distribution can be written as

$$\bar{J}_s(x, y) = \bar{j}(x, y)e^{j(k'_x x + k'_y y)} \quad (3.11)$$

where $\bar{j}(x, y)$ is a two-dimensional periodic function. It can, therefore, be expanded in a Fourier series

$$\bar{j}(x, y) = \sum_{p=-\infty}^{\infty} \sum_{q=-\infty}^{\infty} \hat{j}_{pq} \psi_{pq}(x, y) \quad (3.12)$$

where

$$\hat{j}_{pq} = \frac{1}{T_x T_y} \int \int_{S_p} \bar{j}(x', y') \psi_{pq}^*(x', y') dx' dy' \quad (3.13)$$

$$\psi_{pq}(x, y) = e^{j(k_{xp}x + k_{yq}y)} \quad (3.14)$$

in which S_p denotes the area of a single patch, $k_{xp} = 2\pi p/T_x$, $k_{yq} = 2\pi q/T_y$, and p and q are integers representing the Floquet modes.

3.3 Scattered Field

From Section 2.5, the transverse part of the scattered field for $z > d$ as produced by the current \bar{J}_s , is

$$\bar{E}_T^s(x, y, z) = \int_{-\infty}^{\infty} \int_{-\infty}^{\infty} \bar{G} \cdot \bar{J}_s(x', y') dx' dy' \quad (3.15)$$

and by employing (2.53) in conjunction with (3.11), it becomes

$$\begin{aligned} \bar{E}_T^s(x, y, z) = & \frac{1}{4\pi^2} \int_{-\infty}^{\infty} \int_{-\infty}^{\infty} \left[\int_{-\infty}^{\infty} \int_{-\infty}^{\infty} \bar{G} e^{-jk_2(z-d)} e^{jk_x(x-x')} e^{jk_y(y-y')} dk_x dk_y \right] \\ & \cdot \sum_{p=-\infty}^{\infty} \sum_{q=-\infty}^{\infty} \hat{j}_{pq} e^{j(k'_{xp}x + k'_{yq}y)} dx' dy' \end{aligned} \quad (3.16)$$

where $k'_{xp} = k_{xp} + k_x^i$ and $k'_{yq} = k_{yq} + k_y^i$. Interchanging the order of integration, we now obtain

$$\begin{aligned} \overline{E}_T^s(x, y, z) &= \frac{1}{4\pi^2} \int_{-\infty}^{\infty} \int_{-\infty}^{\infty} \int_{-\infty}^{\infty} \int_{-\infty}^{\infty} \tilde{\tilde{G}} \cdot \sum_{p=-\infty}^{\infty} \sum_{q=-\infty}^{\infty} \hat{j}_{pq} e^{-jk_2(z-d)} \\ &\quad \cdot e^{jk_x x} e^{jk_y y} e^{j(k'_{xp}-k_x)x'} e^{j(k'_{yq}-k_y)y'} dx' dy' dk_x dk_y \end{aligned} \quad (3.17)$$

$$\begin{aligned} &= \int_{-\infty}^{\infty} \int_{-\infty}^{\infty} \tilde{\tilde{G}} \cdot \sum_{p=-\infty}^{\infty} \sum_{q=-\infty}^{\infty} \hat{j}_{pq} e^{-jk_2(z-d)} e^{jk_x x} e^{jk_y y} \\ &\quad \cdot \delta(k'_{xp} - k_x) \delta(k'_{yq} - k_y) dk_x dk_y. \end{aligned} \quad (3.18)$$

Further, by interchanging the orders of summation and integration we obtain

$$\overline{E}_T^s(x, y, z) = \sum_{p=-\infty}^{\infty} \sum_{q=-\infty}^{\infty} \tilde{\tilde{G}}(k'_{xp}, k'_{yq}) \cdot \hat{j}_{pq} e^{j[k'_{xp}x + k'_{yq}y - k'_{2pq}(z-d)]} \quad (3.19)$$

upon evaluation of the integrals, where $\tilde{\tilde{G}}(k'_{xp}, k'_{yq})$ is obtained by replacing k_x and k_y with k'_{xp} and k'_{yq} , respectively, in (2.45)-(2.46) and (2.51)-(2.52).

3.4 Equation for Patch Currents

The equation for the electric currents can be obtained by applying the boundary condition on the patch. This demands a vanishing tangential electric field on the patch, that is

$$\overline{E}_T^i + \overline{E}_T^r + \overline{E}_T^s = 0 \quad \text{on the patch.} \quad (3.20)$$

Upon substitution of (3.19) into (3.20) we then obtain

$$\sum_{p=-\infty}^{\infty} \sum_{q=-\infty}^{\infty} \tilde{\tilde{G}}(k'_{xp}, k'_{yq}) \cdot \hat{j}_{pq} e^{j(k'_{xp}x + k'_{yq}y)} = -\overline{E}_T^i(x, y, d) - \overline{E}_T^r(x, y, d) \quad (3.21)$$

for $0 \leq \theta^i < \pi/2$. In the case when $\pi/2 < \theta^i \leq \pi$, $\overline{E}_T^i + \overline{E}_T^r$ in (3.21) should be replaced by the transverse component of the transmitted field.

We note that an alternative expression for (3.21) is

$$\sum_{p=-\infty}^{\infty} \sum_{q=-\infty}^{\infty} \tilde{\tilde{G}}(k'_{xp}, k'_{yq}) \cdot \hat{j}_{pq} \psi_{pq}(x, y) = \overline{B} \quad (3.22)$$

where \overline{B} is given by

$$\overline{B} = - \left[\overline{E}_T^i(x, y, d) + \overline{E}_T^r(x, y, d) \right] e^{-j(k_x^i x + k_y^i y)} \quad (3.23)$$

and can be shown to be invariant to (x, y) . Specifically, for the TE case

$$\overline{B} = (-\hat{x} \sin \phi^i + \hat{y} \cos \phi^i) E_0 (1 + R^{TE}) e^{jk_0 d \cos \theta^i} \quad (3.24)$$

and for the TM case

$$\overline{B} = (\hat{x} \cos \theta^i \cos \phi^i + \hat{y} \cos \theta^i \sin \phi^i) E_0 (1 - R^{TM}) e^{jk_0 d \cos \theta^i}. \quad (3.25)$$

Solving (3.22), one obtains the current distribution on the patches.

Chapter 4

Numerical Implementation

In this chapter, we describe a numerical procedure for solving (3.22). The procedure employs the Conjugate Gradient-Fast Fourier Transform (CG-FFT) technique which appears to be the natural and best choice for the solution.

4.1 Discretization of Geometry

The first step of the CG-FFT solution is to discretize the geometry. For this, we first divide the region of one period into small rectangular cells of dimension $\Delta x \times \Delta y$. The surface of the patch is then generated based on the premise that any planar area may be approximated by a collection of the rectangular cells. Figure 4.1 shows three examples of such a discretization as applied to square, circular and triangular patches.

4.2 Discretization of Currents

Roof-top functions are used below to expand the patch currents. These allow a better representation of the currents and can provide a faster converging series

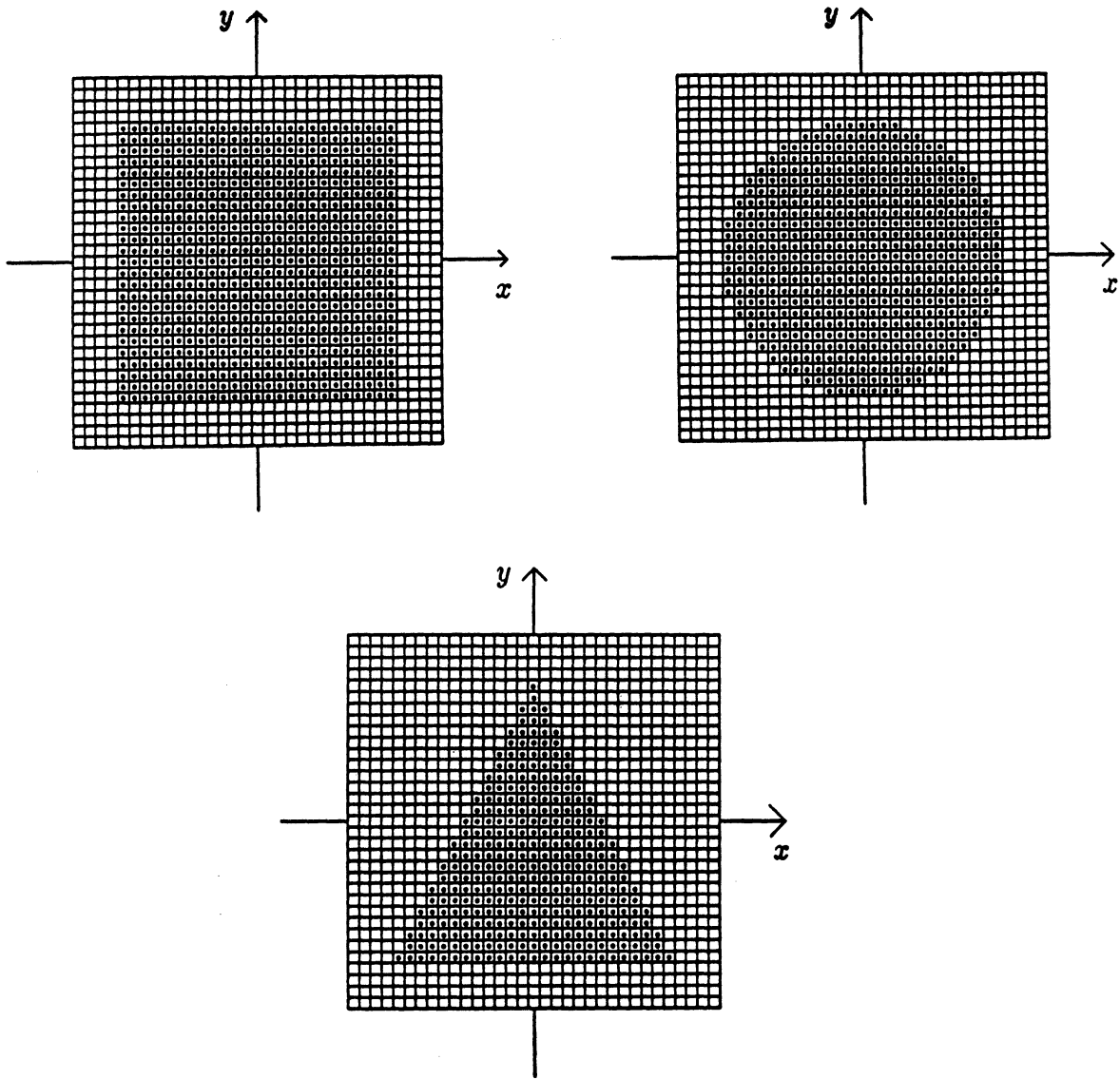


Figure 4.1: Discretization of a square, circular, and triangular patch.

than pulse basis. The current distribution can then be written as

$$j_x(x, y) = \sum_{m=-M/2}^{M/2-1} \sum_{n=-N/2}^{N/2-1} j_{xmn} \Lambda_{m+1/2}(x) \Pi_n(y) \quad (4.1)$$

$$j_y(x, y) = \sum_{m=-M/2}^{M/2-1} \sum_{n=-N/2}^{N/2-1} j_{ymn} \Pi_m(x) \Lambda_{n+1/2}(y) \quad (4.2)$$

where

$$\Lambda_m(x) = \begin{cases} 1 - |x - m\Delta x|/\Delta x, & |x - m\Delta x| < \Delta x \\ 0, & |x - m\Delta x| > \Delta x \end{cases} \quad (4.3)$$

$$\Pi_m(x) = \begin{cases} 1, & |x - m\Delta x| < \Delta x/2 \\ 0, & |x - m\Delta x| > \Delta x/2 \end{cases} \quad (4.4)$$

M and N denote the number of cells along the x and y directions, respectively, and $\bar{j}_{mn} = \hat{x}j_{xmn} + \hat{y}j_{ymn}$ are the unknown constant coefficients of the expansion.

Substituting now (4.1)-(4.2) into (3.13) leads to

$$\begin{aligned} \hat{j}_{xpq} &= \frac{1}{T_x T_y} \sum_{m=-M/2}^{M/2-1} \sum_{n=-N/2}^{N/2-1} j_{xmn} \\ &\quad \cdot \int \Lambda_{m+1/2}(x) e^{-jk_x p x} dx \int \Pi_n(y) e^{-jk_y q y} dy \end{aligned} \quad (4.5)$$

$$\begin{aligned} &= \frac{1}{MN} \text{sinc}^2\left(\frac{p\pi}{M}\right) \text{sinc}\left(\frac{q\pi}{N}\right) e^{-jp\pi/M} \\ &\quad \cdot \sum_{m=-M/2}^{M/2-1} \sum_{n=-N/2}^{N/2-1} j_{xmn} e^{-j(2\pi pm/M + 2\pi qn/N)} \end{aligned} \quad (4.6)$$

where we note that $\Delta x/T_x = 1/M$ and $\Delta y/T_y = 1/N$. Similarly,

$$\begin{aligned} \hat{j}_{ypq} &= \frac{1}{MN} \text{sinc}\left(\frac{p\pi}{M}\right) \text{sinc}^2\left(\frac{q\pi}{N}\right) e^{-jq\pi/N} \\ &\quad \cdot \sum_{m=-M/2}^{M/2-1} \sum_{n=-N/2}^{N/2-1} j_{ymn} e^{-j(2\pi pm/M + 2\pi qn/N)}. \end{aligned} \quad (4.7)$$

The left hand side of (3.22) then becomes

$$\begin{aligned}
& \sum_{p=-\infty}^{\infty} \sum_{q=-\infty}^{\infty} \tilde{\tilde{G}}(k'_{xp}, k'_{yq}) \cdot \hat{j}_{pq} \psi_{pq}(x, y) \\
&= \frac{1}{MN} \sum_{p=-\infty}^{\infty} \sum_{q=-\infty}^{\infty} \operatorname{sinc}\left(\frac{p\pi}{M}\right) \operatorname{sinc}\left(\frac{q\pi}{N}\right) \\
&\quad \cdot \left\{ \left[\hat{x} \hat{x} \tilde{G}_{xx}(k'_{xp}, k'_{yq}) + \hat{y} \hat{x} \tilde{G}_{yx}(k'_{xp}, k'_{yq}) \right] \operatorname{sinc}\left(\frac{p\pi}{M}\right) e^{-jp\pi/M} \right. \\
&\quad \left. + \left[\hat{x} \hat{y} \tilde{G}_{xy}(k'_{xp}, k'_{yq}) + \hat{y} \hat{y} \tilde{G}_{yy}(k'_{xp}, k'_{yq}) \right] \operatorname{sinc}\left(\frac{q\pi}{N}\right) e^{-jq\pi/N} \right\} \\
&\quad \cdot \left[\sum_{m=-M/2}^{M/2-1} \sum_{n=-N/2}^{N/2-1} \bar{j}_{mn} e^{-j(2\pi pm/M + 2\pi qn/N)} \right] e^{j(k_{xp}x + k_{yq}y)}. \tag{4.8}
\end{aligned}$$

4.3 Application of Galerkin's Technique

From (3.22) the equations for determining the constants are

$$\begin{aligned}
& \frac{1}{MN} \sum_{p=-\infty}^{\infty} \sum_{q=-\infty}^{\infty} \left[\hat{x} \hat{x} \tilde{G}_{xx}(k'_{xp}, k'_{yq}) \operatorname{sinc}^2\left(\frac{p\pi}{M}\right) \operatorname{sinc}\left(\frac{q\pi}{N}\right) e^{-jp\pi/M} \right. \\
& \left. + \hat{x} \hat{y} \tilde{G}_{xy}(k'_{xp}, k'_{yq}) \operatorname{sinc}\left(\frac{p\pi}{M}\right) \operatorname{sinc}^2\left(\frac{q\pi}{N}\right) e^{-jq\pi/N} \right] \\
& \cdot \left[\sum_{m=-M/2}^{M/2-1} \sum_{n=-N/2}^{N/2-1} \bar{j}_{mn} e^{-j(2\pi pm/M + 2\pi qn/N)} \right] e^{j(k_{xp}x + k_{yq}y)} \\
&= B_x \tag{4.9}
\end{aligned}$$

for x component and

$$\begin{aligned}
& \frac{1}{MN} \sum_{p=-\infty}^{\infty} \sum_{q=-\infty}^{\infty} \left[\hat{y} \hat{x} \tilde{G}_{yx}(k'_{xp}, k'_{yq}) \operatorname{sinc}^2\left(\frac{p\pi}{M}\right) \operatorname{sinc}\left(\frac{q\pi}{N}\right) e^{-jp\pi/M} \right. \\
& \left. + \hat{y} \hat{y} \tilde{G}_{yy}(k'_{xp}, k'_{yq}) \operatorname{sinc}\left(\frac{p\pi}{M}\right) \operatorname{sinc}^2\left(\frac{q\pi}{N}\right) e^{-jq\pi/N} \right] \\
& \cdot \left[\sum_{m=-M/2}^{M/2-1} \sum_{n=-N/2}^{N/2-1} \bar{j}_{mn} e^{-j(2\pi pm/M + 2\pi qn/N)} \right] e^{j(k_{xp}x + k_{yq}y)} \\
&= B_y \tag{4.10}
\end{aligned}$$

for y component. To solve for \bar{j}_{mn} , (4.9)-(4.10) must now be converted to a system of equations by employing Galerkin's technique. Accordingly, the weighting functions are chosen the same as the current density expansion functions. In so doing, we multiply (4.9) by $\Lambda_{s+1/2}(x)\Pi_t(y)$ and (4.10) by $\Pi_s(x)\Lambda_{t+1/2}(y)$ ($s = -M/2, \dots, M/2 - 1$; $t = -N/2, \dots, N/2 - 1$) and by integrating over the patch, we obtain

$$\begin{aligned}
& \frac{1}{MN} \sum_{p=-\infty}^{\infty} \sum_{q=-\infty}^{\infty} \left[\hat{x}\hat{x}\tilde{G}_{xx}(k'_{xp}, k'_{yq}) \text{sinc}^4\left(\frac{p\pi}{M}\right) \text{sinc}^2\left(\frac{q\pi}{N}\right) \right. \\
& \left. + \hat{x}\hat{y}\tilde{G}_{xy}(k'_{xp}, k'_{yq}) \text{sinc}^3\left(\frac{p\pi}{M}\right) \text{sinc}^3\left(\frac{q\pi}{N}\right) e^{j(p\pi/M - q\pi/N)} \right] \\
& \cdot \left[\sum_{m=-M/2}^{M/2-1} \sum_{n=-N/2}^{N/2-1} \bar{j}_{mn} e^{-j(2\pi pm/M + 2\pi qn/N)} \right] e^{j(2\pi ps/M + 2\pi qt/N)} \\
& = B_x
\end{aligned} \tag{4.11}$$

and

$$\begin{aligned}
& \frac{1}{MN} \sum_{p=-\infty}^{\infty} \sum_{q=-\infty}^{\infty} \left[\hat{y}\hat{x}\tilde{G}_{yx}(k'_{xp}, k'_{yq}) \text{sinc}^3\left(\frac{p\pi}{M}\right) \text{sinc}^3\left(\frac{q\pi}{N}\right) \right. \\
& \left. \cdot e^{-j(p\pi/M - q\pi/N)} + \hat{y}\hat{y}\tilde{G}_{yy}(k'_{xp}, k'_{yq}) \text{sinc}^2\left(\frac{p\pi}{M}\right) \text{sinc}^4\left(\frac{q\pi}{N}\right) \right] \\
& \cdot \left[\sum_{m=-M/2}^{M/2-1} \sum_{n=-N/2}^{N/2-1} \bar{j}_{mn} e^{-j(2\pi pm/M + 2\pi qn/N)} \right] e^{j(2\pi ps/M + 2\pi qt/N)} \\
& = B_y.
\end{aligned} \tag{4.12}$$

Equations (4.11) and (4.12) now form a system of equations for the unknown coefficients \bar{j}_{mn} .

4.4 CG-FFT Technique

It can be shown that (4.11)-(4.12) can be written as

$$\frac{1}{MN} \sum_{p'=-M/2}^{M/2-1} \sum_{q'=-N/2}^{N/2-1} \tilde{\tilde{A}}(k'_{xp'}, k'_{yq'}) \cdot \left[\sum_{m=-M/2}^{M/2-1} \sum_{n=-N/2}^{N/2-1} \bar{j}_{mn} e^{-j(2\pi p'm/M + 2\pi q'n/N)} \right] \cdot e^{j(2\pi p's/M + 2\pi q't/N)} = \bar{B} \quad (4.13)$$

where

$$\tilde{A}_{xx}(k'_{xp'}, k'_{yq'}) = \sum_{u=-\infty}^{\infty} \sum_{v=-\infty}^{\infty} \tilde{G}_{xx}(k'_{xp''}, k'_{yq''}) \text{sinc}^4 \left(\frac{p''\pi}{M} \right) \text{sinc}^2 \left(\frac{q''\pi}{N} \right) \quad (4.14)$$

$$\tilde{A}_{xy}(k'_{xp'}, k'_{yq'}) = \sum_{u=-\infty}^{\infty} \sum_{v=-\infty}^{\infty} \tilde{G}_{xy}(k'_{xp''}, k'_{yq''}) \text{sinc}^3 \left(\frac{p''\pi}{M} \right) \text{sinc}^3 \left(\frac{q''\pi}{N} \right) \cdot e^{j(p''\pi/M - q''\pi/N)} \quad (4.15)$$

$$\tilde{A}_{yx}(k'_{xp'}, k'_{yq'}) = \sum_{u=-\infty}^{\infty} \sum_{v=-\infty}^{\infty} \tilde{G}_{yx}(k'_{xp''}, k'_{yq''}) \text{sinc}^3 \left(\frac{p''\pi}{M} \right) \text{sinc}^3 \left(\frac{q''\pi}{N} \right) \cdot e^{-j(p''\pi/M - q''\pi/N)} \quad (4.16)$$

$$\tilde{A}_{yy}(k'_{xp'}, k'_{yq'}) = \sum_{u=-\infty}^{\infty} \sum_{v=-\infty}^{\infty} \tilde{G}_{yy}(k'_{xp''}, k'_{yq''}) \text{sinc}^2 \left(\frac{p''\pi}{M} \right) \text{sinc}^4 \left(\frac{q''\pi}{N} \right) \quad (4.17)$$

with $p'' = p' + uM$, $q'' = q' + vN$. Here, we note that for large (u, v) the terms of the summations in (4.14)-(4.17) are of the order

$$\frac{1}{(uv)^2(u^2 + v^2)^{1/2}} \quad (4.18)$$

resulting in a rapid series convergence.

In accordance with the definition of the discrete Fourier transform and its inverse [9], (4.13) can be symbolically written as

$$\text{FFT}^{-1} \left\{ \tilde{\tilde{A}}(k'_{xp'}, k'_{yq'}) \cdot [\text{FFT} \{ \bar{j}_{mn} \}] \right\} = \bar{B} \quad (4.19)$$

and it is then clear that (4.19) is suited for a conjugate gradient iterative solution eliminating a need for an explicit generation of a square impedance matrix.

The CG-FFT algorithm for solving (4.19) is described as follows:

Initialize the residual and search vectors:

$$\bar{R}_1 = \bar{B} - \text{FFT}^{-1} \left\{ \tilde{\tilde{A}}(k'_{xp'}, k'_{yq'}) \cdot [\text{FFT} \{ \bar{J}_{mn}^{(1)} \}] \right\} \quad (4.20)$$

$$\bar{X}_1 = \text{FFT}^{-1} \left\{ \left[\tilde{\tilde{A}}^*(k'_{xp'}, k'_{yq'}) \right]^T \cdot [\text{FFT} \{ \bar{R}_1 \}] \right\} \quad (4.21)$$

$$\beta_0 = \frac{1}{\langle \bar{X}_1, \bar{X}_1 \rangle} \quad (4.22)$$

$$\bar{P}_1 = \beta_0 \bar{X}_1. \quad (4.23)$$

Iterate for $k = 1, 2, \dots, NM$:

$$\bar{Y}_k = \text{FFT}^{-1} \left\{ \tilde{\tilde{A}}(k'_{xp'}, k'_{yq'}) \cdot [\text{FFT} \{ \bar{P}_k \}] \right\} \quad (4.24)$$

$$\alpha_k = \frac{1}{\langle \bar{Y}_k, \bar{Y}_k \rangle} \quad (4.25)$$

$$\bar{J}_{mn}^{(k+1)} = \bar{J}_{mn}^{(k)} + \alpha_k \bar{P}_k \quad (4.26)$$

$$\bar{R}_{k+1} = \bar{R}_k - \alpha_k \bar{Y}_k \quad (4.27)$$

$$\bar{X}_{k+1} = \text{FFT}^{-1} \left\{ \left[\tilde{\tilde{A}}^*(k'_{xp'}, k'_{yq'}) \right]^T \cdot [\text{FFT} \{ \bar{R}_{k+1} \}] \right\} \quad (4.28)$$

$$\beta_k = \frac{1}{\langle \bar{X}_{k+1}, \bar{X}_{k+1} \rangle} \quad (4.29)$$

$$\bar{P}_{k+1} = \bar{P}_k + \beta_k \bar{X}_{k+1}. \quad (4.30)$$

Terminate at $k = MN$ or when

$$\frac{\|\bar{R}_{k+1}\|_2}{\|\bar{B}\|_2} < \text{tolerance}. \quad (4.31)$$

Note that the quantity $\left[\tilde{\tilde{A}}^*(k'_{xp'}, k'_{yq'}) \right]^T$ is the adjoint expression for $\tilde{\tilde{A}}(k'_{xp'}, k'_{yq'})$.

Chapter 5

Reflection, Transmission and Diffraction of a Periodic Array

The usual parameters characterizing an infinite periodic patch array are the reflection and transmission coefficients. In high frequency applications, high order Bragg diffractions could also be of interest. In this chapter, we describe the procedure for computing these reflected, transmitted and diffracted fields and present some numerical results.

5.1 Reflection and Transmission Coefficients

Once the currents \vec{j}_{mn} are found from a solution of (4.19), the reflection and transmission coefficients can be evaluated in a straightforward manner. To show this, we refer to (3.19) which is repeated below

$$\vec{E}_T^s(x, y, z) = \sum_{p=-\infty}^{\infty} \sum_{q=-\infty}^{\infty} \vec{\tilde{G}}(k'_{xp}, k'_{yq}) \cdot \hat{j}_{pq} e^{j[k'_{xp}x + k'_{yq}y - k'_{zpq}(z-d)]}. \quad (5.1)$$

It is seen that only the Floquet mode corresponding to $(p, q) = (0, 0)$ contributes the scattered field in the direction of reflection. Thus, the transverse component

of this scattered field is

$$\overline{E}_T^s(x, y, z) = \overline{\overline{G}}(k_x^i, k_y^i) \cdot \hat{j}_{00} e^{j[k_x^i x + k_y^i y - k_z^i(z-d)]} \quad (5.2)$$

where

$$\hat{j}_{00} = \frac{1}{MN} \sum_{m,n} \overline{j}_{mn}. \quad (5.3)$$

The same Floquet mode (0, 0) contributes the scattered field in the direction of transmission and this can again be found in a similar way by employing the dyadic Green's function applicable in the region $z \leq 0$. The transverse component of this scattered field is found as

$$\overline{E}_T^s(x, y, z) = \overline{\overline{G}}(k_x^i, k_y^i) \cdot \hat{j}_{00} e^{j(k_x^i x + k_y^i y + k_z^i z)} \quad (5.4)$$

where \hat{j}_{00} is again given by (5.3).

The total reflected and transmitted fields of the array are then obtained by adding the scattered fields to the reflected field, (3.3) or (3.7), and transmitted field, (3.5) or (3.9), associated with the dielectric slab in isolation.

5.2 Bragg Diffractions

Under certain circumstance, it is possible to obtain higher order Bragg diffractions than the zeroth order (reflection and transmission) considered above. Such diffractions occur when

$$k'_{2pq} > 0 \quad \text{or} \quad k'_{xp}{}^2 + k'_{yq}{}^2 < k_0^2 \quad (5.5)$$

which may be satisfied by certain nonzero (p, q) . The direction (θ_{pq}, ϕ_{pq}) of a possible (p, q) diffraction is determined from the relations

$$\sin \theta_{pq} \cos \phi_{pq} = \sin \theta^i \cos \phi^i + \frac{p\lambda}{T_x} \quad (5.6)$$

$$\sin \theta_{pq} \sin \phi_{pq} = \sin \theta^i \sin \phi^i + \frac{q\lambda}{T_y} \quad (5.7)$$

in which λ is the free-space wavelength, and the magnitude of the corresponding diffracted field in the half space $z > d$ can be obtained from its transverse component given by

$$\bar{E}_T(p, q) = \bar{\tilde{G}}(k'_{xp}, k'_{yq}) \cdot \hat{j}_{pq}. \quad (5.8)$$

From (5.6)-(5.7) it is seen that the diffractions appear in pairs and are symmetric with respect to the x - y plane. The diffracted field in the half space $z < 0$ can be found in a similar way.

5.3 Numerical Results

In the following, we present some numerical results for the reflection by and transmission through an infinite periodic array associated with three types of element patch geometries illustrated in Figure 5.1.

Figure 5.2 shows the reflection and transmission coefficients of a square patch array on a dielectric slab having $d = 0, 0.1$ and 0.2 cm for normal incidence. For the free-standing ($d = 0$) case the result agrees with that obtained by Cwik and Mittra [8]. The general effect of the dielectric layer is seen to shift the resonant frequency of the array. Also, note that at frequencies greater than 15 GHz higher order Bragg

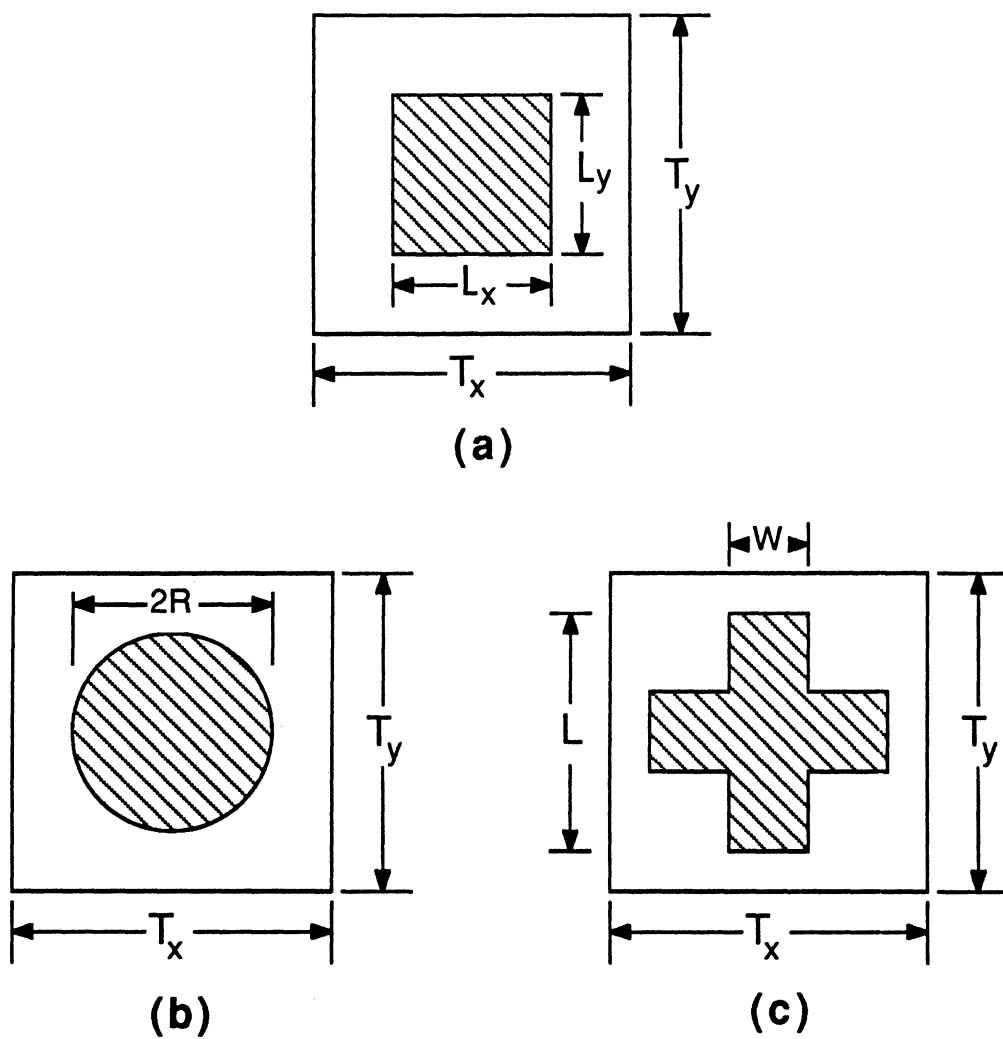
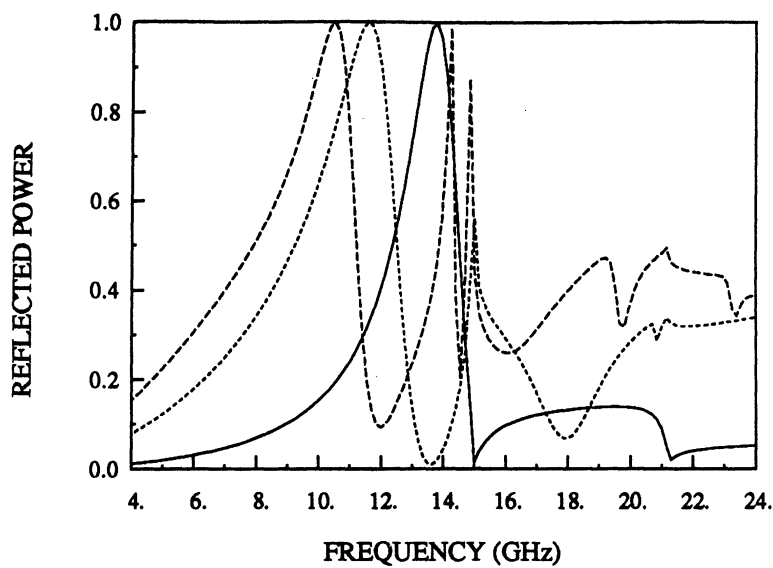
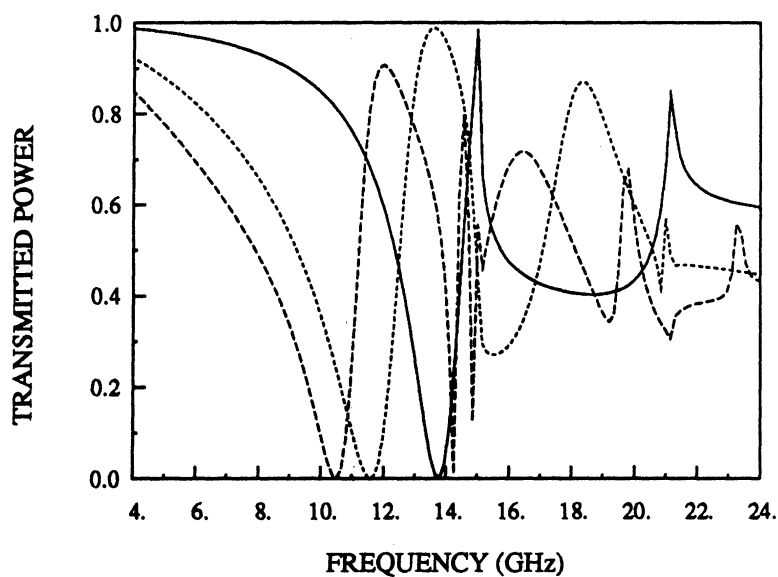


Figure 5.1: Three types of cell geometries. (a) A square patch cell. (b) A circular patch cell. (c) A cross-shaped patch cell.



(a)



(b)

Figure 5.2: (a) Reflection and (b) transmission coefficients vs frequency for an array of square patches with various dielectric slab thicknesses; $T_x = T_y = 2.0$ cm, $L_x = L_y = 1.0$ cm, $\epsilon_r = 3.5$, $\theta^i = 0$, $\phi^i = 0$; (—) $d = 0.0$ cm; (- - -) $d = 0.1$ cm; (- · - ·) $d = 0.2$ cm.

diffractions occur and as a result the reflection and transmission coefficients are no longer complementary.

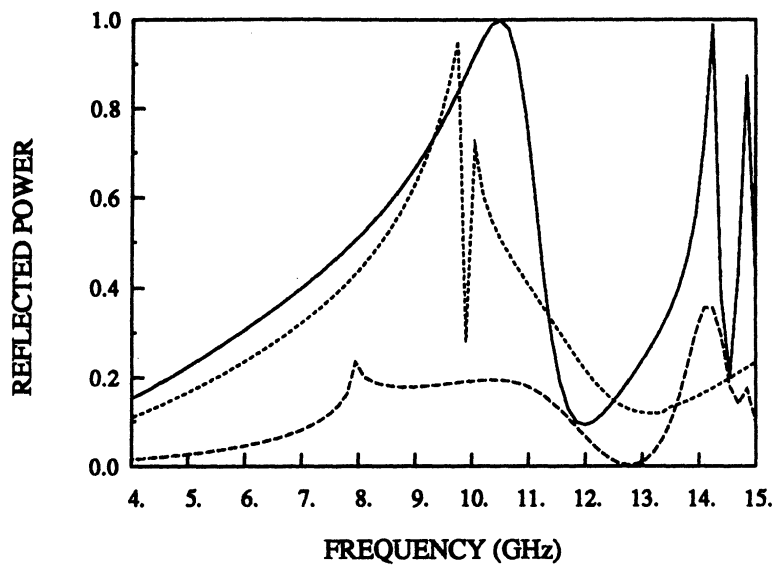
Figures 5.3-5.4 show the reflection and transmission coefficients of the same patch array for three different angles of incidence. As the angle of incidence changes the frequency where the higher order Bragg diffraction occurs also changes.

Figure 5.5 shows the reflection and transmission coefficients of a circular patch array as a function of the angle of incidence. The circular patch is approximately modelled as a collection of square cells. It is seen that higher order Bragg diffractions occur when $\theta^i > 26^\circ$.

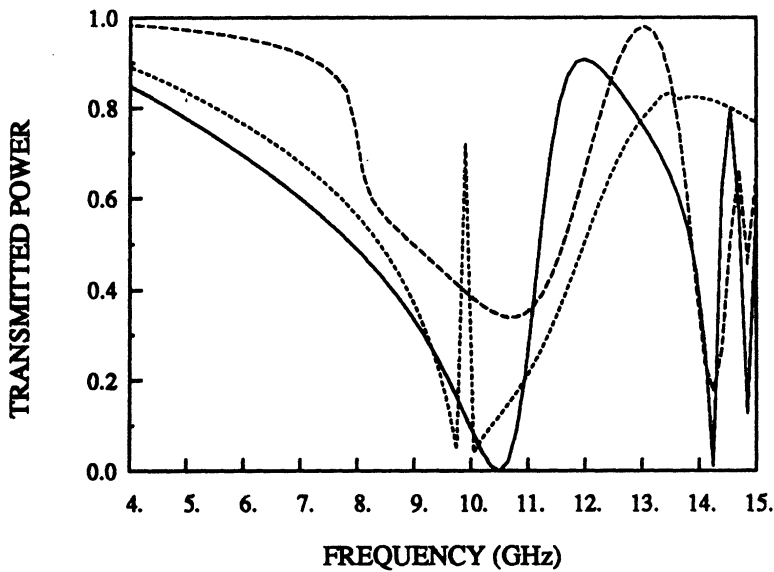
The effect of loss in the dielectric slab is shown in Figure 5.6 where the reflected, transmitted and dissipated power are plotted versus frequency for a cross-shaped patch array. Results are shown for various lossy slabs and the dissipated power is computed in accordance with the relation

$$\begin{aligned} \text{Dissipated Power} = & \text{Incident Power} - \text{Reflected Power} \\ & - \text{Transmitted Power} \end{aligned} \quad (5.9)$$

which is valid up to the frequency where the first order Bragg mode beyond the zeroth order appears.

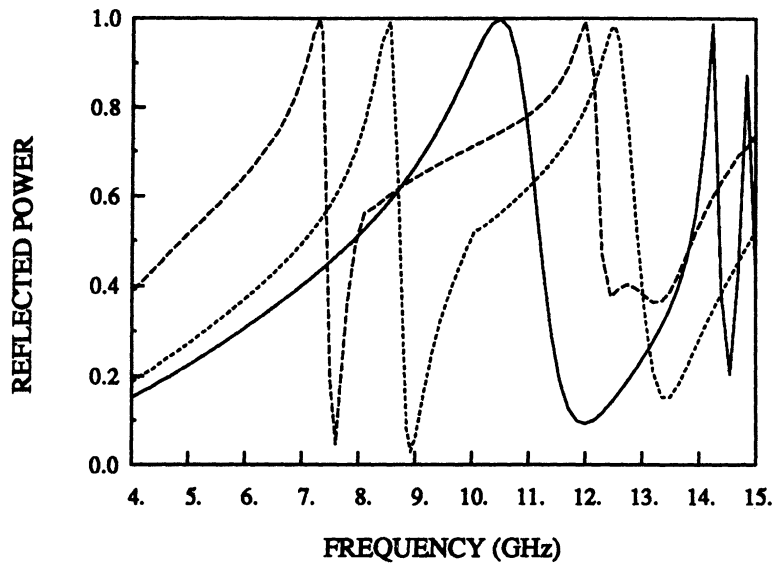


(a)

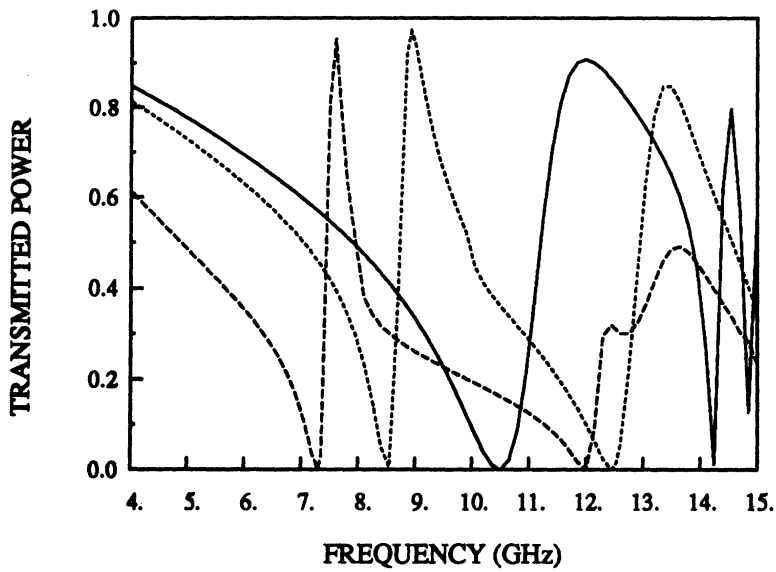


(b)

Figure 5.3: (a) Reflection and (b) transmission coefficients vs frequency for an array of square patches for three incident angles for TM incidence; $T_x = T_y = 2.0$ cm, $L_x = L_y = 1.0$ cm, $\epsilon_r = 3.5$, $d = 0.2$ cm, $\phi^i = 0$; (—) $\theta^i = 0$ degree; (- - -) $\theta^i = 30$ degrees; (- · - ·) $\theta^i = 60$ degrees.32

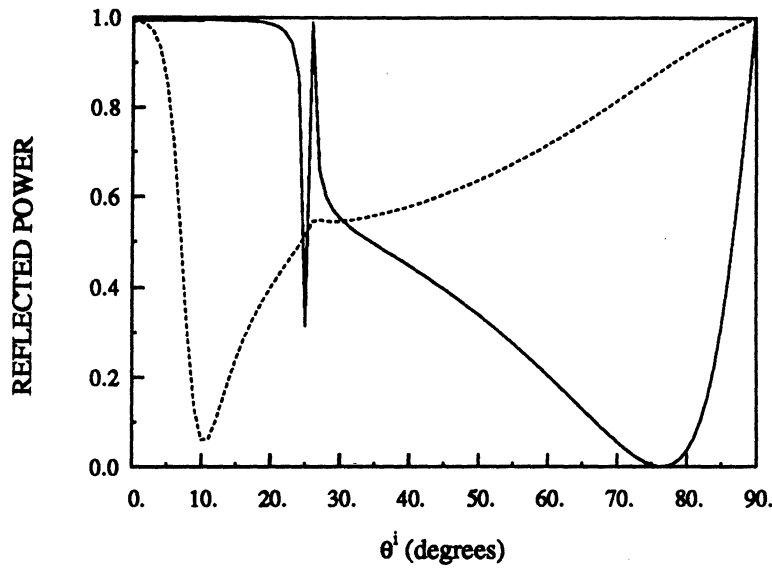


(a)

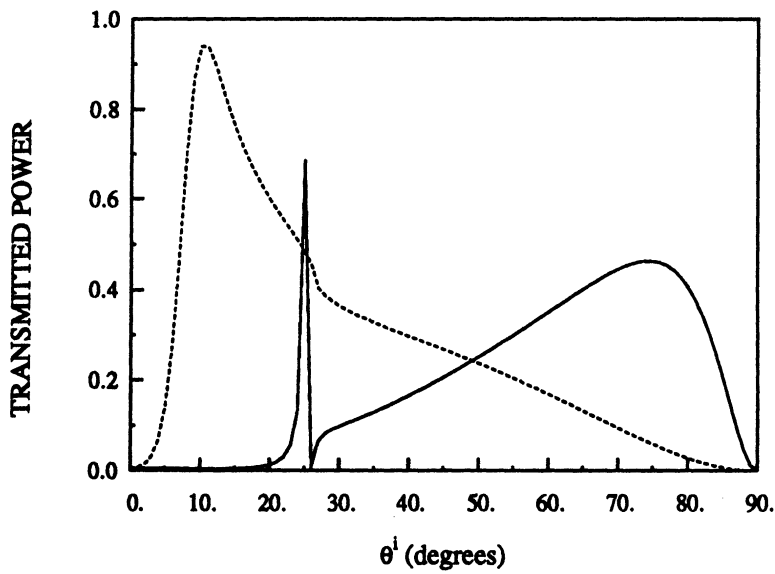


(b)

Figure 5.4: (a) Reflection and (b) transmission coefficients vs frequency for an array of square patches for three incident angles for TE incidence; $T_x = T_y = 2.0$ cm, $L_x = L_y = 1.0$ cm, $\epsilon_r = 3.5$, $d = 0.2$ cm, $\phi^i = 0$; (—) $\theta^i = 0$ degree; (- - -) $\theta^i = 30$ degrees; (- · - ·) $\theta^i = 60$ degrees.33

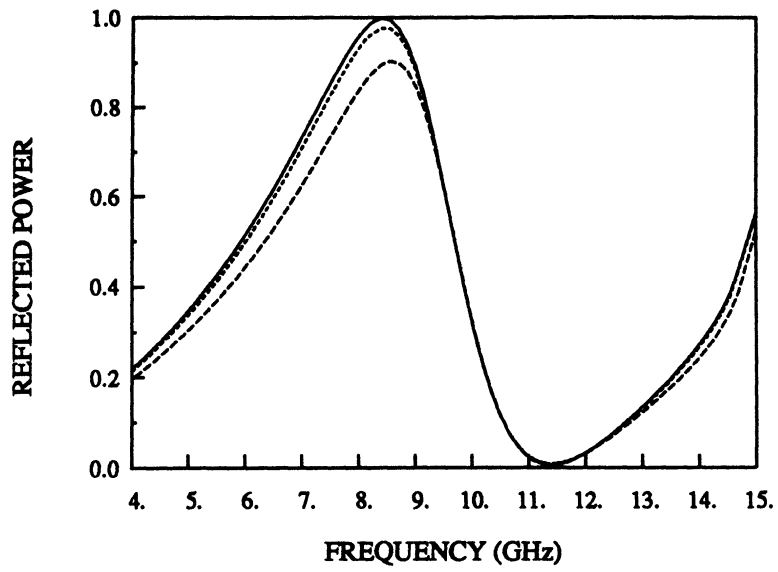


(a)

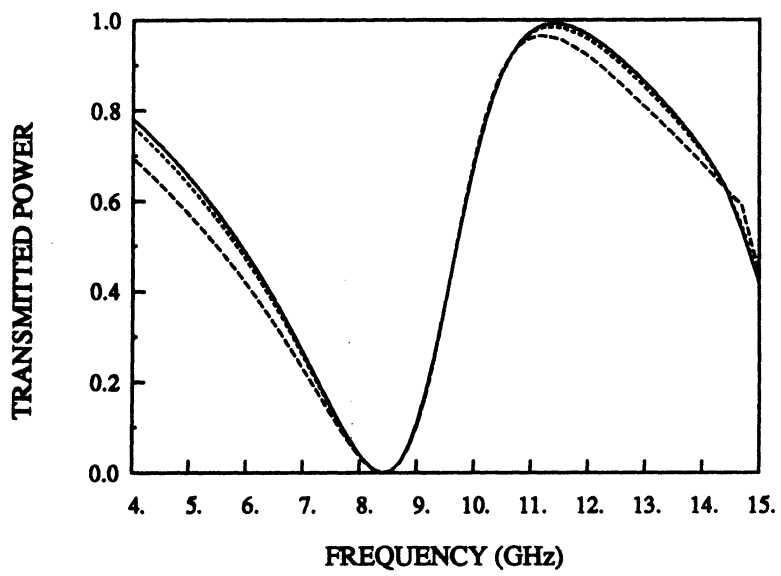


(b)

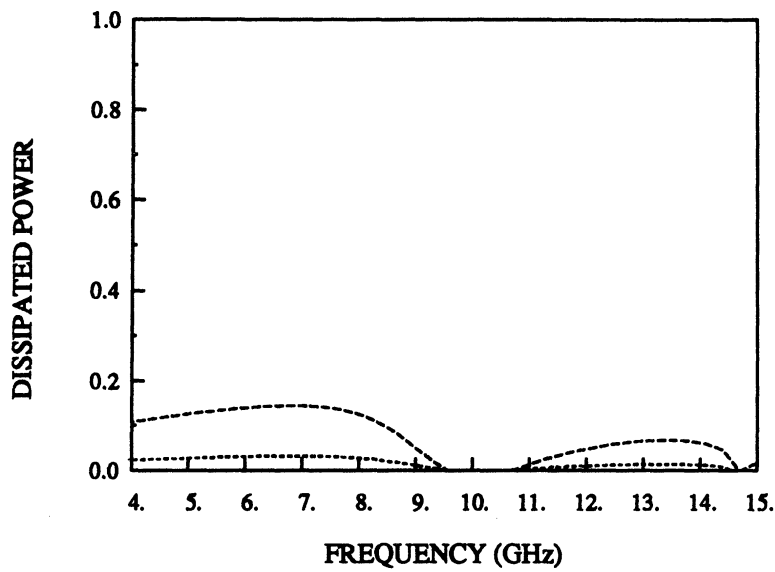
Figure 5.5: (a) Reflection and (b) transmission coefficients vs angle of incidence for an array of circular patches; $T_x = T_y = 2.0$ cm, $R = 0.625$ cm, $\epsilon_r = 3.5$, $d = 0.2$ cm, $\phi^i = 0$, $f = 10.4$ GHz; (—) TM incidence; (- - -) TE incidence.



(a)



(b)



(c)

Figure 5.6: (a) Reflected, (b) transmitted and (c) dissipated power vs frequency for an array of cross-shaped patches with various lossy dielectric slabs; $T_x = T_y = 2.0$ cm, $L = 1.5$ cm, $W = 0.5$ cm, $d = 0.1$ cm, $\theta^i = 0$, $\phi^i = 0$; (—) $\epsilon_r = 4.0$; (- - -) $\epsilon_r = 4.0 - j0.1$; (- · - ·) $\epsilon_r = 4.0 - j0.5$.

Chapter 6

Scattering by a Truncated Array

In practical applications, an infinite periodic patch array is usually truncated but an exact solution in this case is computationally intensive and sometimes impractical because of high memory demand. In this chapter, we, instead, present an approximate solution achieved by integrating the currents \bar{J}_s , obtained in Chapter 4 over the truncated region. Using this procedure, the scattering pattern for the finite array can be written as a product of the element pattern corresponding to a single patch and the pertinent array factor.

6.1 Bidirectionally Truncated Array

To find the far zone radiated field by a single patch, one can proceed by evaluating the Fourier integrals in (2.53) using the stationary-phase formula [10]. Another much easier approach is to employ the reciprocity theorem [11]. Here we discuss both approaches.

Consider the integral

$$I(\Omega) = \int_{-\infty}^{\infty} \int_{-\infty}^{\infty} f(x, y) e^{j\Omega q(x, y)} dx dy, \quad \Omega > 0 \quad (6.1)$$

where $q(x, y)$ is a real function and it has a simple, real stationary point (x_s, y_s) defined by

$$\frac{\partial q}{\partial x} = 0 \text{ and } \frac{\partial q}{\partial y} = 0 \text{ at } (x_s, y_s). \quad (6.2)$$

Provided f is regular near (x_s, y_s) , then an asymptotic approximation of $I(\Omega)$ for large Ω is given by

$$I(\Omega) \approx f(x_s, y_s) e^{j\Omega q(x_s, y_s)} \left(\frac{2\pi}{\Omega} \right) \frac{e^{j(\pi/4)\sigma}}{|\det(\partial^2 q / \partial x_s \partial y_s)|^{1/2}} \quad (6.3)$$

where

$$\sigma = \text{sgn} d_1 + \text{sgn} d_2$$

in which (d_1, d_2) are the eigenvalues of the matrix comprising the elements $\partial^2 q / \partial x_s \partial y_s$.

The above stationary-phase formula can be applied for the evaluation of (2.53)

which can be written as

$$\begin{aligned} \bar{G} &= \frac{1}{4\pi^2} \int_{-\infty}^{\infty} \int_{-\infty}^{\infty} \bar{\bar{G}}(k_x, k_y) e^{j(k_2 d - k_x x' - k_y y')} \\ &\quad \cdot e^{jr(k_x \sin \theta \cos \phi + k_y \sin \theta \sin \phi - k_2 \cos \theta)} dk_x dk_y \end{aligned} \quad (6.4)$$

where (r, θ, ϕ) are the usual spherical coordinates describing the observation point.

Comparing (6.4) to (6.1), the following identifications are possible:

$$f = \frac{1}{4\pi^2} \bar{\bar{G}}(k_x, k_y) e^{j(k_2 d - k_x x' - k_y y')}$$

$$\Omega = r$$

$$q = k_x \sin \theta \cos \phi + k_y \sin \theta \sin \phi - k_2 \cos \theta.$$

The stationary point is found in accordance with (6.2) and is given by

$$k_{xs} = -k_0 \sin \theta \cos \phi, \quad k_{ys} = -k_0 \sin \theta \sin \phi \quad (6.5)$$

and together with

$$|\det(\partial^2 q / \partial k_{xs} \partial k_{ys})|^{1/2} = \frac{1}{k_0 \cos \theta}, \quad \sigma = 2 \quad (6.6)$$

we obtain

$$\bar{G} \approx \frac{jk_0 \cos \theta}{2\pi r} e^{-jk_0 r} \bar{G}(k_{xs}, k_{ys}) e^{jk_0(\cos \theta d + \sin \theta \cos \phi x' + \sin \theta \sin \phi y')} \quad (6.7)$$

for large r . The transverse component of the far field radiated by a single patch with current $\bar{J}_s(x, y)$ is then given by

$$\begin{aligned} \bar{e}_T = & \frac{jk_0 \cos \theta}{2\pi r} e^{-jk_0 r} \bar{G}(k_{xs}, k_{ys}) e^{jk_0 d \cos \theta} \\ & \cdot \int \int_{S_p} \bar{J}_s(x', y') e^{jk_0(\sin \theta \cos \phi x' + \sin \theta \sin \phi y')} dx' dy'. \end{aligned} \quad (6.8)$$

Note that f is not regular at $\theta = \pi/2$ and therefore the above asymptotic expression is not valid there.

We now consider the second approach. In accordance with reciprocity theorem, if \bar{E}_1 is the field due to \bar{J}_1 and \bar{E}_2 is the field due to \bar{J}_2 , then

$$\int \int \int \bar{E}_1 \cdot \bar{J}_2 dV = \int \int \int \bar{E}_2 \cdot \bar{J}_1 dV \quad (6.9)$$

holds. Assume now that a current element Il is situated at point (r, θ, ϕ) and oriented in the $\hat{\theta}$ direction. This current element, if away from the dielectric surface, produces a spherical wave of the form

$$\bar{E}^i = -j \frac{k_0 Z_0 Il}{4\pi r} e^{-jk_0(|\bar{r} - \bar{r}'|)} \hat{\theta} \quad (6.10)$$

where \vec{r}' is a point near the origin. We observe that (6.10) can be approximated as a plane wave with TM polarization and, therefore, the plane wave reflection coefficient (3.8) can be employed to find the reflected field near the origin. The total field at the dielectric surface near the origin is then given by

$$\bar{E} = -j \frac{k_0 Z_0 I l}{4\pi r} e^{-jk_0 r} (1 - R^{TM}) e^{jk_0 (\cos \theta d + \sin \theta \cos \phi x' + \sin \theta \sin \phi y')} \hat{\theta}. \quad (6.11)$$

Let now \bar{e} denote the electric field at (r, θ, ϕ) produced by the patch current \bar{J}_s .

From the reciprocity theorem (6.9), we then have

$$\begin{aligned} \bar{e} \cdot I l \hat{\theta} &= -j \frac{k_0 Z_0 I l}{4\pi r} e^{-jk_0 r} (1 - R^{TM}) e^{jk_0 d \cos \theta} \\ &\quad \cdot \int \int_{S_p} e^{jk_0 (\sin \theta \cos \phi x' + \sin \theta \sin \phi y')} \hat{\theta} \cdot \bar{J}_s(x', y') dx' dy' \end{aligned} \quad (6.12)$$

which yields

$$\begin{aligned} e_\theta &= -j \frac{k_0 Z_0}{4\pi r} e^{-jk_0 r} (1 - R^{TM}) e^{jk_0 d \cos \theta} \\ &\quad \cdot \int \int_{S_p} e^{jk_0 (\sin \theta \cos \phi x' + \sin \theta \sin \phi y')} \hat{\theta} \cdot \bar{J}_s(x', y') dx' dy'. \end{aligned} \quad (6.13)$$

Similarly, by orienting the element current in the $\hat{\phi}$ direction, we find that

$$\begin{aligned} e_\phi &= -j \frac{k_0 Z_0}{4\pi r} e^{-jk_0 r} (1 + R^{TE}) e^{jk_0 d \cos \theta} \\ &\quad \cdot \int \int_{S_p} e^{jk_0 (\sin \theta \cos \phi x' + \sin \theta \sin \phi y')} \hat{\phi} \cdot \bar{J}_s(x', y') dx' dy'. \end{aligned} \quad (6.14)$$

It can be shown that the field given by (6.13)-(6.14) is the same as that in (6.8). They all exhibit a feature of geometrical optics and are, thus, accurate provided the observation point is not near the dielectric surface where the surface wave

contribution may become appreciable. Therefore, in the region $0 \leq \theta < \pi/2$ we have

$$e_\theta = -j \frac{k_0 Z_0}{4\pi} \frac{e^{-jk_0 r}}{r} (1 - R^{TM}) e^{jk_0 d \cos \theta} (\cos \theta \cos \phi I_x + \cos \theta \sin \phi I_y) \quad (6.15)$$

$$e_\phi = -j \frac{k_0 Z_0}{4\pi} \frac{e^{-jk_0 r}}{r} (1 + R^{TE}) e^{jk_0 d \cos \theta} (-\sin \phi I_x + \cos \phi I_y) \quad (6.16)$$

where the components $I_{x,y}$ are integrals given by

$$I_{x,y} = \int \int_{S_p} J_{x,y} e^{jk_0(x \sin \theta \cos \phi + y \sin \theta \sin \phi)} dx dy. \quad (6.17)$$

However, after employing the expansions (4.1)-(4.2) in (3.11), $I_{x,y}$ can be written as summations

$$I_x = \frac{\Delta x \Delta y}{2} \sum_{m,n} (j_{x(m-1)n} + j_{xmn}) \cdot e^{j[(k_0 \sin \theta \cos \phi + k_x^i)x_{mn} + (k_0 \sin \theta \sin \phi + k_y^i)y_{mn}]} \quad (6.18)$$

$$I_y = \frac{\Delta x \Delta y}{2} \sum_{m,n} (j_{ym(n-1)} + j_{ymn}) \cdot e^{j[(k_0 \sin \theta \cos \phi + k_x^i)x_{mn} + (k_0 \sin \theta \sin \phi + k_y^i)y_{mn}]} \quad (6.19)$$

in which (x_{mn}, y_{mn}) denotes the center point of the (mn) th cell.

The above discussion applies to the radiated field in the region $0 \leq \theta < \pi/2$. The radiated field in the region $\pi/2 < \theta \leq \pi$ is obtained in a similar manner. In particular, we find that $e_{\theta,\phi}$ are again given by (6.15)-(6.16) provided $(1 - R^{TM})$ is replaced by T^{TM} given in (3.10) and $(1 + R^{TE})$ by T^{TE} given in (3.6).

The array factor can be easily found in the traditional manner. For an arbitrary array, it is given by

$$AF(\theta, \phi) = \sum_{i=1}^{N_p} e^{j[(k_0 \sin \theta \cos \phi + k_x^i)x_i + (k_0 \sin \theta \sin \phi + k_y^i)y_i]} \quad (6.20)$$

where N_p is the number of patches and (x_i, y_i) is the center point of the i th patch. In particular, for a rectangular array with N_x patches in the x direction and N_y patches in the y direction it is

$$|AF(\theta, \phi)| = \left| \frac{\sin[(N_x T_x/2)(k_0 \sin \theta \cos \phi + k_x^i)]}{\sin[(T_x/2)(k_0 \sin \theta \cos \phi + k_x^i)]} \right| \cdot \left| \frac{\sin[(N_y T_y/2)(k_0 \sin \theta \sin \phi + k_y^i)]}{\sin[(T_y/2)(k_0 \sin \theta \sin \phi + k_y^i)]} \right| \quad (6.21)$$

The scattering pattern of the truncated periodic array is now given by

$$|E_\theta| = |e_\theta| \cdot |AF(\theta, \phi)| \quad (6.22)$$

$$|E_\phi| = |e_\phi| \cdot |AF(\theta, \phi)| \quad (6.23)$$

and the corresponding radar cross section (RCS) can be calculated as

$$\sigma(\theta, \phi) = \lim_{r \rightarrow \infty} 4\pi r^2 \frac{|E_\theta|^2 + |E_\phi|^2}{|E_0|^2}. \quad (6.24)$$

6.2 Unidirectionally Truncated Array

For the special case where the array is truncated only in one direction, say x direction, we can again use the above two approaches to find the element pattern produced by a row of patches along the y axis. The resulting expressions are

$$e_\theta = -Z_0 \sqrt{\frac{jk_0}{8\pi\rho}} e^{-jk_0\rho} (1 - R^{TM}) e^{jk_0 d \cos \theta} \cos \theta I_x / T_y \quad (6.25)$$

$$e_y = -Z_0 \sqrt{\frac{jk_0}{8\pi\rho}} e^{-jk_0\rho} (1 + R^{TE}) e^{jk_0 d \cos \theta} I_y / T_y \quad (6.26)$$

for $0 \leq \theta < \pi/2$ and

$$e_\theta = -Z_0 \sqrt{\frac{jk_0}{8\pi\rho}} e^{-jk_0\rho} T^{TM} e^{jk_0 d \cos \theta} \cos \theta I_x / T_y \quad (6.27)$$

$$e_y = -Z_0 \sqrt{\frac{jk_0}{8\pi\rho}} e^{-jk_0\rho} T^{TE} e^{jk_0d \cos\theta} I_y/T_y \quad (6.28)$$

for $\pi/2 < \theta \leq \pi$, where $\rho = \sqrt{x^2 + z^2}$ and $I_{x,y}$ is as given by (6.18)-(6.19) with $\phi^i, \phi = 0$ or π . The array pattern is then computed by multiplying (6.25)-(6.26) or (6.27)-(6.28) with the array factor

$$|AF(\theta, \phi)| = \left| \frac{\sin[(N_x T_x/2)(k_0 \sin\theta \cos\phi + k_x^i)]}{\sin[(T_x/2)(k_0 \sin\theta \cos\phi + k_x^i)]} \right| \quad (6.29)$$

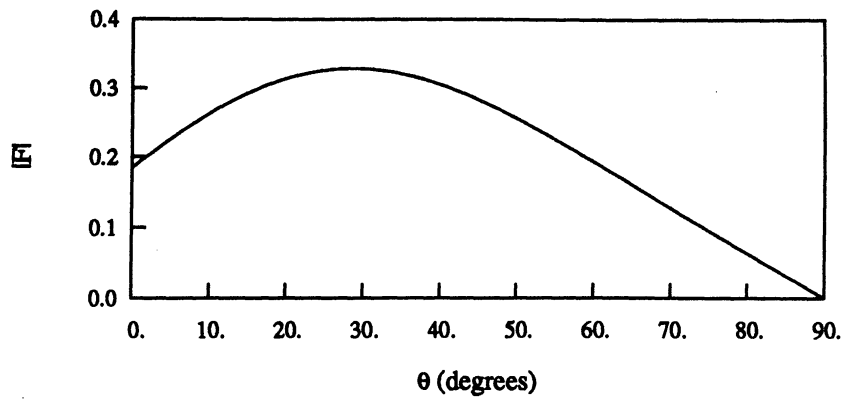
and the RCS is given by (6.24) with $4\pi r^2$ replaced by $2\pi\rho$. That is

$$\sigma(\theta, \phi) = \lim_{\rho \rightarrow \infty} 2\pi\rho \frac{|E_\theta|^2 + |E_y|^2}{|E_0|^2}. \quad (6.30)$$

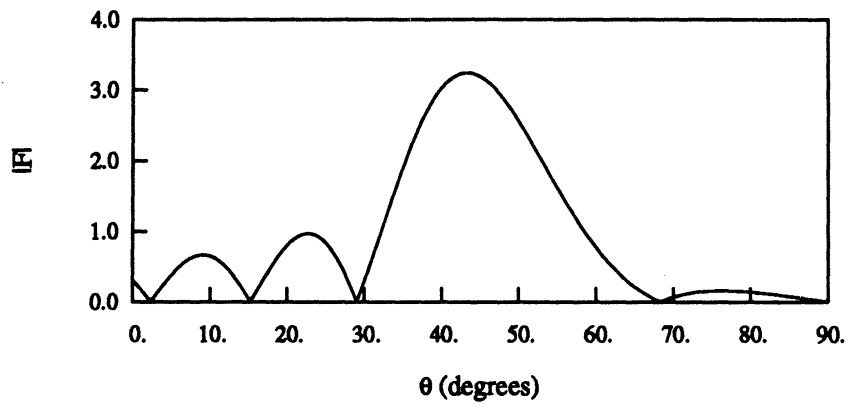
6.3 Numerical Results

Before presenting results relating to the truncated patch array, it is first necessary to examine the accuracy of the approximate solution described above by comparison with the exact solution. While this exact solution is not available for a bidirectionally truncated array, some results do exist for arrays truncated in one direction only [12], [13]. The available data are for free-standing arrays, but this is not as relevant to the comparison.

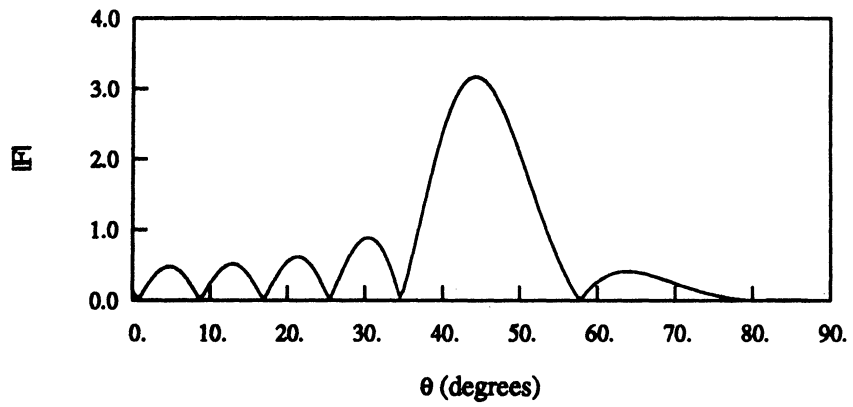
Figure 6.1 shows the approximate scattering pattern corresponding to an array having nine square patches in the x direction and being infinite periodic in the y direction. The incident field is a TM polarized plane wave with $\theta^i = 45^\circ$ and $\phi^i = 0$. Referring to [12], the approximate results in Figure 6.1 are in good agreement with the exact given in Figures 5-9 of [12]. Another comparison is given



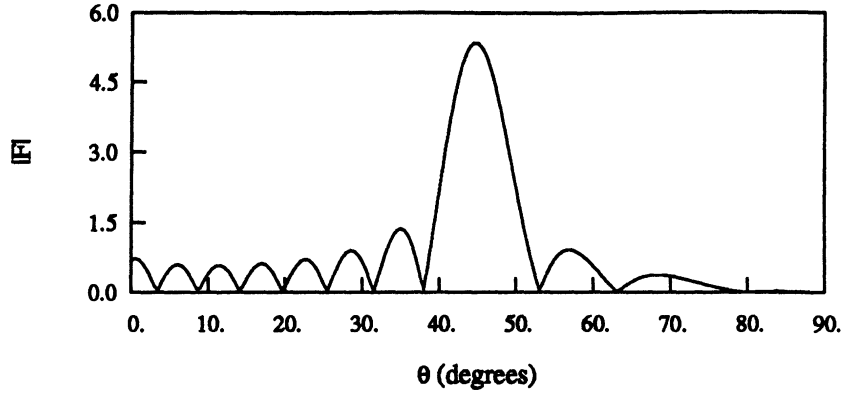
(a)



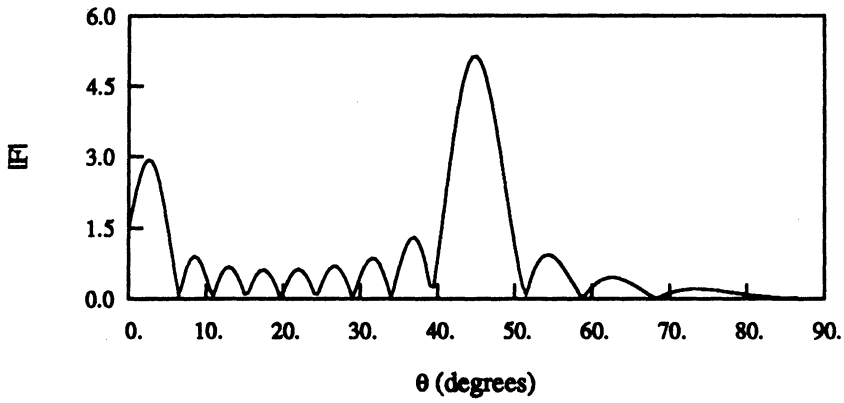
(b)



(c)



(d)



(e)

Figure 6.1: Far field patterns in the $\phi = 180^\circ$ half-plane for a unidirectionally truncated array having nine patches in the x direction; $T_x = T_y = 1.0$ cm, $L_x = L_y = 0.8$ cm, $\theta^i = 45^\circ$, $\phi^i = 0$, TM incidence. (a) $f = 3$ GHz. (b) $f = 15$ GHz. (c) $f = 24$ GHz. (d) $f = 36$ GHz. (e) $f = 45$ GHz.

$$(|F| = |E_\theta| \cdot \sqrt{\rho})$$

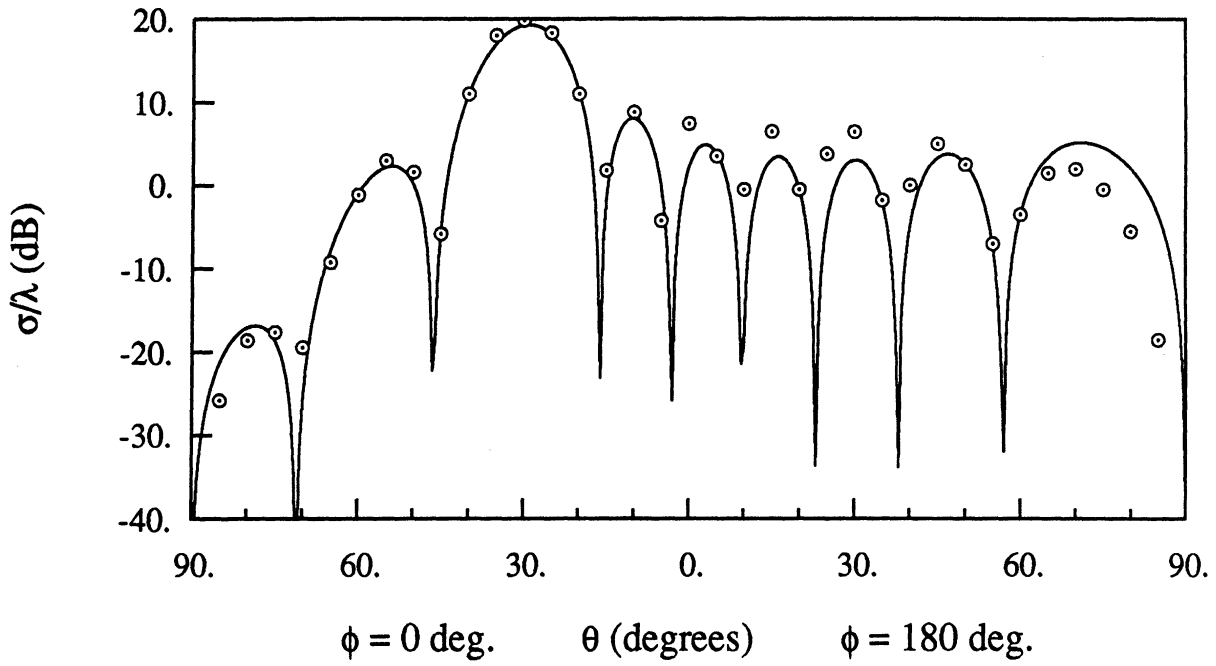
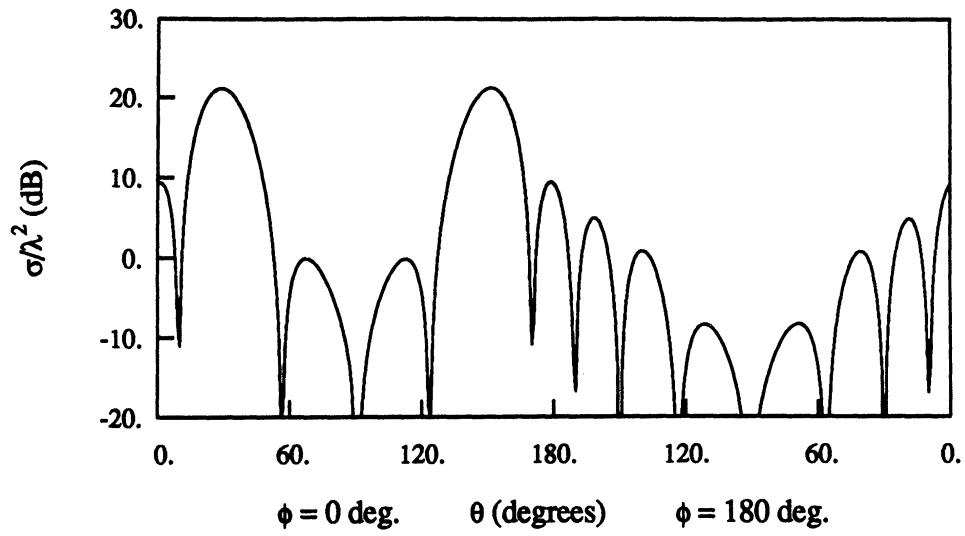


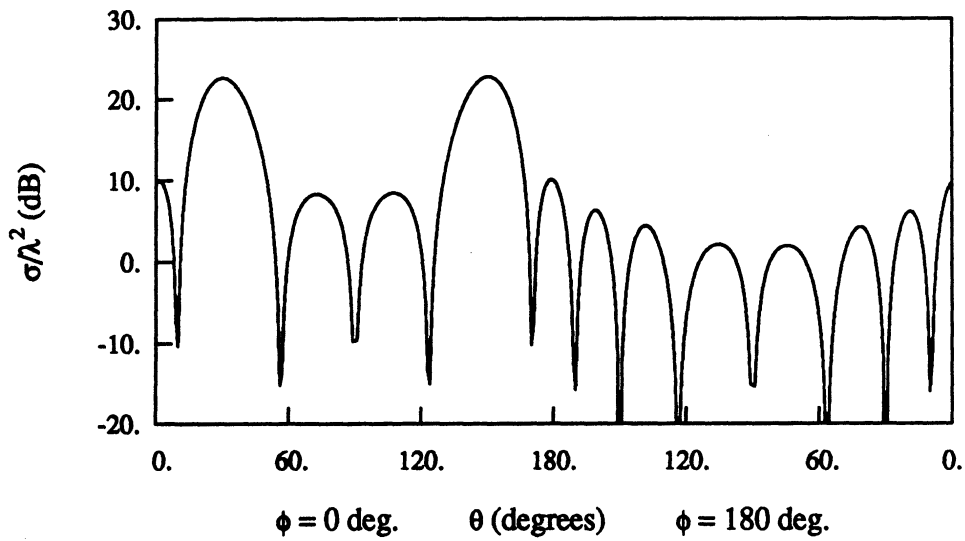
Figure 6.2: Bistatic radar cross section for a unidirectionally truncated array having seven patches in the x direction; $T_x = T_y = 1.78$ cm, $L_x = 1.27$ cm, $L_y = 0.127$ cm, $\theta^i = 30^\circ$, $\phi^i = 180^\circ$, $f = 10.8$ GHz, TM incidence. The circles represent the exact data given in [13].

in Figure 6.2 where the approximate scattering cross section, again for the TM incidence, is plotted and compared with the exact data [13] for an array having seven rectangular patches in the x direction. Note that the approximate solution agrees with the exact to within 1.0 dB in the specular direction and a reasonable agreement is observed overall. Clearly, the data in Figures 6.1 and 6.2 show that for a truncated array the termination effect can be reasonably modelled by the approximate expressions (6.22)-(6.23) provided, of course, the array size is large.

Figures 6.3-6.5 present the bistatic scattering patterns in the x - z plane for a truncated array having nine cross-shaped patches in both x and y directions. The excitation is a plane wave of either TM or TE polarization with $\theta^i = 30^\circ$ and $\phi^i = 180^\circ$. The results are shown for three different frequencies $f = 5, 9$ and 20 GHz. In view of the remarks in the previous paragraph, these are expected to be of reasonable accuracy although no comparative check has been made against the exact solutions.

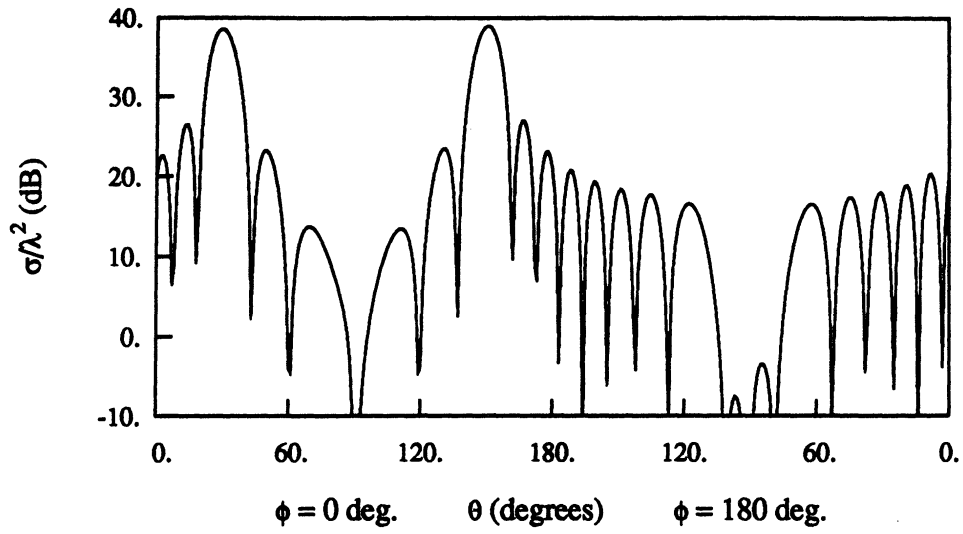


(a)

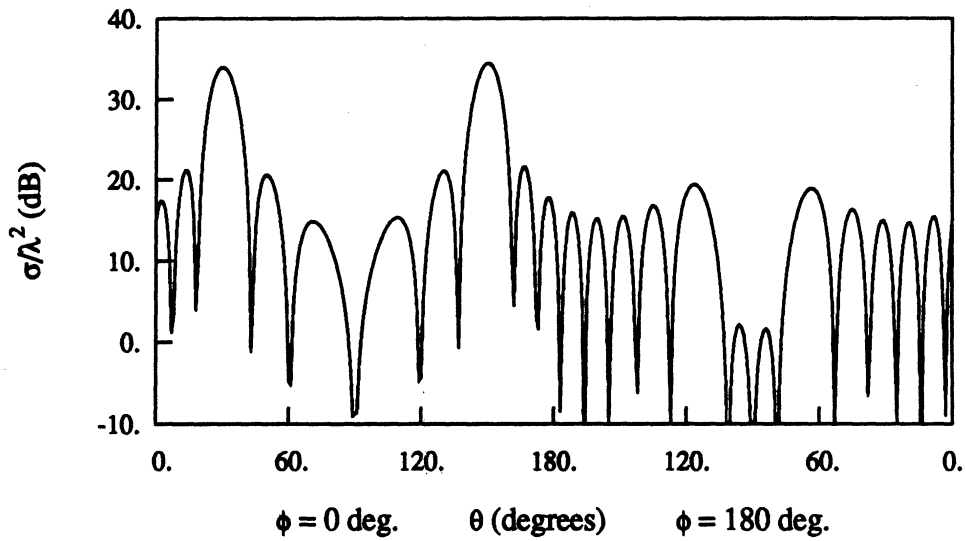


(b)

Figure 6.3: Bistatic radar cross section patterns for a 9×9 cross-shaped patch array at $f = 5$ GHz; $T_x = T_y = 2.0$ cm, $L = 1.5$ cm, $W = 0.5$ cm, $\epsilon_r = 4.0$, $d = 0.1$ cm, $\theta^i = 30^\circ$, $\phi^i = 180^\circ$. (a) TM incidence; (b) TE incidence.

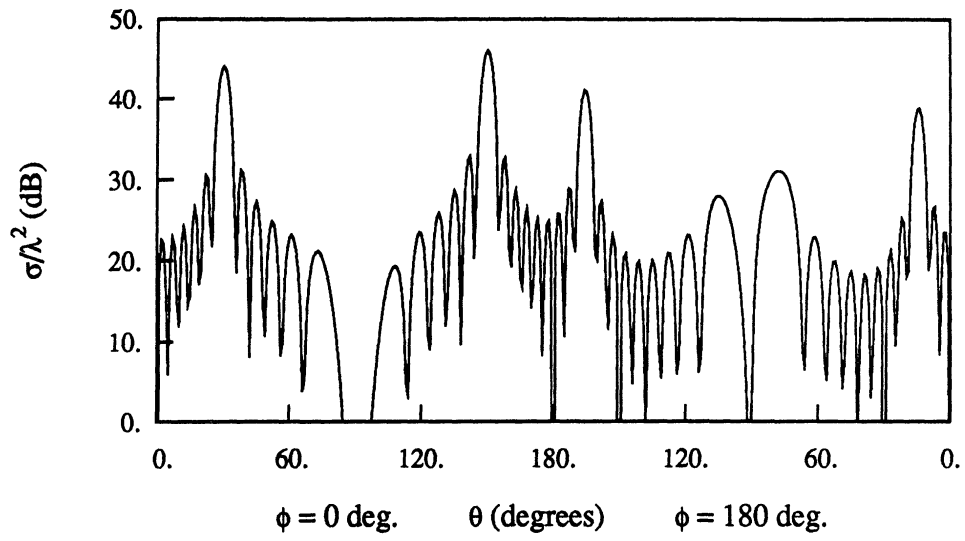


(a)

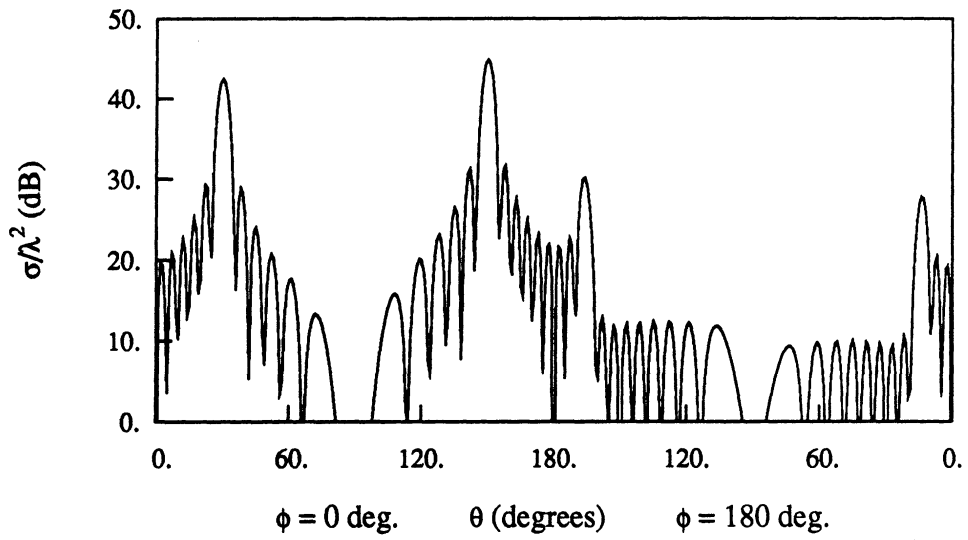


(b)

Figure 6.4: Bistatic radar cross section patterns for a 9×9 cross-shaped patch array at $f = 9$ GHz; $T_x = T_y = 2.0$ cm, $L = 1.5$ cm, $W = 0.5$ cm, $\epsilon_r = 4.0$, $d = 0.1$ cm, $\theta^i = 30^\circ$, $\phi^i = 180^\circ$. (a) TM incidence. (b) TE incidence.



(a)



(b)

Figure 6.5: Bistatic radar cross section patterns for a 9×9 cross-shaped patch array at $f = 20$ GHz; $T_x = T_y = 2.0$ cm, $L = 1.5$ cm, $W = 0.5$ cm, $\epsilon_r = 4.0$, $d = 0.1$ cm, $\theta^i = 30^\circ$, $\phi^i = 180^\circ$. (a) TM incidence. (b) TE incidence.

Chapter 7

Truncation Effect of Dielectric Slab

In Chapter 6, we dealt with a truncated periodic patch array residing on an infinite dielectric slab. If the dielectric slab is also of finite size, the diffraction caused by the edges of the slab will alter the overall scattering pattern. In this chapter, we present an approach to evaluate the diffraction contributed by the truncation of the slab. In particular, a volume integral physical optics approximation is developed to compute the diffracted field by the slab which must be added to the radiated field by the patch currents in determining the total scattering of the configuration.

7.1 Physical Optics Approximation

Consider a finite planar dielectric slab of thickness d occupying the region $0 \leq z \leq d$ (a geometry similar to this is shown in Figure 2.1). The far zone

scattered field by this slab can be written as a volume integral

$$\overline{E}^s = \frac{jk_0 Z_0}{4\pi r} e^{-jk_0 r} \hat{r} \times \hat{r} \times \int \int \int_V \overline{J}(x, y, z) e^{j(k_x x + k_y y + k_z z)} dx dy dz \quad (7.1)$$

where V denotes the volume occupied by the slab, $k_x = k_0 \sin \theta \cos \phi$, $k_y = k_0 \sin \theta \sin \phi$ and $k_z = k_0 \cos \theta$. In addition, \overline{J} is the equivalent polarized current given by

$$\overline{J}(x, y, z) = j\omega\epsilon_0(\epsilon_r - 1)\overline{E}(x, y, z) \quad (7.2)$$

in which \overline{E} is the total electric field in the slab.

In accordance with a physical optics approximation, the total field \overline{E} is approximated by the field \overline{E}' induced in a corresponding infinite slab of the same thickness and property. For the infinite slab, \overline{E}' can be found analytically and for the TE case with the excitation (3.1) it is given by

$$\begin{aligned} \overline{E}' = & \left[A \sin \left(k_0 z \sqrt{\epsilon_r - \sin^2 \theta^i} \right) + B \cos \left(k_0 z \sqrt{\epsilon_r - \sin^2 \theta^i} \right) \right] \\ & \cdot (-\hat{x} \sin \phi^i + \hat{y} \cos \phi^i) e^{j(k_x^i x + k_y^i y)} \end{aligned} \quad (7.3)$$

where A and B are constants given by

$$\begin{aligned} A &= \frac{j \cos \theta^i}{\sqrt{\epsilon_r - \sin^2 \theta^i}} E_0 T^{TE} e^{jk_0 d \cos \theta^i} \\ B &= E_0 T^{TE} e^{jk_0 d \cos \theta^i} \end{aligned}$$

For the TM case with the excitation (3.2), \overline{E}' is given by

$$\overline{E}' = \left\{ \frac{j \sqrt{\epsilon_r - \sin^2 \theta^i}}{\epsilon_r} \left[A \cos \left(k_0 z \sqrt{\epsilon_r - \sin^2 \theta^i} \right) - B \sin \left(k_0 z \sqrt{\epsilon_r - \sin^2 \theta^i} \right) \right] \right\}$$

$$\begin{aligned} & \cdot (\hat{x} \cos \phi^i + \hat{y} \sin \phi^i) - \frac{\sin \theta^i}{\epsilon_r} \left[A \sin \left(k_0 z \sqrt{\epsilon_r - \sin^2 \theta^i} \right) \right. \\ & \left. + B \cos \left(k_0 z \sqrt{\epsilon_r - \sin^2 \theta^i} \right) \right] \hat{z} \} e^{j(k_x^i x + k_y^i y)} \end{aligned} \quad (7.4)$$

where A and B are again the constants

$$\begin{aligned} A &= \frac{j \epsilon_r \cos \theta^i}{\sqrt{\epsilon_r - \sin^2 \theta^i}} E_0 T^{TM} e^{j k_0 d \cos \theta^i} \\ B &= E_0 T^{TM} e^{j k_0 d \cos \theta^i}. \end{aligned}$$

Let us denote \bar{E}' as

$$\bar{E}' = \bar{i}(z) e^{j(k_x^i x + k_y^i y)} \quad (7.5)$$

for both TE and TM cases. When (7.5) now is substituted into (7.1)-(7.2) we obtain

$$\bar{E}^s = -\frac{k_0^2(\epsilon_r - 1)}{4\pi r} e^{-j k_0 r} \hat{r} \times \hat{r} \times \int_0^d \bar{i}(z) e^{j k_z z} dz \int \int_S e^{j(k_x + k_x^i)x + j(k_y + k_y^i)y} dx dy \quad (7.6)$$

where S is the area occupied by the slab in the x - y plane. Introducing the definitions

$$\bar{I} = \int_0^d \bar{i}(z) e^{j k_z z} dz \quad (7.7)$$

$$F = \int \int_S e^{j(k_x + k_x^i)x + j(k_y + k_y^i)y} dx dy \quad (7.8)$$

(7.6) may be written as

$$\bar{E}^s = -\frac{k_0^2(\epsilon_r - 1)}{4\pi r} F e^{-j k_0 r} \hat{r} \times \hat{r} \times \bar{I}. \quad (7.9)$$

It can be shown that

$$\begin{aligned} \hat{r} \times \hat{r} \times \bar{I} &= (-\cos \theta \cos \phi I_x - \cos \theta \sin \phi I_y + \sin \theta I_z) \hat{\theta} \\ &+ (\sin \phi I_x - \cos \phi I_y) \hat{\phi} \end{aligned} \quad (7.10)$$

and when this is substituted into (7.9) we finally have

$$E_{\theta}^s = \frac{k_0^2(\epsilon_r - 1)}{4\pi r} F e^{-jk_0 r} (\cos \theta \cos \phi I_x + \cos \theta \sin \phi I_y - \sin \theta I_z) \quad (7.11)$$

$$E_{\phi}^s = \frac{k_0^2(\epsilon_r - 1)}{4\pi r} F e^{-jk_0 r} (-\sin \phi I_x + \cos \phi I_y). \quad (7.12)$$

While F depends on the specific geometry, \bar{I} can be easily integrated out. In particular, for the TE case we find

$$I_x = -(As + Bc) \sin \phi^i \quad (7.13)$$

$$I_y = (As + Bc) \cos \phi^i \quad (7.14)$$

$$I_z = 0. \quad (7.15)$$

Similarly, for the TM case

$$I_x = \frac{j\sqrt{\epsilon_r - \sin^2 \theta^i}}{\epsilon_r} (ac - Bs) \cos \phi^i \quad (7.16)$$

$$I_y = \frac{j\sqrt{\epsilon_r - \sin^2 \theta^i}}{\epsilon_r} (ac - Bs) \sin \phi^i \quad (7.17)$$

$$I_z = -\frac{\sin \theta^i}{\epsilon_r} (As + Bc). \quad (7.18)$$

In the above, s and c are given by

$$\begin{aligned} s &= \int_0^d \sin \left(k_0 z \sqrt{\epsilon_r - \sin^2 \theta^i} \right) e^{jk_0 z \cos \theta} dz \\ &= \frac{1 - e^{jk_0 \left(\sqrt{\epsilon_r - \sin^2 \theta^i} + \cos \theta \right) d}}{2k_0 \left(\sqrt{\epsilon_r - \sin^2 \theta^i} + \cos \theta \right)} + \frac{1 - e^{-jk_0 \left(\sqrt{\epsilon_r - \sin^2 \theta^i} - \cos \theta \right) d}}{2k_0 \left(\sqrt{\epsilon_r - \sin^2 \theta^i} - \cos \theta \right)} \end{aligned} \quad (7.19)$$

$$\begin{aligned} c &= \int_0^d \cos \left(k_0 z \sqrt{\epsilon_r - \sin^2 \theta^i} \right) e^{jk_0 z \cos \theta} dz \\ &= j \frac{1 - e^{jk_0 \left(\sqrt{\epsilon_r - \sin^2 \theta^i} + \cos \theta \right) d}}{2k_0 \left(\sqrt{\epsilon_r - \sin^2 \theta^i} + \cos \theta \right)} - j \frac{1 - e^{-jk_0 \left(\sqrt{\epsilon_r - \sin^2 \theta^i} - \cos \theta \right) d}}{2k_0 \left(\sqrt{\epsilon_r - \sin^2 \theta^i} - \cos \theta \right)}. \end{aligned} \quad (7.20)$$

For a rectangular $a \times b$ slab, we have

$$\begin{aligned} F &= \int_{-a/2}^{a/2} \int_{-b/2}^{b/2} e^{j(k_x+k_x^i)x+j(k_y+k_y^i)y} dx dy \\ &= ab \operatorname{sinc} \left[(k_x+k_x^i) \frac{a}{2} \right] \operatorname{sinc} \left[(k_y+k_y^i) \frac{b}{2} \right]. \end{aligned} \quad (7.21)$$

We note that while the above scattered field was formulated as that generated by the equivalent polarized currents, some choose to relate it to the concept of edge diffraction which may provide a more understandable interpretation. To do so, we note that

$$\begin{aligned} e^{j(k_x+k_x^i)x+j(k_y+k_y^i)y} = \\ \hat{z} \cdot \nabla \left\{ \left[(k_x+k_x^i)\hat{y} - (k_y+k_y^i)\hat{x} \right] \frac{e^{j(k_x+k_x^i)x+j(k_y+k_y^i)y}}{j \left[(k_x+k_x^i)^2 + (k_y+k_y^i)^2 \right]} \right\} \end{aligned} \quad (7.22)$$

and thus (7.6) can be rewritten as

$$\begin{aligned} \overline{E}^s &= -\frac{k_0^2(\epsilon_r-1)}{4\pi r} e^{-jk_0 r} \hat{r} \times \hat{r} \times \overline{I} \\ &\cdot \oint_C \frac{\hat{t} \cdot \left[(k_x+k_x^i)\hat{y} - (k_y+k_y^i)\hat{x} \right]}{j \left[(k_x+k_x^i)^2 + (k_y+k_y^i)^2 \right]} e^{j(k_x+k_x^i)x+j(k_y+k_y^i)y} dt \end{aligned} \quad (7.23)$$

upon the use of Stoke's theorem, where C is the contour enclosing the area S and \hat{t} is the unit vector tangential to C . The corresponding expression for the field radiated by a line source of current $\overline{K}(t)$ is

$$\overline{E} = \frac{jk_0 Z_0}{4\pi r} e^{-jk_0 r} \hat{r} \times \hat{r} \times \oint_C \overline{K}(t) e^{j(k_x x + k_y y)} dt \quad (7.24)$$

and by comparison with (7.23) we observe that the edge diffraction may be attributed to an equivalent current given by

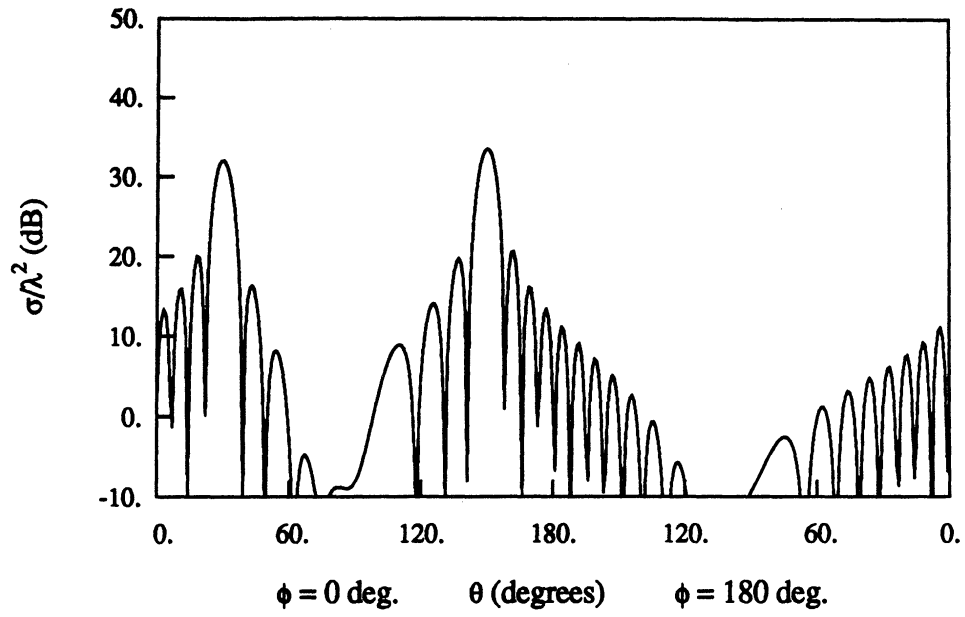
$$\overline{K}(t) = k_0 Y_0 (\epsilon_r - 1) \overline{I} \frac{\hat{t} \cdot \left[(k_x+k_x^i)\hat{y} - (k_y+k_y^i)\hat{x} \right]}{\left[(k_x+k_x^i)^2 + (k_y+k_y^i)^2 \right]} e^{jk_x^i x + jk_y^i y}. \quad (7.25)$$

We also note that $\bar{K}(t)$ can be further splitted into the equivalent electric and magnetic currents flowing along the edge [14, ch. 2].

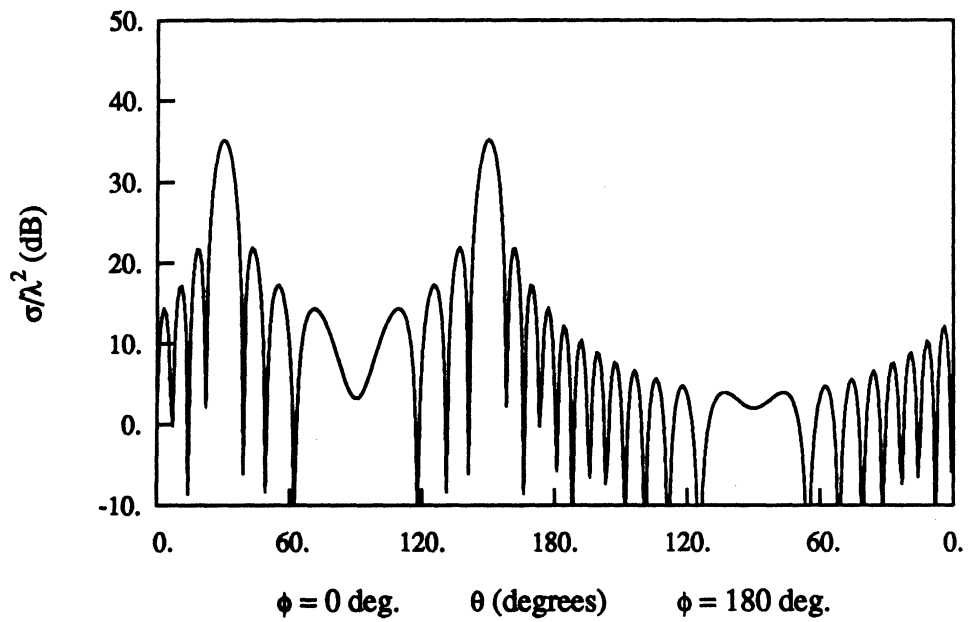
7.2 Numerical Results

In the following, we present the approximate solution for the scattering by a 9×9 cross-shaped patch array on a $26 \text{ cm} \times 26 \text{ cm}$ dielectric slab with all other parameters the same as those given in Figures 6.4 and 6.5.

Figures 7.1 and 7.2 show the physical optics solutions for the bistatic scattering patterns of the slab at frequencies 9 GHz and 20 GHz, respectively. When these slab scattered fields are added to the scattered fields by the patch array (Figures 6.4-6.5), we obtain the total scattered fields of the truncated array on a finite slab. The results are shown in Figures 7.3 and 7.4. Comparing these with the corresponding data in Figures 6.4-6.5 and Figures 7.1-7.2, we observe that the fields radiated by the patch currents are dominant at 9 GHz while at 20 GHz the fields diffracted by the slab are dominant.

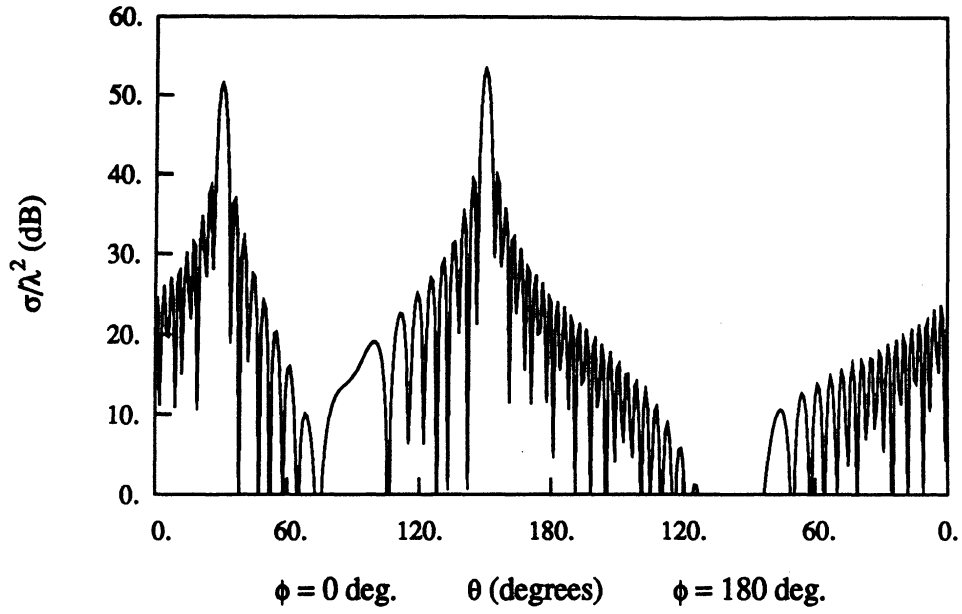


(a)

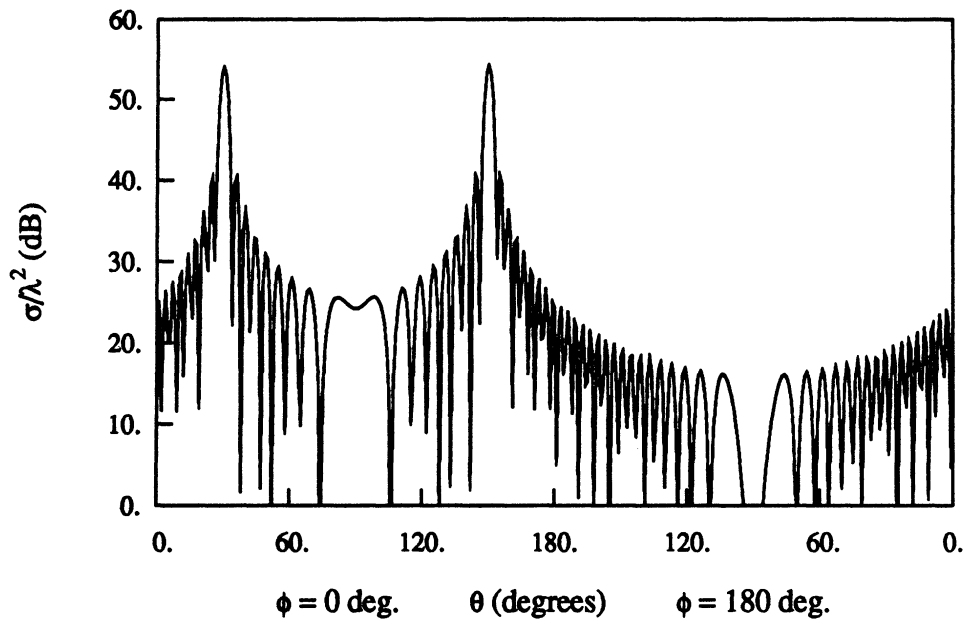


(b)

Figure 7.1: Bistatic radar cross section patterns for a $26 \text{ cm} \times 26 \text{ cm}$ dielectric slab at 9 GHz; $\epsilon_r = 4.0$, $d = 0.1 \text{ cm}$, $\theta^i = 30^\circ$, $\phi^i = 180^\circ$. (a) TM incidence. (b) TE incidence.

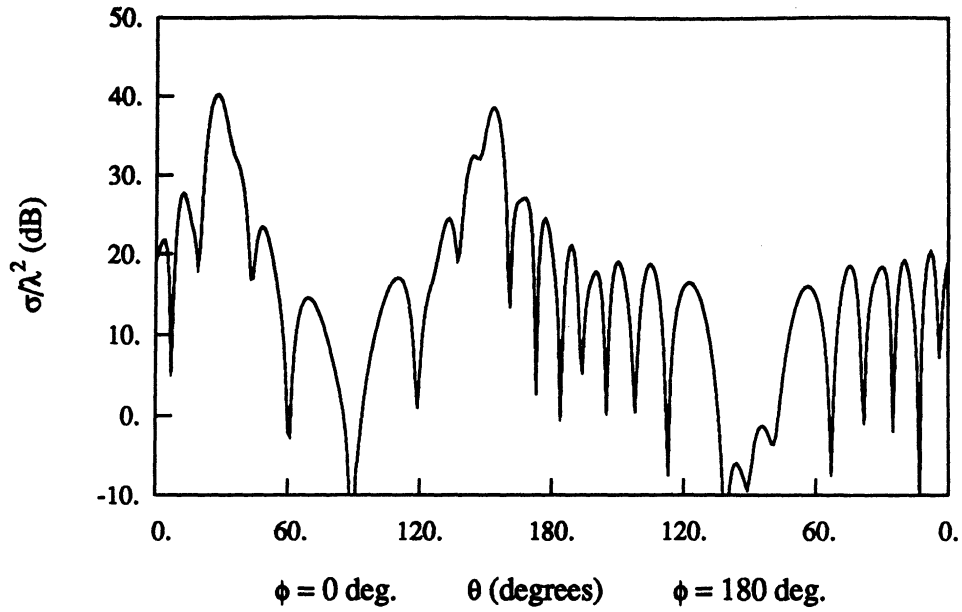


(a)

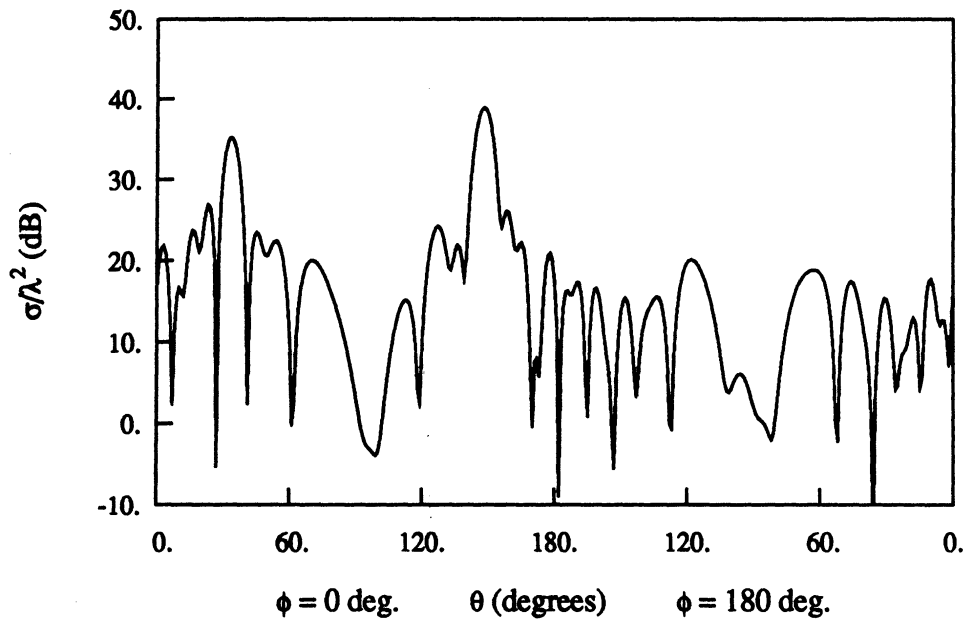


(b)

Figure 7.2: Bistatic radar cross section patterns for a 26 cm \times 26 cm dielectric slab at 20 GHz; $\epsilon_r = 4.0$, $d = 0.1$ cm, $\theta^i = 30^\circ$, $\phi^i = 180^\circ$. (a) TM incidence. (b) TE incidence.

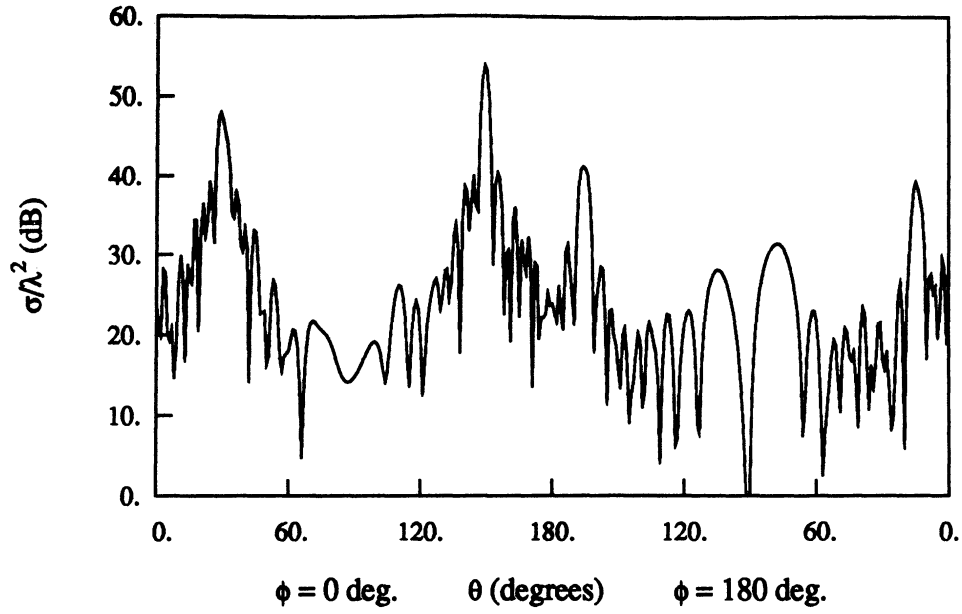


(a)

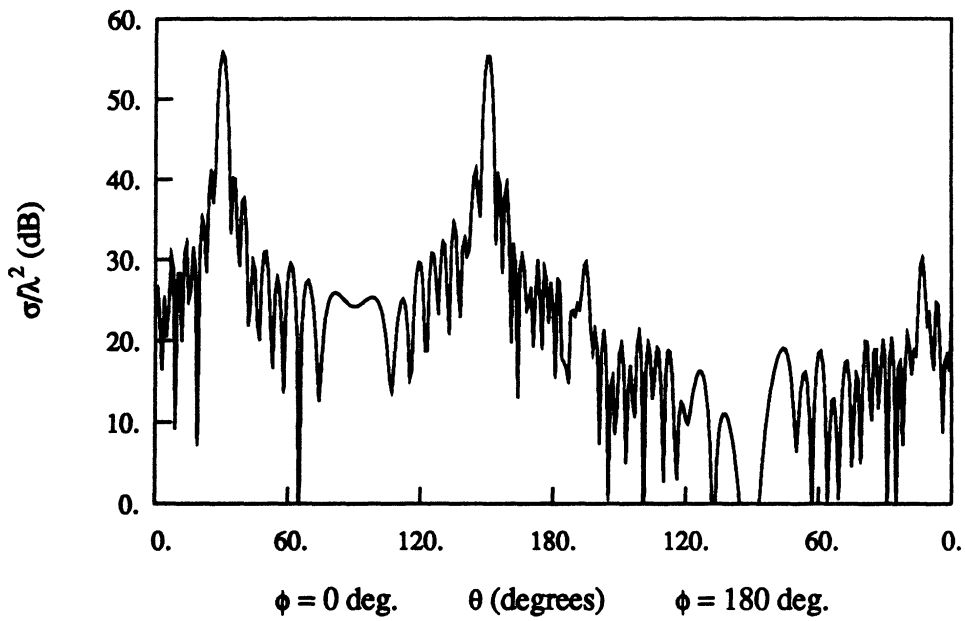


(b)

Figure 7.3: Bistatic radar cross section patterns for a 9×9 cross-shaped patch array on a $26 \text{ cm} \times 26 \text{ cm}$ dielectric slab at 9 GHz ; $T_x = T_y = 2.0 \text{ cm}$, $L = 1.5 \text{ cm}$, $W = 0.5 \text{ cm}$, $\epsilon_r = 4.0$, $d = 0.1 \text{ cm}$, $\theta^i = 30^\circ$, $\phi^i = 180^\circ$. (a) TM incidence. (b) TE incidence.



(a)



(b)

Figure 7.4: Bistatic radar cross section patterns for a 9×9 cross-shaped patch array on a $26 \text{ cm} \times 26 \text{ cm}$ dielectric slab at 20 GHz; $T_x = T_y = 2.0 \text{ cm}$, $L = 1.5 \text{ cm}$, $W = 0.5 \text{ cm}$, $\epsilon_r = 4.0$, $d = 0.1 \text{ cm}$, $\theta^i = 30^\circ$, $\phi^i = 180^\circ$. (a) TM incidence. (b) TE incidence.

Chapter 8

Conclusion

In this report, a spectral expression was derived for the dyadic Green's function associated with a dielectric slab. This was subsequently employed together with Floquet's theorem to formulate an equation for the patch currents on an infinite periodic array. A system of equations was then obtained by employing subdomain roof-top basis functions to expand the patch currents and applying Galerkin's technique. The conjugate gradient method in conjunction with the fast Fourier transform (CG-FFT) procedure for the solution of the system of equations was described in detail. This CG-FFT technique avoids the problem of large computer storage requirement and thus allows the treatment of large size arrays of practical interest.

Based on the computed patch currents, an exact numerical solution was presented for the infinite periodic array scattering. An approximate solution for the truncated periodic array scattering was also given and its accuracy was examined by comparison with available exact numerical data for unidirectionally truncated arrays. It was found that the approximate solution is of reasonable accuracy in pre-

dicting the scattering by the truncated array. Furthermore, the truncation effect of the dielectric slab was also studied by employing a physical optics approximation to compute the scattering by the slab.

The FORTRAN computer program which was used to generate the numerical data is described and listed in the appendix.

References

- [1] S. W. Lee, "Scattering by dielectric-loaded screen," *IEEE Trans. Antennas Propagat.*, vol. AP-19, pp. 656-665, Sept. 1971.
- [2] C. C. Chen, "Transmission of microwave through perforated flat plates," *IEEE Trans. Microwave Theory Tech.*, vol. MTT-21, pp. 1-6, Jan. 1973.
- [3] J. P. Montgomery, "Scattering by an infinite periodic array of thin conductors on a dielectric sheet," *IEEE Trans. Antennas Propagat.*, vol. AP-23, pp. 70-75, Jan. 1975.
- [4] T. A. Cwik and R. Mittra, "The cascade connection of planar periodic surfaces and lossy dielectric layers to form an arbitrary periodic screen," *IEEE Trans. Antennas Propagat.*, vol. AP-35, pp. 1397-1405, Dec. 1987.
- [5] R. C. Hall, R. Mittra, and K. M. Mitzner, "Analysis of multilayered periodic structures using generalized scattering matrix theory," *IEEE Trans. Antennas Propagat.*, vol. AP-36, pp. 511-517, April 1988.
- [6] B. J. Rubin and H. L. Bertoni, "Reflection from a periodically perforated plane using a subsectional current approximation," *IEEE Trans. Antennas*

- Propagat.*, vol. AP-31, pp. 829-836, Nov. 1983.
- [7] S. Contu and R. Tascone, "Scattering from passive arrays in plane stratified regions," *Electromagnetics*, vol. 5, no. 4, pp. 285-306, 1985.
- [8] T. A. Cwik and R. Mittra, "Scattering from a periodic array of free-standing arbitrarily shaped perfectly conducting or resistive patches," *IEEE Trans. Antennas Propagat.*, vol. AP-35, pp. 1226-1234, Nov. 1987.
- [9] W. H. Press, B. P. Flannery, S. A. Teukolsky, and W. T. Vetterling, *Numerical Recipes*, chap.12, Cambridge Univ. Press, 1986.
- [10] L. B. Felsen and N. Marcuvitz, *Radiation and Scattering of Waves*, chap.4, Prentice-Hall, Inc., Englewood Cliffs, N.J., 1973.
- [11] R. F. Harrington, *Time-Harmonic Electromagnetic Fields*. chap.3, New York: McGraw-Hill, 1961.
- [12] W. L. Ko and R. Mittra, "Scattering by a truncated periodic array," *IEEE Trans. Antennas Propagat.*, vol. AP-36, pp. 496-503, April 1988.
- [13] P. W. Grounds and K. J. Webb, "Numerical analysis of finite frequency selective surfaces," *1988 IEEE AP-S International Symposium Digest*, vol. II, pp. 746-749, June 1988.
- [14] R. J. Marhefka, O. M. Buyukdura, and W. Ebihara, "Radar cross section studies, phase III," The Ohio State University ElectroScience Laboratory Report No. 716621-1, April 1986.

Appendix

This appendix contains a brief description and a list of Fortran program and subroutines for the solution of the problem considered in this report.

1. INPUT DATA

There are three sets of input data describing the geometry of the problem, the numerical discretization and the incident field. All of them are contained and explained in the main program ARRAY. By looking through ARRAY, one should have no difficulty to understand and change these data.

2. OUTPUT DATA

The current output format is shown by an example computation listed below. If other output format is desired, one can change the main program ARRAY or the subroutine PCPA.

****ARRAY GEOMETRY INFORMATION UNIT=CM****

ARRAY PERIODICITY: TX = 2.000 TY = 2.000
RECTANGULAR PATCH: LX = 1.000 LY = 1.000
SLAB PERMITTIVITY: EPS = 4.000 0.000J
SLAB THICKNESS: D = 0.100

****INCIDENT FIELD INFORMATION****

POLARIZATION: TRANSVERSE MAGNETIC (TM)
WAVELENGTH: LAMBDA = 3.333 CM
INCIDENT ANGLE: PHI = 180.0 DEGREES

THETA = 30.0 DEGREES

FREQ(GHz)= 9.00 REFL(%)= 48.9904 TRANS(%)= 51.1338

SCATTERING PATTERN FOR THE TRUNCATED ARRAY

NO. OF PATCHES IN X-DIRECTION = 9

NO. OF PATCHES IN Y-DIRECTION = 9

PHI(DEG)	THETA(DEG)	RCS(DB)	ELMT PATT
0.0000	0.0000	15.24	-3.846
0.0000	30.00	33.18	-4.995
0.0000	60.00	-9.256	-9.608
0.0000	120.0	-9.165	-9.516
0.0000	150.0	33.57	-4.596
0.0000	180.0	15.70	-3.380
180.0	0.0000	15.24	-3.846
180.0	30.00	13.80	-5.283
180.0	60.00	13.70	-10.12
180.0	120.0	13.79	-10.02
180.0	150.0	14.20	-4.885
180.0	180.0	15.70	-3.380

SCATTERING PATTERN FOR THE TRUNCATED ARRAY

ON A TRUNCATED SLAB

A(CM)= 26.000 B(CM)= 26.000

PHI(DEG)	THETA(DEG)	RCS(DB)	EDGE DIFFRAC
0.0000	0.0000	15.22	2.096
0.0000	30.00	24.23	32.05
0.0000	60.00	-0.1905	-3.052
0.0000	120.0	6.472	5.120
0.0000	150.0	25.49	33.58
0.0000	180.0	16.98	2.154
180.0	0.0000	15.22	2.096
180.0	30.00	15.58	1.126
180.0	60.00	13.10	-0.3070
180.0	120.0	13.99	-8.452
180.0	150.0	15.06	-0.3098
180.0	180.0	16.98	2.153

3. PROGRAM DESCRIPTION

ARRAY - This program is a driver for subroutine PCPA.

PCPA - Computes the currents on a periodic patch array residing on a dielectric slab. Calls subroutines COEFF, FARF and FAFSFF.

COEFF - Computes the reflection and transmission coefficients of the periodic array.

- FARF - Computes the scattering pattern of a truncated patch array on an infinite dielectric slab.
- FAFSFF - Computes the scattering pattern of a truncated patch array on a finite dielectric slab.
- PAD - Generates the coded geometry for a patch.
- FINC - Computes the incident field vector \bar{B} as given by (3.24) and (3.25).
- GREENF - Computes \tilde{A}_{xx} , \tilde{A}_{xy} , \tilde{A}_{yx} and \tilde{A}_{yy} given in (4.14)-(4.17).
- SPECTRA - Decides whether to call SPECT1 or SPECT2.
- SPECT1 - Calls FFTN to perform FFT computation.
- SPECT2 - Calls PFFFT2 to perform FFT computation.
- FFTN - Ordinary FFT algorithm.
- PFFFT2 - Prime factor FFT algorithm.
- TABLE - Finds prime factors for FFT.
- VNORM - Calculates the euclidian norm of a vector.
- PRODUCT - Multiplies two vectors.
- CPRODUCT - Multiplies the conjugate of a vector with a vector.
- REFL - Computes the reflected field by a slab in isolation.
- TRANS - Computes the transmitted field through a slab in isolation.

Note that though the program treats rectangular, circular and cross-shaped patches, other patch geometries can also be treated by a simple modification on subroutine PAD. Also note that if one has a pad size larger than 32×32 , he or she needs to change the number $1024 = (32 \times 32)$ into a proper number in PCPA and SPECT2.

```

C*****C
          PROGRAM ARRAY
C*****C
C THIS PROGRAM IS A DRIVER FOR SUBROUTINE PCPA. THE PROGRAM COMPUTES C
C ELECTROMAGNETIC SCATTERING FROM A PERFECTLY CONDUCTING PATCH ARRAY C
C ON A DIELECTRIC SLAB. C
C FOR THE DETAILS OF THE FORMULATION, PLEASE REFER TO THE ATTACHED C
C UNIVERSITY OF MICHIGAN TECHNICAL REPORT 389604-7-T. C
C C
C PCPA -- THIS SUBROUTINE HAS FOUR TASKS: C
C 1: COMPUTES CURRENTS ON A PERIODIC CONDUCTING PATCH C
C ARRAY RESIDING ON AN UNGROUNDED DIELECTRIC SLAB FOR A C
C PLANE WAVE INCIDENCE. C
C 2: COMPUTES THE REFLECTION AND TRANSMISSION COEFFICIENTS C
C OF THE PERIODIC ARRAY. C
C 3: COMPUTES THE SCATTERING PATTERN IN RCS FOR THE C
C CORRESPONDING TRUNCATED PATCH ARRAY. C
C 4: COMPUTES THE SCATTERING PATTERN IN RCS FOR THE C
C TRUNCATED PATCH ON THE TRUNCATED SLAB. C
C*****C
C JIANMING JIN C
C RADIATION LABORATORY C
C DEPT. OF ELECTRICAL ENGINEERING & COMPUTER SCIENCE C
C THE UNIVERSITY OF MICHIGAN C
C ANN ARBOR, MICHIGAN 48109 C
C MARCH 20, 1989 C
C*****C

```

```

COMPLEX EPS
REAL LX,LY,L

```

```

C*****C
C.....FIRST SET INPUT DATA DESCRIPTION CONCERNING THE GEOMETRY: C
C C
C IS - INTEGER TYPE OF PATCH C
C IS=1 FOR RECTANGULAR PATCH C
C IS=2 FOR CIRCULAR PATCH C
C IS=3 FOR CROSS PATCH C
C OTHER GEOMETRIES COULD BE TREATED BY C
C MODIFYING SUBROUTINE PAD C
C TX - REAL PERIODIC LENGTH IN X-RECTION C
C TY - REAL PERIODIC LENGTH IN Y-RECTION C
C FOR IS=1 C
C LX - REAL PATCH DIMENSION IN X-DIRECTION C
C LY - REAL PATCH DIMENSION IN Y-DIRECTION C
C FOR IS=2 C
C RP - REAL PATCH RADIUS C
C FOR IS=3 C
C W - REAL WIDTH OF CROSS C
C L - REAL LENGTH OF CROSS C
C EPS - COMPLEX RELATIVE PERMITTIVITY OF SLAB C
C D - REAL THICKNESS OF SLAB C
C MX - INTEGER NUMBER OF PATCHES IN THE X-DIRECTION C
C MY - INTEGER NUMBER OF PATCHES IN THE Y-DIRECTION C
C A - REAL TRUNCATED SLAB DIMENSION IN X-DIRECTION C
C B - REAL TRUNCATED SLAB DIMENSION IN Y-DIRECTION C
C*****C
IS=1
TX=2.0
TY=2.0
LX=1.

```

LY=1.
 RP=0.625
 W=0.5
 L=1.5
 EPS=(4.0,0.0)
 D=0.1
 A=26.0
 B=26.0
 MX=9
 MY=9

```

C*****C
C.....SECOND SET INPUT DATA DESCRIPTION CONCERNING THE DISCRETIZATION: C
C  NX - INTEGER    NUMBER OF CELLS IN X-DIRECTION          C
C  NY - INTEGER    NUMBER OF CELLS IN Y-DIRECTION          C
C  IFFT - INTEGER  TYPE OF FFT ALGORITHM TO USE           C
C                                     THERE ARE TWO SUBROUTINES FOR FFT COMPUTATION: C
C                                     ONE IS ORDINARY FFT ALGORITHM AND THE OTHER IS C
C                                     THE PRIME FACTOR FFT ALGORITHM.                 C
C  FOR IFFT=1      USE THE ORDINARY FFT ALGORITHM          C
C                                     NX AND NY CAN BE ANY NUMBER FROM THE SET (8, 16, C
C                                     32, 64, 128, 256, 512, ...)                     C
C  FOR IFFT=2      USE THE PRIME FACTOR FFT ALGORITHM      C
C                                     NX(=NY) CAN BE ANY NUMBER FROM THE SET (8, 9, 10,C
C                                     12, 14, 15, 16, 18, 20, 21, 24, 28, 30, 35, 36, C
C                                     40, 42, 45, 48, 56, 60, 63, 70, 72, 80, 84, 90, C
C                                     105, 112, 120, 126, 140, 144, 168, 180, 210, 240,C
C                                     252, 280, 315, 336, 360, 420, 560, ...)         C
C  TOL - REAL      TOLERANCE (USUALLY .001 TO .01)        C
C  ITHAX - INTEGER MAXIMUM ITERATION NUMBER               C
  
```

```

C*****C
  IFFT=2
  NX=16
  NY=16
  TOL=0.005
  ITHAX=501
  
```

```

C*****C
C.....THIRD SET INPUT DATA DESCRIPTION CONCERNING THE INCIDENT FIELD: C
C                                     C
C  WAVE - REAL     FREE-SPACE WAVELENGTH                   C
C  IPOL - INTEGER  POLARIZATION                           C
C                                     IPOL=1 E-POLARIZATION (TE) (Ez=0)           C
C                                     IPOL=2 H-POLARIZATION (TM) (Hz=0)           C
C  PHINC - REAL   INCIDENT PHI ANGLE IF KODE=1 (DEGREES) C
C  THINC - REAL   INCIDENT THETA ANGLE IF KODE=1 (DEGREES) C
C  PH1 - REAL     INITIAL PHI ANGLE (DEGREES)             C
C  PH2 - REAL     FINAL PHI ANGLE (DEGREES)              C
C  TH1 - REAL     INITIAL THETA ANGLE (DEGREES)          C
C  TH2 - REAL     FINAL THETA ANGLE (DEGREES)            C
C  DPH - REAL     INCREMENT OF PHI ANGLE (DEGREES)       C
C  DTH - REAL     INCREMENT OF THETA ANGLE (DEGREES)     C
  
```

```

C*****C
  WAVE=3.333333333
  IPOL=2
  PHINC=180.0
  THINC=30.0
  PH1=0.0
  PH2=270.0
  TH1=0.0
  
```

```
TH2=180.0  
DPH=180.0  
DTH=30.
```

```
C....CALL SUBROUTINE TO COMPUTE CURRENT DISTRIBUTION AND THEN THE  
C ... REFLECTION, TRANSMISSION, SCATTERING PATTERNS, ETC.  
CALL PCPA(WAVE,EPS,D,TX,TY,LX,LY,RP,W,L,IS,IFFT,MX,MY,PH1,PH2,  
&TH1,TH2,DPH,DTH,PHINC,THINC,IPOL,TOL,ITMAX,MX,MY,A,B)  
STOP  
END
```

```

SUBROUTINE PCPA(WAVE, EPS, DD, TX, TY, LX, LY, RP, W, L, IS, IFFT, NX, NY, PH1,
&PH2, TH1, TH2, DPH, DTH, PHINC, THINC, IPOL, TOL, ITMAX, MX, MY, A, BS)
C*****
C THIS SUBROUTINE SOLVES THE CURRENT DISTRIBUTION ON A PERIODIC C
C CONDUCTING PATCH ARRAY RESIDING ON AN UNGROUNDED DIELECTRIC SLAB C
C FOR A PLANE WAVE INCIDENCE. THE APPROACH IS BASED ON THE CG-FFT C
C METHOD. C
C ONCE THE CURRENT IS COMPUTED, THE SUBROUTINE COMPUTES THE C
C REFLECTION AND TRANSMISSION OF THE ARRAY, THE SCATTERING PATTERNS C
C FOR THE TRUNCATED ARRAY. C
C*****
C....NM = NX*NY
PARAMETER (NM=1024)
COMPLEX CUX(NM), CUY(NM), EX(NM), EY(NM), EPS, XT(NM), YT(NM), AX(NM),
& AY(NM), AXT(NM), AYT(NM), GXI(NM), GXY(NM), GYY(NM), GYX(NM),
& RX(NM), RY(NM), PX(NM), PY(NM)
REAL L, LX, LY, KO, KXI, KYI
INTEGER SG(NM), SGX(NM), SGY(NM), SIGN, MF(4)
PI=3.141592654

C....FIND PRIME FACTORS OF NX
IF (IFFT.EQ.2) CALL TABLE(NX, MF, MF)

CALL PAD(NE, SG, SGX, SGY, DX, DY, TX, TY, NX, NY, LX, LY, RP, W, L, IS)
C*****
C....OUTPUT DATA DESCRIPTION: C
C NE - INTEGER NUMBER OF CELLS IN THE PATCH C
C SG - INTEGER VECTOR TAG ARRAY FOR THE PATCH C
C SG(I)=0 CELL OUTSIDE THE PATCH C
C SG(I)=1 CELL INSIDE THE PATCH C
C SGX - INTEGER VECTOR SHIFTED TAG FOR ROOF-TOP FOR X CURRENT C
C SGY - INTEGER VECTOR SHIFTED TAG FOR ROOF-TOP FOR Y CURRENT C
C*****

NT=NX*NY

CALL FINC(IPOL, WAVE, EPS, DD, DX, DY, PHINC, THINC, NT, EX, EY, KO, KXI, KYI)
C*****
C....OUTPUT DATA DESCRIPTION: C
C EX - COMPLEX VECTOR X-COMPONENT OF INCIDENT FIELD C
C EY - COMPLEX VECTOR Y-COMPONENT OF INCIDENT FIELD C
C*****

CALL GREENF(GXI, GXY, GYY, GYX, NX, NY, KXI, KYI, KO, EPS, DD, TX, TY)
C*****
C....OUTPUT DATA DESCRIPTION: C
C GXI - COMPLEX VECTOR GREEN'S FUNCTION COMPONENT C
C GXY - COMPLEX VECTOR GREEN'S FUNCTION COMPONENT C
C GYY - COMPLEX VECTOR GREEN'S FUNCTION COMPONENT C
C GYX - COMPLEX VECTOR GREEN'S FUNCTION COMPONENT C
C*****

SNT=FLOAT(NT)
DO I=1, NT
GXI(I)=GXI(I)/SNT
GXY(I)=GYX(I)/SNT
GYY(I)=GYY(I)/SNT
GYX(I)=GXY(I)/SNT
ENDDO

```

```

VHRM=VNORM(EX,KY,NT,SGX,SGY)
RSS=0.0
ITER=0

C.....INITIALIZE CURRENT DISTRIBUTION
DO I=1,NT
  CUX(I)=(0.0,0.0)
  CUY(I)=(0.0,0.0)
ENDDO

SIGN=-1
CALL SPECTRA(CUX,XT,NX,NY,SIGN,MF,NF,IFFT)
CALL SPECTRA(CUY,YT,NX,NY,SIGN,MF,NF,IFFT)
C*****C
C.....OUTPUT DATA DESCRIPTION: C
C  XT - COMPLEX VECTOR  FOURIER TRANSFORMED X-COMPONENT CURRENT C
C  YT - COMPLEX VECTOR  FOURIER TRANSFORMED Y-COMPONENT CURRENT C
C*****C

CALL PRODUCT(AXT,GXX,GXY,XT,YT,NT)
CALL PRODUCT(AYT,GYY,GXY,YT,XT,NT)
C*****C
C.....OUTPUT DATA DESCRIPTION: C
C  AXT - COMPLEX VECTOR  PRODUCT TO TE TRANSFORMED C
C  AYT - COMPLEX VECTOR  PRODUCT TO TE TRANSFORMED C
C*****C

SIGN=1
CALL SPECTRA(AX,AXT,NX,NY,SIGN,MF,NF,IFFT)
CALL SPECTRA(AY,AYT,NX,NY,SIGN,MF,NF,IFFT)
C*****C
C.....OUTPUT DATA DESCRIPTION: C
C  AX - COMPLEX VECTOR  PRODUCT AFTER TRANSFORMATION C
C  AY - COMPLEX VECTOR  PRODUCT AFTER TRANSFORMATION C
C*****C

C.....COMPUTE THE RESIDUAL FOR THE INTIAL CURRENTS
DO 10 I=1,NT
  IF(SGX(I).EQ.1) THEN
    RX(I) = EX(I)-AX(I)
  ELSE
    RX(I) = (0.0,0.0)
  END IF
  IF(SGY(I).EQ.1) THEN
    RY(I) = EY(I)-AY(I)
  ELSE
    RY(I) = (0.0,0.0)
  END IF
10 CONTINUE

SIGN=-1
CALL SPECTRA(RX,XT,NX,NY,SIGN,MF,NF,IFFT)
CALL SPECTRA(RY,YT,NX,NY,SIGN,MF,NF,IFFT)

CALL CPRODUCT(AXT,GXX,GXY,XT,YT,NT)
CALL CPRODUCT(AYT,GYY,GXY,YT,XT,NT)

SIGN=1
CALL SPECTRA(AX,AXT,NX,NY,SIGN,MF,NF,IFFT)
CALL SPECTRA(AY,AYT,NX,NY,SIGN,MF,NF,IFFT)

```

```

      B=1./VNORM(AX,AY,NT,SGX,SGY)

C.....COMPUTE THE SEARCH VECTORS
      DO 20 I = 1,NT
      IF(SGX(I).EQ.1) THEN
        PX(I) = B*AX(I)
      ELSE
        PX(I) = (0.0,0.0)
      END IF
      IF(SGY(I).EQ.1) THEN
        PY(I) = B*AY(I)
      ELSE
        PY(I) = (0.0,0.0)
      END IF
20    CONTINUE

C.....BEGIN ITERATION TO FIND SOLUTION TO THE CURRENT
30    CONTINUE

      SIGN=-1
      CALL SPECTRA(PX,XT,NX,NY,SIGN,MF,NF,IFFT)
      CALL SPECTRA(PY,YT,NX,NY,SIGN,MF,NF,IFFT)

      CALL PRODUCT(AXT,GXX,GXY,XT,YT,NT)
      CALL PRODUCT(AYT,GYY,GYX,YT,XT,NT)

      SIGN=1
      CALL SPECTRA(AX,AXT,NX,NY,SIGN,MF,NF,IFFT)
      CALL SPECTRA(AY,AYT,NX,NY,SIGN,MF,NF,IFFT)

      T = 1./VNORM(AX,AY,NT,SGX,SGY)
      DO 70 I = 1,NT
      IF(SGX(I).EQ.1) THEN
        CUX(I) = CUX(I)+T*PX(I)
        RX(I) = RX(I)-T*AX(I)
      ELSE
        CUX(I) = (0.0,0.0)
        RX(I) = (0.0,0.0)
      END IF
      IF(SGY(I).EQ.1) THEN
        CUY(I) = CUY(I)+T*PY(I)
        RY(I) = RY(I)-T*AY(I)
      ELSE
        CUY(I) = (0.0,0.0)
        RY(I) = (0.0,0.0)
      END IF
70    CONTINUE

      SIGN=-1
      CALL SPECTRA(RX,XT,NX,NY,SIGN,MF,NF,IFFT)
      CALL SPECTRA(RY,YT,NX,NY,SIGN,MF,NF,IFFT)

      CALL CPRODUCT(AXT,GXX,GYX,XT,YT,NT)
      CALL CPRODUCT(AYT,GYY,GYX,YT,XT,NT)

      SIGN=1
      CALL SPECTRA(AX,AXT,NX,NY,SIGN,MF,NF,IFFT)
      CALL SPECTRA(AY,AYT,NX,NY,SIGN,MF,NF,IFFT)

```



```

      B=1./VNORM(AX,AY,NT,SGX,SGY)
      DO 50 I = 1,NT
      IF(SGX(I).EQ.1) THEN
        PX(I) = PX(I)+B*AX(I)
      ELSE
        PX(I) = (0.0,0.0)
      END IF
      IF(SGY(I).EQ.1) THEN
        PY(I) = PY(I)+B*AY(I)
      ELSE
        PY(I) = (0.0,0.0)
      END IF
50    CONTINUE

      ITER = ITER+1

      VVRMR=VNORM(RX,RY,NT,SGX,SGY)
      RSS = SQRT(VVRMR/VNRM)

C.....IF NOT TO MONITOR THE ITERATIVE PROCEDURE, COMMENT THE NEXT LINE
C      PRINT 140,ITER,RSS

C.....IF THE CRITERIA IS SARISFIED, THEN
      IF(RSS.LE.TOL) THEN
        PRINT 120

C.....PRINT THE INFORMATION ABOUT THE ARRAY
      PRINT 200, TX, TY
      IF(IS.EQ.1) PRINT 220, LX, LY
      IF(IS.EQ.2) PRINT 240, RP
      IF(IS.EQ.3) PRINT 260, L, W
      PRINT 280, EPS, DD
C.....PRINT THE INCIDENT FIELD INFORMATION
      PRINT 300
      IF(IPOL.EQ.1) PRINT 320
      IF(IPOL.EQ.2) PRINT 340
      PRINT 360, WAVE, PHINC, THINC

C.....IF THE CURRENT DATA ARE DESIRED, UNCOMMENT THE FOLLOWING 11 LINES
C ... THE FIRST TASK IS COMPLETED HERE
C      PRINT 150
C      DO I=1,NT
C      IF(CUX(I).EQ.(0.,0.)) PHX=0.
C      IF(CUX(I).NE.(0.,0.)) PHX=ATAN2(AIMAG(CUX(I)),REAL(CUX(I)))*
C      & 180./PI
C      IF(CUY(I).EQ.(0.,0.)) PHY=0.
C      IF(CUY(I).NE.(0.,0.)) PHY=ATAN2(AIMAG(CUY(I)),REAL(CUY(I)))*
C      & 180./PI
C      PRINT 90,CABS(CUX(I)),PHX,CABS(CUY(I)),PHY
C 90    FORMAT(4G13.4)
C      ENDDO

C.....CALL COEFF TO COMPUTE THE REFLECTION AND TRANSMISSION COEFFICIENTS
C ... THE SECOND TASK IS COMPLETED HERE
      CALL COEFF(CUX,CUY,SGX,SGY,NX,NY,KXI,KYI,KO,EPS,DD,TX,TY,THINC,
      &          PHINC,IPOL)

C.....CALL FARF TO COMPUTE THE SCATTERING PATTERN FOR THE CORRESPONDING
C ... TRUNCATED PATCH ARRAY. THE THIRD TASK IS COMPLETED HERE
      PRINT 160,MX,MY

```

```

      CALL FARF(CUX,CUY,SG,NX,NY,KXI,KYI,KO,EPS,DD,TX,TY,PH1,PH2,DPH,
&          TH1,TH2,DTH,MX,MY)

C.....CALL FAFSFF TO COMPUTE THE SCATTERING PATTERN FOR THE TRUNCATED ON
C ... A TRUNCATED SLAB. THE FOURTH OR FINAL TASK IS COMPLETED HERE
      PRINT 170,A,BS
      CALL FAFSFF(CUX,CUY,SG,NX,NY,PHINC,THINC,KO,EPS,DD,TX,TY,PH1,
&          PH2,DPH,TH1,TH2,DTH,MX,MY,A,BS,IPOL)

C.....IF THE CRITERIA IS NOT SATISFIED, THEN
      ELSE
        IF(ITER.EQ.ITMAX) THEN
          PRINT 130
        ELSE
          GO TO 30
        END IF
      END IF

120  FORMAT('CONVERGENCE ACHIEVED, WOW!!'//)
130  FORMAT('ITMAX EXCEEDED; NO CONVERGENCE.')
140  FORMAT('ITER=',I4,' RSS=',G14.4)
150  FORMAT('          THE CURRENT DISTRIBUTION ON A PATCH'/
&          ' MAG(J_X)  PHASE(J_X)  MAG(J_Y)  PHASE(J_Y)')
160  FORMAT('//          SCATTERING PATTERN FOR THE TRUNCATED ARRAY'/
&          '          NO. OF PATCHES IN X-DIRECTION =',I4/
&          '          NO. OF PATCHES IN Y-DIRECTION =',I4/
&          ' PHI(DEG)  THETA(DEG)  RCS(DB)  ELMT PATT')
170  FORMAT('//          SCATTERING PATTERN FOR THE TRUNCATED ARRAY'/
&          '          ON A TRUNCATED SLAB          '/
&          '          A(CM)=',F8.3,' B(CM)=',F8.3/
&          ' PHI(DEG)  THETA(DEG)  RCS(DB)  EDGE DIFFRAC')
200  FORMAT('          ****ARRAY GEOMETRY INFORMATION UNIT=CM****'//
&          '          ARRAY PERIODICITY: TX =',F8.3,' TY =',F8.3)
220  FORMAT('          RECTANGULAR PATCH: LX =',F8.3,' LY =',F8.3)
240  FORMAT('          CIRCULAR PATCH: RADIUS =',F8.3)
260  FORMAT('          CROSS SHAPED PATCH: L =',F8.3,' W =',F8.3)
280  FORMAT('          SLAB PERMITTIVITY: EPS =',2F8.3,'J'/
&          '          SLAB THICKNESS: D =',F8.3//)
300  FORMAT('          ****INCIDENT FIELD INFORMATION****'//)
320  FORMAT('          POLARIZATION: TRANSVERSE ELECTRIC (TE)')
340  FORMAT('          POLARIZATION: TRANSVERSE MAGNETIC (TM)')
360  FORMAT('          WAVELENGTH: LAMBDA =',F8.3,' CM'/
&          '          INCIDENT ANGLE: PHI =',F8.1,' DEGREES'/
&          '          THETA =',F8.1,' DEGREES'//)

      RETURN
      END

```

```

      SUBROUTINE PAD(NE,SG,SGX,SGY,DX,DY,TX,TY,NX,NY,LX,LY,R,W,L,IS)
C*****
C THIS SUBROUTINE GENERATES A CODED GEOMETRY FOR A RECTANGULAR OR A C
C CIRCULAR OR A CROSS PATCH. C
C IS=1 --- RECTANGULAR; IS=2 --- CIRCULAR; IS=3 --- CROSS. C
C*****C
      INTEGER SG(*),SGX(*),SGY(*)
      REAL LX,LY,L
      NT=NX*NY
      DO K=1,NT
      SGX(K)=0
      SGY(K)=0
      ENDDO
      HLX=0.5*LX
      HLY=0.5*LY
      DX=TX/NX
      DY=TY/NY
      HW=0.5*W
      HL=0.5*L
      XO=-0.5*TX+0.5*DX
      YO=-0.5*TY+0.5*DY
      K=0
      NE=0
C.....FOR RECTANGULAR PATCH
      IF(IS.EQ.1) THEN
      DO J=1,NY
      Y=YO+FLOAT(J-1)*DY
      DO I=1,NX
      X=XO+FLOAT(I-1)*DX
      K=K+1
      IF(ABS(X).LT.HLX) THEN
      IF(ABS(Y).LT.HLY) THEN
      SG(K)=1
      NE=NE+1
      ELSE
      SG(K)=0
      END IF
      ELSE
      SG(K)=0
      END IF
      ENDDO
      ENDDO
      GOTO 1
      ELSE
      END IF
C.....FOR CIRCULAR PATCH
      IF(IS.EQ.2) THEN
      DO J=1,NY
      Y=YO+FLOAT(J-1)*DY
      DO I=1,NX
      X=XO+FLOAT(I-1)*DX
      K=K+1
      RSQ=X*X+Y*Y
      IF(RSQ.LT.R*R) THEN
      SG(K)=1
      NE=NE+1
      ELSE
      SG(K)=0
      END IF
      ENDDO

```

```

        ENDDO
        GOTO 1
    ELSE
        END IF
C.....FOR CROSS PATCH
    IF (IS.EQ.3) THEN
        DO J=1,NY
            Y=Y0+FLOAT(J-1)*DY
        DO I=1,NX
            X=X0+FLOAT(I-1)*DX
            K=K+1
            IF (ABS(X).LT.HW.AND.ABS(Y).LT.HL) THEN
                SG(K)=1
            ELSE
                IF (ABS(X).LT.HL.AND.ABS(Y).LT.HW) THEN
                    SG(K)=1
                ELSE
                    SG(K)=0
                END IF
            END IF
            NE=NE+1
        ENDDO
    ENDDO
    ELSE
        END IF
C.....SHIFT LABELS IN X AND Y DIRECTION
1 CONTINUE
    K=0
    DO J=1,NY
        DO I=1,NX
            K=K+1
            IF (SG(K).EQ.1.AND.SG(K+1).EQ.0) THEN
                SGX(K)=0
            ELSE
                SGX(K)=SG(K)
            END IF
        END DO
    END DO
    DO I=1,NX
        DO J=1,NY-1
            K1=(J-1)*NX+I
            K2=J*NX+I
            IF (SG(K1).EQ.1.AND.SG(K2).EQ.0) THEN
                SGY(K1)=0
            ELSE
                SGY(K1)=SG(K1)
            END IF
        END DO
    END DO
    RETURN
END

```

```

SUBROUTINE FING(IFLAG,WAVE,EPS,D,DX,DY,PH,TH,WT,EX,EY,KO,KX,KY)
C*****C
C THIS SUBROUTINE COMPUTES THE INCIDENT AND REFLECTED TANGENTIAL C
C ELECTRIC FIELD ON THE PATCH. C
C*****C
C IFLAG=1 --- TE INCIDENCE (Ez=0) C
C IFLAG=2 --- TM INCIDENCE (Hz=0) C
C*****C
COMPLEX EI(*),EY(*),EPS
REAL KO,KX,KY
COMPLEX CJ,CO,C1,C2,C3,C4,R,EXTE,EYTE,EXTM,EYTM
DATA TPI,RAD/.6283185E+01,.1745329E-01/
CJ=CHPLX(0.,1.)
KO=TPI/WAVE
SIP=SIN(RAD*PH)
COP=COS(RAD*PH)
SIT=SIN(RAD*TH)
COT=COS(RAD*TH)
SID=SIN(KO*D*COT)
COD=COS(KO*D*COT)
KX=KO*SIT+COP
KY=KO*SIT+SIP
C1=CSQRT(EPS-SIT*SIT)
C2=CSIN(KO*D*C1)
C3=CCOS(KO*D*C1)
CO=(CJ*C1+C2+COT*C3)/(CJ*C1+C3-COT*C2)
IF(IFLAG.EQ.2) GOTO 10
R=(CJ*COT+CO*C1)/(CJ*COT-CO*C1)
C4=(1.+R)*CHPLX(COD,SID)
EXTE=SIP*C4
EYTE=-COP*C4
DO I=1,WT
EX(I)=EXTE
EY(I)=EYTE
ENDDO
RETURN
10 CO=(CJ*C1+C2+EPS*COT*C3)/(CJ*C1+C3-EPS*COT*C2)
R=(EPS*COT-CJ*C1+CO)/(EPS*COT+CJ*C1+CO)
C4=(1.-R)*CHPLX(COD,SID)
EXTM=-COT*COP*C4
EYTM=-COT*SIP*C4
DO I=1,WT
EX(I)=EXTM
EY(I)=EYTM
ENDDO
RETURN
END

```

```

SUBROUTINE GREENF(GXX,GXY,GYY,GYX,NX,NY,KXI,KYI,KO,EPS,D,TX,TY)
C*****
C THIS SUBROUTINE COMPUTES GREEN'S FUNCTIONS G_XX, G_YX, G_YY AND *
C G_XY (=G_YX) FOR A GEOMETRY OF A DIELECTRIC SLAB HAVING THICK- *
C -NESS D AND PERMITTIVITY EPS. THE OUTPUT IS THOSE FUNCTIONS MUL- *
C TIPLIED BY EXPANSION AND TESTING FACTORS. *
C*****
INTEGER P,Q
REAL KXI,KYI,KXP,KYQ,KO,K2S
COMPLEX GAM1,GAM2,SI,CO,CJ,K1,K2,C1,C2,C3,C4,C5,C6,FAC4,EPS,
& GXX(*),GYY(*),GXY(*),GYX(*)
PI=3.141592654
TPI=6.283185308
ZO=377.
CJ=CMPLX(0.,1.)
HDX=TX/FLOAT(2*NX)
HDY=TY/FLOAT(2*NY)
IJ=3
C....BEGIN TO GENERATE ELEMENTS
K=0
DO 100 J=1,NY
DO 100 I=1,NX
K=K+1
GXX(K)=(0.,0.)
GYY(K)=(0.,0.)
GXY(K)=(0.,0.)
GYX(K)=(0.,0.)
IF(J.LE.NY/2) THEN
Q=J-1
ELSE
Q=-NY-1+J
END IF
IF(I.LE.NX/2) THEN
P=I-1
ELSE
P=-NX-1+I
END IF
DO 90 JV=-IJ,IJ
DO 90 IU=-IJ,IJ
KXP=KXI+TPI*FLOAT(P+IU*NX)/TX
KYQ=KYI+TPI*FLOAT(Q+JV*NY)/TY
BETA2=KXP*KXP+KYQ*KYQ
K1=CSQRT(EPS*KO*KO-BETA2)
K1=CMPLX(REAL(K1),-AIMAG(K1))
K2S=KO*KO-BETA2
IF(K2S.GE.0.0) THEN
K2=SQRT(K2S)
ELSE
K2=-1.0*CJ*SQRT(ABS(K2S))
END IF
IF(ABS(K1*D).LE.80.) THEN
SI=CSIN(K1*D)
CO=CCOS(K1*D)
GAM1=(EPS*K2*SI-CJ*K1*CO)/(EPS*K2*CO+CJ*K1*SI)
GAM2=(K2*CO+CJ*K1*SI)/(K2*SI-CJ*K1*CO)
ELSE
GAM1=-CJ
GAM2=CJ
KXP=TPI*FLOAT(P+IU*NX)/TX
KYQ=TPI*FLOAT(Q+JV*NY)/TY

```

```

END IF
IF(KXP.EQ.0.) THEN
SINCX=1.
ELSE
SINCX=SIN(KXP*HDX)/(KXP*HDX)
END IF
IF(KYQ.EQ.0.) THEN
SINCY=1.
ELSE
SINCY=SIN(KYQ*HDY)/(KYQ*HDY)
END IF
FAC=SINCX*SINCX+SINCY*SINCY
FAC1=FAC+SINCX*SINCX
FAC2=FAC+SINCY*SINCY
FAC3=FAC+SINCX*SINCY
FAC4=CEXP(CJ*(KXP*HDX-KYQ*HDY))
IF(BETA2.EQ.0.0) THEN
GXX(K)=GXX(K)-ZO/(1.0+CJ*CSQRT(EPS)*GAM1)*FAC1
GYY(K)=GYY(K)-ZO/(1.0+CJ*CSQRT(EPS)*GAM1)*FAC2
ELSE
Z1=ZO/(KO*BETA2)
C1=CJ*K1*K2*KXP*KXP/(EPS*K2*GAM1-CJ*K1)
C2=KYQ*KYQ*KO*KO/(CJ*K1*GAM2-K2)
C3=CJ*K1*K2*KYQ*KYQ/(EPS*K2*GAM1-CJ*K1)
C4=KXP*KXP*KO*KO/(CJ*K1*GAM2-K2)
C5=CJ*K1*K2*KXP*KYQ/(EPS*K2*GAM1-CJ*K1)
C6=KXP*KYQ*KO*KO/(CJ*K1*GAM2-K2)
GXX(K)=GXX(K)+Z1*(C1+C2)*FAC1
GYY(K)=GYY(K)+Z1*(C3+C4)*FAC2
GXY(K)=GXY(K)+Z1*(C5-C6)*FAC3+FAC4
GYI(K)=GYI(K)+Z1*(C5-C6)*FAC3*CONJG(FAC4)
END IF
90 CONTINUE
100 CONTINUE
RETURN
END

```

```

C*****C
C  THIS SUBROUTINE CALCULATES THE EUCLIDIAN NORM OF A VECTOR  C
C*****C
      REAL    FUNCTION VNORM(A,B,N,SG1,SG2)
      COMPLEX A(N),B(N)
      INTEGER SG1(N),SG2(N)
      SUM=0.
      DO 10 I=1,N
      IF(SG1(I).EQ.1) THEN
      SUM=SUM+CABS(A(I))**2
      ELSE
      END IF
      IF(SG2(I).EQ.1) THEN
      SUM=SUM+CABS(B(I))**2
      ELSE
      END IF
10  CONTINUE
      VNORM=SUM
      RETURN
      END

      SUBROUTINE PRODUCT(A,GX,GY,X,Y,N)
      COMPLEX A(*),GX(*),GY(*),X(*),Y(*)
      DO I=1,N
      A(I)=GX(I)*X(I)+GY(I)*Y(I)
      ENDDO
      RETURN
      END

      SUBROUTINE CPRODUCT(A,GX,GY,X,Y,N)
      COMPLEX A(*),GX(*),GY(*),X(*),Y(*)
      DO I=1,N
      A(I)=CONJG(GX(I))*X(I)+CONJG(GY(I))*Y(I)
      ENDDO
      RETURN
      END

```



```

C*****C
C          FOURIER TRANSFORM VIA FFT          C
C*****C
C          PARAMETER DESCRIPTION
C=====C
C      Z.....DATA IN SPATIAL DOMAIN; SIZE M  C
C      ZT.....DATA IN SPECTRAL DOMAIN; SIZE N C
C=====C
      SUBROUTINE SPECTRA(Z,ZT,MZ,NZ,ISIGN,MF,NF,IFFT)
      INTEGER      N(2),NF(4)
      COMPLEX      Z(*),ZT(*)

      IF(IFFT.EQ.1) CALL SPECT1(Z,ZT,MZ,NZ,ISIGN)
      IF(IFFT.EQ.2) CALL SPECT2(Z,ZT,MZ,NZ,ISIGN,MF,NF)

      RETURN
      END

      SUBROUTINE SPECT1(Z,ZT,MZ,NZ,ISIGN)
C.....CALL THE ORDINARY FFT ALGORITHM
      INTEGER      N(2)
      COMPLEX      Z(*),ZT(*)

      N(1) = MZ
      N(2) = NZ
      NT = MZ*NZ

C      |-----|
C      | FORWARD FOURIER TRANSFORM |
C      |-----|

      IF(ISIGN.EQ.-1) THEN
        DO K=1,NT
          ZT(K)=Z(K)
        ENDDO
        CALL FFTN(ZT,N,2,-1)
C      |-----|
C      | INVERSE FOURIER TRANSFORM |
C      |-----|

      ELSE
        DO J=1,NT
          Z(J)=ZT(J)
        ENDDO
        CALL FFTN(Z,N,2,1)
      END IF
      RETURN
      END

      SUBROUTINE SPECT2(Z,ZT,MZ,NZ,ISIGN,MF,NF)
C.....CALL THE PRIME FACTOR FFT ALGORITHM
      INTEGER      NF(4)
      COMPLEX      Z(*),ZT(*)
      REAL X(1024),Y(1024)

      NT = MZ*NZ
      LP=MZ-2

```

```

C -----
C | FORWARD FOURIER TRANSFORM |
C -----

      IF(ISIGN.EQ.-1) THEN
        DO K=1,NT
          X(K)=REAL(Z(K))
          Y(K)=AIMAG(Z(K))
        ENDDO
        CALL PFFFT2(MZ,LP,MF,WF,X,Y,ISIGN)
        DO K=1,NT
          ZT(K)=CMPLX(X(K),Y(K))
        ENDDO

C -----
C | INVERSE FOURIER TRANSFORM |
C -----

      ELSE
        DO K=1,NT
          X(K)=REAL(ZT(K))
          Y(K)=AIMAG(ZT(K))
        ENDDO
        CALL PFFFT2(MZ,LP,MF,WF,X,Y,ISIGN)
        DO K=1,NT
          Z(K)=CMPLX(X(K),Y(K))
        ENDDO
      END IF
      RETURN
      END

```

```

      SUBROUTINE COEFF(CUX,CUY,SGX,SGY,NX,NY,KXI,KYI,KO,EPS,D,TX,TY,TH,
&
&      PH,IFLAG)
C*****
C   THIS SUBROUTINE COMPUTES REFLECTION AND TRANSMISSION COEFFICIENTS*
C   OF THE INFINITE ARRAY USING THE COMPUTED CURRENT *
C*****
      INTEGER SGX(*),SGY(*)
      REAL KXI,KYI,KO,K2S
      COMPLEX GAM1,GAM2,SI,CO,CJ,K1,K2,Z1,C1,C2,C3,C4,C5,C6,FAC3,FAC4,
&EPS,GXX,GYY,GXY,GYX,CUX(*),CUY(*),EX,EY,SCUX,SCUY,EXT,EYT,EXR,EYR
      DATA TPI,RAD/.6283185E+01,.1745329E-01/
      COT=COS(RAD*TH)
      COT2=COT*COT
      PI=3.141592654
      TPI=6.283185308
      ZO=377.
      CJ=CMPLX(0.,1.)
      HDX=TX/FLOAT(2*NX)
      HDY=TY/FLOAT(2*NY)
C.... COMPUTE G_XX, G_YY, G_XY AND G_YX FOR REFLECTED FIELD
      BETA2=KXI*KXI+KYI*KYI
      K1=CSQRT(EPS*KO*KO-BETA2)
      K1=CMPLX(REAL(K1),-AIMAG(K1))
      K2S=KO*KO-BETA2
      IF(K2S.GE.0.0) THEN
      K2=SQRT(K2S)
      ELSE
      K2=-1.0+CJ*SQRT(ABS(K2S))
      END IF
      IF(ABS(K1*D).LE.80.) THEN
      SI=CSIN(K1*D)
      CO=CCOS(K1*D)
      GAM1=(EPS*K2+SI-CJ*K1*CO)/(EPS*K2+CO+CJ*K1*SI)
      GAM2=(K2*CO+CJ*K1*SI)/(K2*SI-CJ*K1*CO)
      ELSE
      GAM1=-CJ
      GAM2=CJ
      END IF
      IF(BETA2.EQ.0.0) THEN
      GXX=-ZO/(1.0+CJ*CSQRT(EPS)*GAM1)
      GYY=-ZO/(1.0+CJ*CSQRT(EPS)*GAM1)
      GXY=(0.,0.)
      GYX=(0.,0.)
      ELSE
      Z1=ZO/(KO*BETA2)
      C1=CJ*K1*K2*KXI*KXI/(EPS*K2+GAM1-CJ*K1)
      C2=KYI*KYI*KO*KO/(CJ*K1+GAM2-K2)
      C3=CJ*K1*K2*KYI*KYI/(EPS*K2+GAM1-CJ*K1)
      C4=KXI*KXI*KO*KO/(CJ*K1+GAM2-K2)
      C5=CJ*K1*K2*KXI*KYI/(EPS*K2+GAM1-CJ*K1)
      C6=KXI*KYI*KO*KO/(CJ*K1+GAM2-K2)
      GXX=Z1*(C1+C2)
      GYY=Z1*(C3+C4)
      GXY=Z1*(C5-C6)
      GYX=Z1*(C5-C6)
      END IF
C.... COMPUTE THE SUMMATION OF THE CURRENT
      NT=NX*NY
      SCUX=(0.,0.)
      SCUY=(0.,0.)

```

```

DO 70 I = 1,NT
  IF(SGX(I).EQ.1) THEN
    SCUX = SCUX+CUX(I)
  ELSE
    END IF
  IF(SGY(I).EQ.1) THEN
    SCUY = SCUY+CUY(I)
  ELSE
    END IF
70 CONTINUE
C.....COMPUTE REFLECTED FIELD
EX=(GXX+SCUX+GXY+SCUY)/NT
EY=(GYX+SCUX+GY+SCUY)/NT
CALL REFL(IFLAG,KO,EPS,D,PH,TH,EXR,EYR)
IF(IFLAG.EQ.1) THEN
  SEX=CABS(EX+EXR)**2
  SEY=CABS(EY+EYR)**2
ELSE
  SEX=CABS(EX/COT+EXR)**2
  SEY=CABS(EY/COT+EYR)**2
END IF
R=SEX+SEY
C.....COMPUTE G_XX, G_YY, G_XY AND G_YX FOR TRANSMITTED FIELD
IF(BETA2.EQ.0.0) THEN
  GXX=CJ*ZO*CSQRT(EPS)/(CSQRT(EPS)*GAM1-CJ)/(CJ*SI+CSQRT(EPS)*CO)
  GYY=GXX
  GXY=(0.,0.)
  GYX=(0.,0.)
ELSE
  Z1=ZO/(KO*BETA2)
  C1=CJ*EPS*K1*K2*K2*KXI/(EPS*K2*GAM1-CJ*K1)/(CJ*K1*SI+EPS*K2*CO)
  C2=CJ*K1*KO*KO*KYI/(CJ*K1*GAM2-K2)/(K2*SI-CJ*K1*CO)
  C3=CJ*EPS*K1*K2*K2*KYI/(EPS*K2*GAM1-CJ*K1)/(CJ*K1*SI+EPS*K2*CO)
  C4=CJ*K1*KO*KO*KXI/(CJ*K1*GAM2-K2)/(K2*SI-CJ*K1*CO)
  GXX=Z1*(C1*KXI-C2*KYI)
  GYY=Z1*(C3*KYI-C4*KXI)
  GXY=Z1*(C1*KYI+C2*KXI)
  GYX=Z1*(C1*KYI+C2*KXI)
END IF
C.....COMPUTE TRANSMITTED FIELD
EX=(GXX+SCUX+GXY+SCUY)/NT
EY=(GYX+SCUX+GY+SCUY)/NT
CALL TRANS(IFLAG,KO,EPS,D,PH,TH,EXT,EYT)
IF(IFLAG.EQ.1) THEN
  SEX=CABS(EX+EXT)**2
  SEY=CABS(EY+EYT)**2
ELSE
  SEX=CABS(EX/COT+EXT)**2
  SEY=CABS(EY/COT+EYT)**2
END IF
T=SEX+SEY
DIS=1.-R-T
WRITE(6,90) KO/TPI*30.,R*100.,T*100.
90 FORMAT(//'FREQ(GHz)=' ,F6.2, ' REFL(%)=' ,F8.4, ' TRANS(%)=' ,F8.4)
RETURN
END

```

```

SUBROUTINE REFL(IFLAG,KO,EPS,D,PH,TH,EX,EY)
C*****C
C THIS SUBROUTINE COMPUTES THE REFLECTED FIELD BY SLAB IN ISOLATION C
C*****C
C IFLAG=1 --- TE INCIDENCE (Ez=0) C
C IFLAG=2 --- TM INCIDENCE (Hz=0) C
C*****C
COMPLEX EX,EY,EPS,CJ,CO,C1,C2,C3,C4,R,T
REAL KO,KX,KY
DATA TPI,RAD/.6283185E+01,.1745329E-01/
CJ=CMPLX(0.,1.)
SIP=SIN(RAD*PH)
COP=COS(RAD*PH)
SIT=SIN(RAD*TH)
COT=COS(RAD*TH)
SID=SIN(KO*D*COT)
COD=COS(KO*D*COT)
C1=CSQRT(EPS-SIT*SIT)
C2=CSIN(KO*D*C1)
C3=CCOS(KO*D*C1)
CO=(CJ*C1*C2+COT*C3)/(CJ*C1*C3-COT*C2)
IF(IFLAG.EQ.2) GOTO 10
R=(CJ*COT+CO*C1)/(CJ*COT-CO*C1)*CMPLX(COD,SID)
EX=-SIP*R
EY=COP*R
RETURN
10 CO=(CJ*C1*C2+EPS*COT*C3)/(CJ*C1*C3-EPS*COT*C2)
R=(EPS*COT-CJ*C1*CO)/(EPS*COT+CJ*C1*CO)*CMPLX(COD,SID)
EX=-COP*R
EY=-SIP*R
RETURN
END

```

```

SUBROUTINE TRANS(IFLAG,KO,EPS,D,PH,TH,EX,EY)
C*****C
C THIS SUBROUTINE COMPUTES THE TRANSMITTED FIELD THROUGH THE SLAB IN C
C ISOLATION C
C*****C
C IFLAG=1 --- TE INCIDENCE (Ez=0) C
C IFLAG=2 --- TM INCIDENCE (Hz=0) C
C*****C
COMPLEX EX,EY,EPS,CJ,CO,C1,C2,C3,C4,R,T
REAL KO,KX,KY
DATA TPI,RAD/.6283185E+01,.1745329E-01/
CJ=CMPLX(0.,1.)
SIP=SIN(RAD*PH)
COP=COS(RAD*PH)
SIT=SIN(RAD*TH)
COT=COS(RAD*TH)
SID=SIN(KO*D*COT)
COD=COS(KO*D*COT)
C1=CSQRT(EPS-SIT*SIT)
C2=CSIN(KO*D*C1)
C3=CCOS(KO*D*C1)
CO=(CJ*C1*C2+COT*C3)/(CJ*C1*C3-COT*C2)
IF(IFLAG.EQ.2) GOTO 10
R=(CJ*COT+CO*C1)/(CJ*COT-CO*C1)
T=(1.+R)/(CJ*COT*C2/C1+C3)*CMPLX(COD,SID)
EX=-SIP*T

```

```
EY=COP*T
RETURN
10 CO=(CJ*C1*C2+EPS*COT*C3)/(CJ*C1*C3-EPS*COT*C2)
R=(EPS*COT-CJ*C1*C0)/(EPS*COT+CJ*C1*C0)
T=(1.+R)/(CJ*EPS*COT*C2/C1+C3)*CMPLX(COD,SID)
EX=COP*T
EY=SIP*T
RETURN
END
```

```

      SUBROUTINE FARF(CUX,CUY,SG,NX,NY,KXI,KYI,KO,EPS,D,TX,TY,PH1,PH2,
&      DPH,TH1,TH2,DTH,MX,MY)
C*****
C   THIS SUBROUTINE COMPUTES SCATTERED FIELD OF THE FINITE ARRAY   *
C   ON THE INFINIT SLAB USING THE COMPUTED CURRENT                 *
C*****
      INTEGER SG(*)
      REAL KXI,KYI,KO,KX,KY
      COMPLEX CO,CJ,C1,C2,C3,EPS,CUX(*),CUY(*),PHASE,RTE,RTM,SCUX,SCUY,
&ETH,EPH,TTE,TTM
      DATA TPI,RAD/.6283185E+01,.1745329E-01/
      ZO=377.
      WAVE=TPI/KO

      MPH=INT((PH2-PH1)/DPH)
      MTH=INT((TH2-TH1)/DTH)
      DO 1000 I=0,MPH
      PH=PH1+FLOAT(I)*DPH
      DO 1000 J=0,MTH
      TH=TH1+FLOAT(J)*DTH
      IF(TH.EQ.90.) GOTO 1000

C.....COMPUTE THE REFLECTION COEFFICIENT
      CJ=CMPLX(0.,1.)
      SIP=SIN(RAD*PH)
      COP=COS(RAD*PH)
      SIT=SIN(RAD*TH)
      COT=COS(RAD*TH)
      SID=SIN(KO*D*COT)
      COD=COS(KO*D*COT)
      C1=CSQRT(EPS-SIT*SIT)
      C2=CSIN(KO*D*C1)
      C3=CCOS(KO*D*C1)
      CO=(CJ*C1+C2+COT*C3)/(CJ*C1+C3-COT*C2)
      RTE=(CJ*COT+CO*C1)/(CJ*COT-CO*C1)
      CO=(CJ*C1+C2+EPS*COT*C3)/(CJ*C1+C3-EPS*COT*C2)
      RTM=(EPS*COT-CJ*C1*CO)/(EPS*COT+CJ*C1*CO)
      KX=KO*SIT+COP+KXI
      KY=KO*SIT+SIP+KYI

      IF(TH.LT.90.) GOTO 100

C.....COMPUTE THE TRANSMISSION COEFFICIENT
      TTE=(1.+RTE)/(CJ*COT+C2/C1+C3)
      TTM=(1.+RTM)/(CJ*EPS*COT+C2/C1+C3)

100 CONTINUE
C.....INTEGRATE THE PATCH CURRENT
      SCUX=(0.,0.)
      SCUY=(0.,0.)
      DX=TX/NX
      DY=TY/NY
      XO=-0.5*TX+0.5*DX
      YO=-0.5*TY+0.5*DY
      K=0
      DO JJ=1,NY
      Y=YO+FLOAT(JJ-1)*DY
      DO II=1,NX
      X=XO+FLOAT(II-1)*DX
      K=K+1
      IF(SG(K).EQ.1) THEN

```

```

        PHASE=CEXP(CJ*(X*KX+Y*KY))
        SCUX=SCUX+0.5*(CUX(K)+CUX(K-1))*PHASE
        SCUY=SCUY+0.5*(CUY(K)+CUY(K-NX))*PHASE
    ELSE
    END IF
ENDDO
ENDDO
SCUX=SCUX+DX*DY
SCUY=SCUY+DY*DY

C.....ELEMENTARY PATTERN
IF(TH.GT.90.) GOTO 200
ETH=CJ*KO*ZO*(1.-RTM)/(2.*TPI)*(COT*COP*SCUX+COT*SIP*SCUY)
EPH=CJ*KO*ZO*(1.+RTE)/(2.*TPI)*(-SIP*SCUX+COP*SCUY)
GOTO 300
200 ETH=CJ*KO*ZO*TTM/(2.*TPI)*(COT*COP*SCUX+COT*SIP*SCUY)
    EPH=CJ*KO*ZO*TTE/(2.*TPI)*(-SIP*SCUX+COP*SCUY)

300 CONTINUE
C.....ARRAY FACTOR
IF(KX.EQ.0.) THEN
    FACX=FLOAT(MX)
ELSE
    FACX=SIN(0.5*FLOAT(MX)*TX*KX)/SIN(0.5*TX*KX)
END IF
IF(KY.EQ.0.) THEN
    FACY=FLOAT(MY)
ELSE
    FACY=SIN(0.5*FLOAT(MY)*TY*KY)/SIN(0.5*TY*KY)
END IF
FAC=FACX*FACY

C.....SCATTERING CROSS SECTION
SIGMA=2.*TPI*(CABS(ETH)**2+CABS(EPH)**2)*FAC*FAC
SIGMA=10.*LOG10(SIGMA/WAVE/WAVE)
SIGMA1=2.*TPI*(CABS(ETH)**2+CABS(EPH)**2)
SIGMA1=10.*LOG10(SIGMA1/WAVE/WAVE)
WRITE(6,90) PH,TH,SIGMA,SIGMA1
90  FORMAT(4G13.4)
1000 CONTINUE
RETURN
END

```



```

SUBROUTINE FAFSFF(CUX,CUY,SG,IX,MY,PHINC,THINC,KO,EPS,D,TX,TY,PH1,
&
PH2,DPH,TH1,TH2,DTH,MY,A,B,IPOL)
C*****
C THIS SUBROUTINE COMPUTES SCATTERED FIELD OF THE FINITE ARRAY *
C ON A FINITE SLAB THROUGH A SUPERPOSITION OF THE FIELD RADIATED *
C BY THE PATCH CURRENTS AND THE FIELD DIFFRACTED BY THE SLAB EDGES *
C OBTAINED USING THE VOLUME INTEGRAL PHYSICAL OPTICS METHOD. *
C*****
INTEGER SG(*)
REAL KXI,KYI,KO,KX,KY,IX,IY,IT
COMPLEX CO,CJ,C1,C2,C3,C4,EPS,CUX(*),CUY(*),PHASE,RTE,RTM,SCUX,
&SCUY,ETH,EPH,TTE,TTH,JX,JY,JZ,FTHR,FPHR,FTHD,FPHD,AA,BB,
&CC,DD,SIC1,COC1,SIC2,COC2,SIC,COC,JX1,JY1,JZ1,FAC,C11
DATA TPI,RAD/.6283185E+01,.1745329E-01/
CJ=CMPLX(0.,1.)
ZO=377.
WAVE=TPI/KO

C....CALCULATE THE REFLECTLECTION COEFFICIENTS WITH INCIDENT ANGLE
SIP=SIN(RAD*PHINC)
COP=COS(RAD*PHINC)
SIT=SIN(RAD*THINC)
COT=COS(RAD*THINC)
SID=SIN(KO*D*COT)
COD=COS(KO*D*COT)
KXI=KO*SIT*COP
KYI=KO*SIT*SIP
C1=CSQRT(EPS-SIT*SIT)
C11=C1
C2=CSIN(KO*D*C1)
C3=CCOS(KO*D*C1)
CO=(CJ*C1*C2+COT*C3)/(CJ*C1*C3-COT*C2)
RTE=(CJ*COT+CO*C1)/(CJ*COT-CO*C1)
CO=(CJ*C1*C2+EPS*COT*C3)/(CJ*C1*C3-EPS*COT*C2)
RTM=(EPS*COT-CJ*C1*CO)/(EPS*COT+CJ*C1*CO)

C....CALCULATE THE EQUIVALENT POLARIZED CURRENTS
C4=KO*KO/(2.*TPI)*(EPS-1.)
IF(IPOL.EQ.2) GOTO 500
AA=(1.+RTE)/(C2-CJ*C1/COT*C3)*CMPLX(COD,SID)
BB=-CJ*C1/COT*AA
JX1=-C4*SIP
JY1=C4*COP
JZ1=CMPLX(0.,0.)
GOTO 600
500 AA=(1.+RTM)/(C2-CJ*C1/COT/EPS*C3)*CMPLX(COD,SID)
BB=-CJ*C1/COT/EPS*AA
JX1=C4*COP
JY1=C4*SIP
JZ1=-C4
600 CONTINUE

C....START TO COMPUTE THE SCATTERED FAR FIELD AT DIFFERENT ANGLES
NPH=INT((PH2-PH1)/DPH)
NTH=INT((TH2-TH1)/DTH)
DO 1000 I=0,NPH
PH=PH1+FLOAT(I)*DPH
DO 1000 J=0,NTH
TH=TH1+FLOAT(J)*DTH
IF(TH.EQ.90.) GOTO 1000

```

```

C.....COMPUTE THE REFLECTION COEFFICIENTS WITH OBSERVATION ANGLE
  SIP=SIN(RAD*PH)
  COP=COS(RAD*PH)
  SIT=SIN(RAD*TH)
  COT=COS(RAD*TH)
  SID=SIN(KO*D*COT)
  COD=COS(KO*D*COT)
  C1=CSQRT(EPS-SIT*SIT)
  C2=CSIN(KO*D*C1)
  C3=CCOS(KO*D*C1)
  CO=(CJ*C1*C2+COT*C3)/(CJ*C1*C3-COT*C2)
  RTE=(CJ*COT+CO*C1)/(CJ*COT-CO*C1)
  CO=(CJ*C1*C2+EPS*COT*C3)/(CJ*C1*C3-EPS*COT*C2)
  RTM=(EPS*COT-CJ*C1*CO)/(EPS*COT+CJ*C1*CO)
  KX=KO*SIT*COP+KXI
  KY=KO*SIT*SIP+KYI

C.....COMPUTE THE CORRESPONDING TRANSMISSION COEFFICIENTS
  IF(TH.LT.90.) GOTO 100
  TTE=(1.+RTE)/(CJ*COT+C2/C1+C3)
  TTM=(1.+RTM)/(CJ*EPS*COT+C2/C1+C3)
100 CONTINUE

C.....INTEGRATE THE PATCH CURRENTS
  SCUX=(0.,0.)
  SCUY=(0.,0.)
  DX=TX/NX
  DY=TY/NY
  X0=-0.5*TX+0.5*DX
  Y0=-0.5*TY+0.5*DY
  K=0
  DO JJ=1,NY
  Y=Y0+FLOAT(JJ-1)*DY
  DO II=1,NX
  X=X0+FLOAT(II-1)*DX
  K=K+1
  IF(SG(K).EQ.1) THEN
    PHASE=CEXP(CJ*(X*KX+Y*KY))
    SCUX=SCUX+0.5*(CUX(K)+CUX(K-1))*PHASE
    SCUY=SCUY+0.5*(CUY(K)+CUY(K-NX))*PHASE
  ELSE
    END IF
  ENDDO
  ENDDO
  SCUX=SCUX*DX*DY
  SCUY=SCUY*DX*DY

C.....COMPUTE THE ELEMENTARY PATTERN
  IF(TH.GT.90.) GOTO 200
  ETH=-CJ*KO*ZO*(1.-RTM)/(2.*TPI)*(COT*COP*SCUX+COT*SIP*SCUY)
  EPH=-CJ*KO*ZO*(1.+RTE)/(2.*TPI)*(-SIP*SCUX+COP*SCUY)
  GOTO 300
200 ETH=-CJ*KO*ZO*TTM/(2.*TPI)*(COT*COP*SCUX+COT*SIP*SCUY)
  EPH=-CJ*KO*ZO*TTE/(2.*TPI)*(-SIP*SCUX+COP*SCUY)
300 CONTINUE
  ETH=ETH*CMPLX(C3,C2)
  EPH=EPH*CMPLX(C3,C2)

C.....COMPUTE THE ARRAY FACTOR

```

```

IF(KX.EQ.0.) THEN
FACX=FLOAT(MX)
ELSE
FACX=SIN(0.5*FLOAT(MX)*TX*KX)/SIN(0.5*TX*KX)
END IF
IF(KY.EQ.0.) THEN
FACY=FLOAT(MY)
ELSE
FACY=SIN(0.5*FLOAT(MY)*TY*KY)/SIN(0.5*TY*KY)
END IF
FAC=FACX*FACY*CEXP(CJ*0.5*FLOAT(MX-1)*TX*KX)
&*CEXP(CJ*0.5*FLOAT(MY-1)*TY*KY)

C.....COMPUTE THE FIELD RADIATED BY THE PATCH CURRENTS
FTHR=FAC*ETH
FPHR=FAC*EPH

C.....START TO COMPUTE THE DIFFRACTED FIELD BY THE SLAB
IF(KX.EQ.0.) THEN
IX=A
ELSE
IX=A*SIN(0.5*A*KX)/(0.5*A*KX)
END IF
IF(KY.EQ.0.) THEN
IY=B
ELSE
IY=B*SIN(0.5*B*KY)/(0.5*B*KY)
END IF
IT=IX*IY
C1=C11
SIC1=CSIN(KO*D*(C1+COT))
COC1=CCOS(KO*D*(C1+COT))
SIC2=CSIN(KO*D*(C1-COT))
COC2=CCOS(KO*D*(C1-COT))
SIC=(1.-CMPLX(COC1,SIC1))/(2.*KO*(C1+COT))+
& (1.-CMPLX(COC2,-SIC2))/(2.*KO*(C1-COT))
COC=((1.-CMPLX(COC1,SIC1))/(2.*KO*(C1+COT))-
& (1.-CMPLX(COC2,-SIC2))/(2.*KO*(C1-COT)))*CJ
IF(IPOL.EQ.2) GOTO 700
CC=AA*SIC+BB*COC
JX=JX1+CC
JY=JY1+CC
JZ=0.
GOTO 800
700 CC=CJ*C1/EPS*(AA*COC-BB*SIC)
DD=-SIT/EPS*(AA*SIC+BB*COC)
JX=JX1+CC
JY=JY1+CC
JZ=JZ1+DD
800 CONTINUE
FTHD=(COT*COP*JX+COT*SIP*JY-SIT*JZ)*IT
FPHD=(-SIP*JX+COP*JY)*IT

C.....FIND THE TOTAL SCATTERED FIELD
ETH=FTHR+FTHD
EPH=FPHR+FPHD

C.....SCATTERING CROSS SECTION
SIGMA=2.*TPI*(CABS(ETH)**2+CABS(EPH)**2)
SIGMA=10.*LOG10(SIGMA/WAVE/WAVE)

```

```
SIGMA1=2.*TPI*(CABS(FTHD)**2+CABS(FPHD)**2)
SIGMA1=10.*LOG10(SIGMA1/WAVE/WAVE)
WRITE(6,90) PH,TH,SIGMA,SIGMA1
90 FORMAT(4G13.4)
1000 CONTINUE
RETURN
END
```

```

C *****
C * FFT ROUTINE FOR COMPUTATION OF N DIMENSIONAL FOURIER TRANSFORM *
C * TASKS: 1)BIT REVERSAL 2)TRIGONOMETRIC RECURRENCE 3)TRANSFORM *
C * ALL DONE IN THIS PROGRAM *
C *****
C
C PARAMETER DESCRIPTION
C =====
C DATA.....A REAL ARRAY IN WHICH DATA ARE STORED AS IN
C A MULTIDIMENSIONAL COMPLEX FORTRAN ARRAY
C NDIM.....DIMENSION OF DATA AND THE FFT
C NN.....INTEGER ARRAY OF LENGTH NDIM
C ISIGN.....DIRECTION OF THE TRANSFORM:
C 1 -FORWARD FFT
C -1 -INVERSE FFT TIMES THE PRODUCT OF
C LENGTHS OF ALL DIMENSIONS
C =====
C
C SUBROUTINE FFTN(DATA,NN,NDIM,ISIGN)
C REAL*8 WR,WI,WPR,WPI,WTEMP,THETA
C DIMENSION NN(NDIM),DATA(*)
C NTOT=1
C DO IDIM=1,NDIM
C NTOT=NTOT*NN(IDIM)
C ENDDO
C NPREV=1
C DO IDIM=1,NDIM
C N=NN(IDIM)
C NREM=NTOT/(N*NPREV)
C IP1=2*NPREV
C IP2=IP1*N
C IP3=IP2*NREM
C I2REV=1
C BIT REVERSAL SECTION
C DO I2=1,IP2,IP1
C IF(I2.LT.I2REV)THEN
C DO I1=I2,I2+IP1-2,2
C DO I3=I1,IP3,IP2
C I3REV=I2REV+I3-I2
C TEMPR=DATA(I3)
C TEMPI=DATA(I3+1)
C DATA(I3)=DATA(I3REV)
C DATA(I3+1)=DATA(I3REV+1)
C DATA(I3REV)=TEMPR
C DATA(I3REV+1)=TEMPI
C ENDDO
C ENDDO
C END IF
C IBIT=IP2/2
C IF((IBIT.GE.IP1).AND.(I2REV.GT.IBIT))THEN
C I2REV=I2REV-IBIT
C IBIT=IBIT/2
C GO TO 1
C END IF
C I2REV=I2REV+IBIT
C ENDDO
C DANIELSON-LANCZOS FORMULA
C IFP1=IP1
C IF(IFP1.LT.IP2)THEN
C IFP2=2*IFP1
C THETA=ISIGN*6.28318530717959DO/(IFP2/IP1)
C WPR=-2.DO*DSIN(0.5DO*THETA)**2

```

```

WPI=DSIN(THETA)
WR=1.DO
WI=0.DO
DO I3=1,IFP1,IP1
  DO I1=I3,I3+IP1-2,2
    DO I2=I1,IP3,IFP2
      K1=I2
      K2=K1+IFP1
      TEMPR=SNGL(WR)*DATA(K2)-SNGL(WI)*DATA(K2+1)
      TEMPI=SNGL(WR)*DATA(K2+1)+SNGL(WI)*DATA(K2)
      DATA(K2)=DATA(K1)-TEMPR
      DATA(K2+1)=DATA(K1+1)-TEMPI
      DATA(K1)=DATA(K1)+TEMPR
      DATA(K1+1)=DATA(K1+1)+TEMPI
    ENDDO
  ENDDO
  WTEMP=WR
C  TRIGONOMETRIC RECURRENCE
  WR=WR+WPR-WI*WPI+WR
  WI=WI+WPR+WTEMP+WPI+WI
  ENDDO
  IFP1=IFP2
  GO TO 2
END IF
WPREV=W+WPREV
ENDDO
RETURN
END

```

```

SUBROUTINE PFFFT2(L,LP,M,N,X,Y,SIGN)
C*****C
C THIS SUBROUTINE COMPUTES A TWO - DIMENSIONAL FFT USING C
C A PRIME FACTOR ALGORITHM C
C*****C
C C
C*****C
C ALLOWED FFT DIMENSIONS FROM THE SET (2,3,4,5,7,8,9,16) C
C C
C L=2 L=14 L=36 L=80 L=180 L=560 C
C L=3 L=15 L=40 L=84 L=210 L=630 C
C L=4 L=16 L=42 L=90 L=240 L=720 C
C L=5 L=18 L=45 L=105 L=252 L=840 C
C L=6 L=20 L=48 L=112 L=280 L=1008 C
C L=7 L=21 L=56 L=120 L=315 L=1260 C
C L=8 L=24 L=60 L=126 L=336 L=1680 C
C L=9 L=28 L=63 L=140 L=360 L=2520 C
C L=10 L=30 L=70 L=144 L=420 L=5040 C
C L=12 L=35 L=72 L=168 L=504 C
C C
C*****C
C INPUT VARIABLE DESCRIPTIONS: C
C C
C L - I*4 ROW AND COLUMN DIMENSION OF FFT C
C LP - I*4 ROW WIDTH AND COLUMN WIDTH OF NON-ZERO DATA C
C M - I*4 NUMBER OF PRIME FACTORS C
C N(1:4) - I*4 PRIME FACTORS (MAY BE IN ANY ORDER) C
C X(1:L*L) - R*4 REAL PART OF INPUT C
C Y(1:L*L) - R*4 IMAGINARY PART OF INPUT C
C SIGN - I*4 SIGN=1 FOR FORWARD AND -1 FOR INVERSE TRANSFORM C
C C
C OUTPUT VARIABLE DESCRIPTIONS: C
C C
C X(1:L*L) - R*4 REAL PART OF TRANSFORM C
C Y(1:L*L) - R*4 IMAGINARY PART OF TRANSFORM C
C*****C
REAL X(*),Y(*)
INTEGER N(*),MA(16),MB(16),KI(16),SIGN
DATA C31,C32,C51,C52 /.86602540,.50000000,.95105652,1.5388418/
DATA C53,C54,C55,C71 /.36327126,.55901699,-1.250000,-1.1666667/
DATA C72,C73,C74,C75 /.79015647,.05585427,.7343022,.44095855/
DATA C76,C77,C78,C81 /.34087293,.53396936,.87484229,.70710678/
DATA C92,C93,C94,C96 /.93969262,-.17364818,.76604444,-.34202014/
DATA C97,C98,C162,C163 /-.98480775,-.64278761,.38268343,1.306563/
DATA C164,C165 /.54119610,.92387953/
IF(SIGN .EQ. 1) THEN
DO 1 I=1,L*L
Y(I)=-Y(I)
1 CONTINUE
ELSE
END IF
C*****C
C STEP THROUGH ROW AND COLUMN TRANSFORMS DOING ROWS FIRST AND C
C THEN COLUMNS C
C*****C
IC1=2-L
IC2=2*L-1
DO 2 IRC=1,2
IC1=IC1+L-1
IC2=IC2-L+1

```

```

C*****C
C  STEP THROUGH THE M STEPS C
C*****C
      DO 3 I=1,M
        K=L/N(I)
C*****C
C  COMPUTE THE PERMUTATION OUTPUT MAP FOR THE ROTATED DFTS C
C*****C
      DO 4 II=1,N(I)
        JT=(II-1)*K
        MB(II)=MOD(JT,N(I))+1
4      CONTINUE
C*****C
C  INITIALIZE THE FIRST GROUP OF POINTS AND CALL THE APPROPRIATE DFT C
C*****C
      DO 5 IJ=0,N(I)-1
        KI(MB(IJ+1))=IC2*(IJ*K+1)+1-IC2
5      CONTINUE
        IF ( ((SIGN .EQ. -1) .AND. (IRC .EQ. 1))
          & .OR. ((SIGN .EQ. 1) .AND. (IRC .EQ. 2)) ) THEN
          ILIM=LP+2-1
        ELSE
          ILIM=L-1
        END IF
        IF (N(I) .EQ. 2) GO TO 100
        IF (N(I) .EQ. 3) GO TO 101
        IF (N(I) .EQ. 4) GO TO 102
        IF (N(I) .EQ. 5) GO TO 103
        IF (N(I) .EQ. 7) GO TO 104
        IF (N(I) .EQ. 8) GO TO 105
        IF (N(I) .EQ. 9) GO TO 106
        IF (N(I) .EQ. 16) GO TO 107
100     CONTINUE
C*****C
C  2 POINT DFT C
C*****C
      DO 6 J=1,K
        MA(1)=KI(1)
        MA(2)=KI(2)
        DO 7 IG=0,ILIM
          IO=IG+IC1
          I1=MA(1)+IO
          I2=MA(2)+IO
C*****2-POINT DFT KERNEL*****C
          T1=X(I1)
          X(MA(MB(1))+IO)=T1+X(I2)
          X(MA(MB(2))+IO)=T1-X(I2)
          T1=Y(I1)
          Y(MA(MB(1))+IO)=T1+Y(I2)
          Y(MA(MB(2))+IO)=T1-Y(I2)
C*****C
7      CONTINUE
          KI(1)=MA(2)+IC2
          KI(2)=MA(1)+IC2
6      CONTINUE
          GO TO 998
101    CONTINUE
C*****C
C  3 POINT DFT C
C*****C

```



```

DO 8 J=1,K
MA(1)=KI(1)
MA(2)=KI(2)
MA(3)=KI(3)
DO 9 IG=0,ILIM
IO=IG*IC1
I1=MA(1)+IO
I2=MA(2)+IO
I3=MA(3)+IO
C*****3-POINT DFT KERNEL*****C
T1=(X(I2)-X(I3))*C31
U1=(Y(I2)-Y(I3))*C31
R1=X(I2)+X(I3)
S1=Y(I2)+Y(I3)
T2=X(I1)-R1*C32
U2=Y(I1)-S1*C32
X(MA(MB(1))+IO)=X(I1)+R1
Y(MA(MB(1))+IO)=Y(I1)+S1
X(MA(MB(2))+IO)=T2+U1
Y(MA(MB(2))+IO)=U2-T1
X(MA(MB(3))+IO)=T2-U1
Y(MA(MB(3))+IO)=U2-T1
C*****C
9 CONTINUE
KI(1)=MA(3)+IC2
KI(2)=MA(1)+IC2
KI(3)=MA(2)+IC2
8 CONTINUE
GO TO 998
102 CONTINUE
C*****C
C 4 POINT DFT C
C*****C
DO 10 J=1,K
MA(1)=KI(1)
MA(2)=KI(2)
MA(3)=KI(3)
MA(4)=KI(4)
DO 11 IG=0,ILIM
IO=IG*IC1
I1=MA(1)+IO
I2=MA(2)+IO
I3=MA(3)+IO
I4=MA(4)+IO
C*****4-POINT DFT KERNEL*****C
R1=X(I1)+X(I3)
R2=X(I1)-X(I3)
S1=Y(I1)+Y(I3)
S2=Y(I1)-Y(I3)
R3=X(I2)+X(I4)
R4=X(I2)-X(I4)
S3=Y(I2)+Y(I4)
S4=Y(I2)-Y(I4)
X(MA(MB(1))+IO)=R1+R3
X(MA(MB(3))+IO)=R1-R3
Y(MA(MB(1))+IO)=S1+S3
Y(MA(MB(3))+IO)=S1-S3
X(MA(MB(2))+IO)=R2+S4
X(MA(MB(4))+IO)=R2-S4
Y(MA(MB(2))+IO)=S2-R4

```

```

      Y(MA(MB(4))+I0)=S2+R4
C*****C
11  CONTINUE
      KI(1)=MA(4)+IC2
      KI(2)=MA(1)+IC2
      KI(3)=MA(2)+IC2
      KI(4)=MA(3)+IC2
10  CONTINUE
      GO TO 998
103 CONTINUE
C*****C
C 5 POINT DFT C
C*****C
      DO 12 J=1,K
      MA(1)=KI(1)
      MA(2)=KI(2)
      MA(3)=KI(3)
      MA(4)=KI(4)
      MA(5)=KI(5)
      DO 13 IG=0,ILIM
      IO=IG*IC1
      I1=MA(1)+IO
      I2=MA(2)+IO
      I3=MA(3)+IO
      I4=MA(4)+IO
      I5=MA(5)+IO
C*****5-POINT DFT KERNEL*****C
      R1=X(I2)+X(I5)
      R2=X(I2)-X(I5)
      S1=Y(I2)+Y(I5)
      S2=Y(I2)-Y(I5)
      R3=X(I3)+X(I4)
      R4=X(I3)-X(I4)
      S3=Y(I3)+Y(I4)
      S4=Y(I3)-Y(I4)
      T1=(R2+R4)*C51
      U1=(S2+S4)*C51
      R2=T1-R2*C52
      S2=U1-S2*C52
      R4=T1-R4*C53
      S4=U1-S4*C53
      T1=(R1-R3)*C54
      U1=(S1-S3)*C54
      T2=R1+R3
      U2=S1+S3
      X(MA(MB(1))+I0)=X(I1)+T2
      Y(MA(MB(1))+I0)=Y(I1)+U2
      T2=X(MA(MB(1))+I0)+T2*C55
      U2=Y(MA(MB(1))+I0)+U2*C55
      R1=T2+T1
      R3=T2-T1
      S1=U2+U1
      S3=U2-U1
      X(MA(MB(2))+I0)=R1+S4
      X(MA(MB(5))+I0)=R1-S4
      Y(MA(MB(2))+I0)=S1-R4
      Y(MA(MB(5))+I0)=S1+R4
      X(MA(MB(3))+I0)=R3-S2
      X(MA(MB(4))+I0)=R3+S2
      Y(MA(MB(3))+I0)=S3+R2

```

```

      Y(MA(MB(4))+I0)=S3-R2
C*****C
13  CONTINUE
      KI(1)=MA(5)+IC2
      KI(2)=MA(1)+IC2
      KI(3)=MA(2)+IC2
      KI(4)=MA(3)+IC2
      KI(5)=MA(4)+IC2
12  CONTINUE
      GO TO 998
104 CONTINUE
C*****C
C   7 POINT DFT                               C
C*****C
      DO 14 J=1,K
      MA(1)=KI(1)
      MA(2)=KI(2)
      MA(3)=KI(3)
      MA(4)=KI(4)
      MA(5)=KI(5)
      MA(6)=KI(6)
      MA(7)=KI(7)
      DO 15 IG=0,ILIM
      IO=IG*IC1
      I1=MA(1)+IO
      I2=MA(2)+IO
      I3=MA(3)+IO
      I4=MA(4)+IO
      I5=MA(5)+IO
      I6=MA(6)+IO
      I7=MA(7)+IO
C*****7-POINT DFT KERNAL*****C
      R1=X(I2)+X(I7)
      R2=X(I2)-X(I7)
      S1=Y(I2)+Y(I7)
      S2=Y(I2)-Y(I7)
      R3=X(I3)+X(I6)
      R4=X(I3)-X(I6)
      S3=Y(I3)+Y(I6)
      S4=Y(I3)-Y(I6)
      R5=X(I4)+X(I5)
      R6=X(I4)-X(I5)
      S5=Y(I4)+Y(I5)
      S6=Y(I4)-Y(I5)
      T1=R1+R3+R5
      U1=S1+S3+S5
      X(MA(MB(1))+I0)=X(I1)+T1
      Y(MA(MB(1))+I0)=Y(I1)+U1
      T1=X(MA(MB(1))+I0)+T1*C71
      U1=Y(MA(MB(1))+I0)+U1*C71
      T2=(R1-R5)*C72
      U2=(S1-S5)*C72
      T3=(R5-R3)*C73
      U3=(S5-S3)*C73
      T4=(R3-R1)*C74
      U4=(S3-S1)*C74
      R1=T1+T2+T3
      R3=T1-T2-T4
      R5=T1-T3+T4
      S1=U1+U2+U3

```

```

S3=U1-U2-U4
S5=U1-U3+U4
U1=(S2+S4-S6)*C75
T1=(R2+R4-R6)*C75
T2=(R2+R6)*C76
U2=(S2+S6)*C76
T3=(R4+R6)*C77
U3=(S4+S6)*C77
T4=(R4-R2)*C78
U4=(S4-S2)*C78
R2=T1+T2+T3
R4=T1-T2-T4
R6=T1-T3+T4
S2=U1+U2+U3
S4=U1-U2-U4
S6=U1-U3+U4
X(MA(MB(2))+IO)=R1+S2
X(MA(MB(7))+IO)=R1-S2
Y(MA(MB(2))+IO)=S1-R2
Y(MA(MB(7))+IO)=S1+R2
X(MA(MB(3))+IO)=R3+S4
X(MA(MB(6))+IO)=R3-S4
Y(MA(MB(3))+IO)=S3-R4
Y(MA(MB(6))+IO)=S3+R4
X(MA(MB(4))+IO)=R5-S6
X(MA(MB(5))+IO)=R5+S6
Y(MA(MB(4))+IO)=S5+R6
Y(MA(MB(5))+IO)=S5-R6
C*****C
15  CONTINUE
    KI(1)=MA(7)+IC2
    KI(2)=MA(1)+IC2
    KI(3)=MA(2)+IC2
    KI(4)=MA(3)+IC2
    KI(5)=MA(4)+IC2
    KI(6)=MA(5)+IC2
    KI(7)=MA(6)+IC2
14  CONTINUE
    GO TO 998
105 CONTINUE
C*****C
C  8 POINT DFT  C
C*****C
DO 16 J=1,K
  MA(1)=KI(1)
  MA(2)=KI(2)
  MA(3)=KI(3)
  MA(4)=KI(4)
  MA(5)=KI(5)
  MA(6)=KI(6)
  MA(7)=KI(7)
  MA(8)=KI(8)
DO 17 IG=0,ILIM
  IO=IG+IC1
  I1=MA(1)+IO
  I2=MA(2)+IO
  I3=MA(3)+IO
  I4=MA(4)+IO
  I5=MA(5)+IO
  I6=MA(6)+IO

```

```

I7=MA(7)+I0
I8=MA(8)+I0
C*****8-POINT DFT KERNEL*****C
R1=X(I1)+X(I5)
R2=X(I1)-X(I5)
S1=Y(I1)+Y(I5)
S2=Y(I1)-Y(I5)
R3=X(I2)+X(I8)
R4=X(I2)-X(I8)
S3=Y(I2)+Y(I8)
S4=Y(I2)-Y(I8)
R5=X(I3)+X(I7)
R6=X(I3)-X(I7)
S5=Y(I3)+Y(I7)
S6=Y(I3)-Y(I7)
R7=X(I4)+X(I6)
R8=X(I4)-X(I6)
S7=Y(I4)+Y(I6)
S8=Y(I4)-Y(I6)
T1=R1+R5
T2=R1-R5
U1=S1+S5
U2=S1-S5
T3=R3+R7
R3=(R3-R7)*C81
U3=S3+S7
S3=(S3-S7)*C81
T4=R4-R8
R4=(R4+R8)*C81
U4=S4-S8
S4=(S4+S8)*C81
T5=R2+R3
T6=R2-R3
U5=S2+S3
U6=S2-S3
T7=R4+R6
T8=R4-R6
U7=S4+S6
U8=S4-S6
X(MA(MB(1))+I0)=T1+T3
X(MA(MB(5))+I0)=T1-T3
Y(MA(MB(1))+I0)=U1+U3
Y(MA(MB(5))+I0)=U1-U3
X(MA(MB(2))+I0)=T5+U7
X(MA(MB(8))+I0)=T5-U7
Y(MA(MB(2))+I0)=U5-T7
Y(MA(MB(8))+I0)=U5+T7
X(MA(MB(3))+I0)=T2+U4
X(MA(MB(7))+I0)=T2-U4
Y(MA(MB(3))+I0)=U2-T4
Y(MA(MB(7))+I0)=U2+T4
X(MA(MB(4))+I0)=T6+U8
X(MA(MB(6))+I0)=T6-U8
Y(MA(MB(4))+I0)=U6-T8
Y(MA(MB(6))+I0)=U6+T8
17 CONTINUE
C*****C
KI(1)=MA(8)+IC2
KI(2)=MA(1)+IC2
KI(3)=MA(2)+IC2

```

```

      KI(4)=MA(3)+IC2
      KI(5)=MA(4)+IC2
      KI(6)=MA(5)+IC2
      KI(7)=MA(6)+IC2
      KI(8)=MA(7)+IC2
16   CONTINUE
      GO TO 998
106  CONTINUE
C*****C
C   9 POINT DFT C
C*****C
      DO 18 J=1,K
      MA(1)=KI(1)
      MA(2)=KI(2)
      MA(3)=KI(3)
      MA(4)=KI(4)
      MA(5)=KI(5)
      MA(6)=KI(6)
      MA(7)=KI(7)
      MA(8)=KI(8)
      MA(9)=KI(9)
      DO 19 IG=0,ILIM
      IO=IG*IC1
      I1=MA(1)+IO
      I2=MA(2)+IO
      I3=MA(3)+IO
      I4=MA(4)+IO
      I5=MA(5)+IO
      I6=MA(6)+IO
      I7=MA(7)+IO
      I8=MA(8)+IO
      I9=MA(9)+IO
C*****9-POINT DFT KERNAL*****C
      R1=X(I2)+X(I9)
      R2=X(I2)-X(I9)
      S1=Y(I2)+Y(I9)
      S2=Y(I2)-Y(I9)
      R3=X(I3)+X(I8)
      R4=X(I3)-X(I8)
      S3=Y(I3)+Y(I8)
      S4=Y(I3)-Y(I8)
      R5=X(I4)+X(I7)
      T=(X(I7)-X(I4))*C31
      S5=Y(I4)+Y(I7)
      U=(Y(I7)-Y(I4))*C31
      R7=X(I5)+X(I6)
      R8=X(I5)-X(I6)
      S7=Y(I5)+Y(I6)
      S8=Y(I5)-Y(I6)
      R9=X(I1)+R5
      S9=Y(I1)+S5
      T1=X(I1)-R5*C32
      U1=Y(I1)-S5*C32
      T2=(R3-R7)*C92
      U2=(S3-S7)*C92
      T3=(R1-R7)*C93
      U3=(S1-S7)*C93
      T4=(R1-R3)*C94
      U4=(S1-S3)*C94
      R10=R1+R3+R7

```

```

S10=S1+S3+S7
R1=T1+T2+T4
R3=T1-T2-T3
R7=T1+T3-T4
S1=U1+U2+U4
S3=U1-U2-U3
S7=U1+U3-U4
X(MA(MB(1))+IO)=R9+R10
Y(MA(MB(1))+IO)=S9+S10
R5=R9-R10*C32
S5=S9-S10*C32
R6=(R4-R2-R8)*C31
S6=(S4-S2-S8)*C31
T2=(R4+R8)*C96
U2=(S4+S8)*C96
T3=(R2-R8)*C97
U3=(S2-S8)*C97
T4=(R2+R4)*C98
U4=(S2+S4)*C98
R2=T+T2+T4
R4=T-T2-T3
R8=T+T3-T4
S2=U+U2+U4
S4=U-U2-U3
S8=U+U3-U4
X(MA(MB(2))+IO)=R1-S2
X(MA(MB(9))+IO)=R1+S2
Y(MA(MB(2))+IO)=S1+R2
Y(MA(MB(9))+IO)=S1-R2
X(MA(MB(3))+IO)=R3+S4
X(MA(MB(8))+IO)=R3-S4
Y(MA(MB(3))+IO)=S3-R4
Y(MA(MB(8))+IO)=S3+R4
X(MA(MB(4))+IO)=R5-S6
X(MA(MB(7))+IO)=R5+S6
Y(MA(MB(4))+IO)=S5+R6
Y(MA(MB(7))+IO)=S5-R6
X(MA(MB(5))+IO)=R7-S8
X(MA(MB(6))+IO)=R7+S8
Y(MA(MB(5))+IO)=S7+R8
Y(MA(MB(6))+IO)=S7-R8
C*****C
19  CONTINUE
    KI(1)=MA(9)+IC2
    KI(2)=MA(1)+IC2
    KI(3)=MA(2)+IC2
    KI(4)=MA(3)+IC2
    KI(5)=MA(4)+IC2
    KI(6)=MA(5)+IC2
    KI(7)=MA(6)+IC2
    KI(8)=MA(7)+IC2
    KI(9)=MA(8)+IC2
18  CONTINUE
    GO TO 998
107 CONTINUE
C*****C
C  16 POINT DFT C
C*****C
    DO 20 J=1,K
      MA(1)=KI(1)

```

```

MA(2)=KI(2)
MA(3)=KI(3)
MA(4)=KI(4)
MA(5)=KI(5)
MA(6)=KI(6)
MA(7)=KI(7)
MA(8)=KI(8)
MA(9)=KI(9)
MA(10)=KI(10)
MA(11)=KI(11)
MA(12)=KI(12)
MA(13)=KI(13)
MA(14)=KI(14)
MA(15)=KI(15)
MA(16)=KI(16)
DO 21 IG=0,ILIM
  IO=IG*IC1
  I1=MA(1)+IO
  I2=MA(2)+IO
  I3=MA(3)+IO
  I4=MA(4)+IO
  I5=MA(5)+IO
  I6=MA(6)+IO
  I7=MA(7)+IO
  I8=MA(8)+IO
  I9=MA(9)+IO
  I10=MA(10)+IO
  I11=MA(11)+IO
  I12=MA(12)+IO
  I13=MA(13)+IO
  I14=MA(14)+IO
  I15=MA(15)+IO
  I16=MA(16)+IO

```

C*****16-POINT DFT KERNEL*****C

```

R1=X(I1)+X(I9)
R2=X(I1)-X(I9)
S1=Y(I1)+Y(I9)
S2=Y(I1)-Y(I9)
R3=X(I2)+X(I10)
R4=X(I2)-X(I10)
S3=Y(I2)+Y(I10)
S4=Y(I2)-Y(I10)
R5=X(I3)+X(I11)
R6=X(I3)-X(I11)
S5=Y(I3)+Y(I11)
S6=Y(I3)-Y(I11)
R7=X(I4)+X(I12)
R8=X(I4)-X(I12)
S7=Y(I4)+Y(I12)
S8=Y(I4)-Y(I12)
R9=X(I5)+X(I13)
R10=X(I5)-X(I13)
S9=Y(I5)+Y(I13)
S10=Y(I5)-Y(I13)
R11=X(I6)+X(I14)
R12=X(I6)-X(I14)
S11=Y(I6)+Y(I14)
S12=Y(I6)-Y(I14)
R13=X(I7)+X(I15)
R14=X(I7)-X(I15)

```


$S13=Y(I7)+Y(I15)$
 $S14=Y(I7)-Y(I15)$
 $R15=X(I8)+X(I16)$
 $R16=X(I8)-X(I16)$
 $S15=Y(I8)+Y(I16)$
 $S16=Y(I8)-Y(I16)$
 $T1=R1+R9$
 $T2=R1-R9$
 $U1=S1+S9$
 $U2=S1-S9$
 $T3=R3+R11$
 $T4=R3-R11$
 $U3=S3+S11$
 $U4=S3-S11$
 $T5=R5+R13$
 $T6=R5-R13$
 $U5=S5+S13$
 $U6=S5-S13$
 $T7=R7+R15$
 $T8=R7-R15$
 $U7=S7+S15$
 $U8=S7-S15$
 $T9=(T4+T8)*C81$
 $T10=(T4-T8)*C81$
 $U9=(U4+U8)*C81$
 $U10=(U4-U8)*C81$
 $R1=T1+T5$
 $R3=T1-T5$
 $S1=U1+U5$
 $S3=U1-U5$
 $R5=T3+T7$
 $R7=T3-T7$
 $S5=U3+U7$
 $S7=U3-U7$
 $R9=T2+T10$
 $R11=T2-T10$
 $S9=U2+U10$
 $S11=U2-U10$
 $R13=T6+T9$
 $R15=T6-T9$
 $S13=U6+U9$
 $S15=U6-U9$
 $T1=R4+R16$
 $T2=R4-R16$
 $U1=S4+S16$
 $U2=S4-S16$
 $T3=(R6+R14)*C81$
 $T4=(R6-R14)*C81$
 $U3=(S6+S14)*C81$
 $U4=(S6-S14)*C81$
 $T5=R8+R12$
 $T6=R8-R12$
 $U5=S8+S12$
 $U6=S8-S12$
 $T7=(T2-T6)*C162$
 $T8=T2*C163-T7$
 $T9=T6*C164-T7$
 $T10=R2+T4$
 $T11=R2-T4$
 $R2=T10+T8$

$R4=T10-T8$
 $R6=T11+T9$
 $R8=T11-T9$
 $U7=(U2-U6)*C162$
 $U8=U2+C163-U7$
 $U9=U6+C164-U7$
 $U10=S2+U4$
 $U11=S2-U4$
 $S2=U10+U8$
 $S4=U10-U8$
 $S6=U11+U9$
 $S8=U11-U9$
 $T7=(T1+T5)*C165$
 $T8=T7-T1+C164$
 $T9=T7-T5*C163$
 $T10=R10+T3$
 $T11=R10-T3$
 $R10=T10+T8$
 $R12=T10-T8$
 $R14=T11+T9$
 $R16=T11-T9$
 $U7=(U1+U5)*C165$
 $U8=U7-C164*U1$
 $U9=U7-C163*U5$
 $U10=S10+U3$
 $U11=S10-U3$
 $S10=U10+U8$
 $S12=U10-U8$
 $S14=U11+U9$
 $S16=U11-U9$
 $X(MA(MB(1))+IO)=R1+R5$
 $X(MA(MB(9))+IO)=R1-R5$
 $Y(MA(MB(1))+IO)=S1+S5$
 $Y(MA(MB(9))+IO)=S1-S5$
 $X(MA(MB(2))+IO)=R2+S10$
 $X(MA(MB(16))+IO)=R2-S10$
 $Y(MA(MB(2))+IO)=S2-R10$
 $Y(MA(MB(16))+IO)=S2+R10$
 $X(MA(MB(3))+IO)=R9+S13$
 $X(MA(MB(15))+IO)=R9-S13$
 $Y(MA(MB(3))+IO)=S9-R13$
 $Y(MA(MB(15))+IO)=S9+R13$
 $X(MA(MB(4))+IO)=R8-S16$
 $X(MA(MB(14))+IO)=R8+S16$
 $Y(MA(MB(4))+IO)=S8+R16$
 $Y(MA(MB(14))+IO)=S8-R16$
 $X(MA(MB(5))+IO)=R3+S7$
 $X(MA(MB(13))+IO)=R3-S7$
 $Y(MA(MB(5))+IO)=S3-R7$
 $Y(MA(MB(13))+IO)=S3+R7$
 $X(MA(MB(6))+IO)=R6+S14$
 $X(MA(MB(12))+IO)=R6-S14$
 $Y(MA(MB(6))+IO)=S6-R14$
 $Y(MA(MB(12))+IO)=S6+R14$
 $X(MA(MB(7))+IO)=R11-S15$
 $X(MA(MB(11))+IO)=R11+S15$
 $Y(MA(MB(7))+IO)=S11+R15$
 $Y(MA(MB(11))+IO)=S11-R15$
 $X(MA(MB(8))+IO)=R4-S12$
 $X(MA(MB(10))+IO)=R4+S12$

```

      Y(MA(MB(8))+I0)=S4+R12
      Y(MA(MB(10))+I0)=S4-R12
21  CONTINUE
C*****C
      KI(1)=MA(16)+IC2
      KI(2)=MA(1)+IC2
      KI(3)=MA(2)+IC2
      KI(4)=MA(3)+IC2
      KI(5)=MA(4)+IC2
      KI(6)=MA(5)+IC2
      KI(7)=MA(6)+IC2
      KI(8)=MA(7)+IC2
      KI(9)=MA(8)+IC2
      KI(10)=MA(9)+IC2
      KI(11)=MA(10)+IC2
      KI(12)=MA(11)+IC2
      KI(13)=MA(12)+IC2
      KI(14)=MA(13)+IC2
      KI(15)=MA(14)+IC2
      KI(16)=MA(15)+IC2
20  CONTINUE
998 CONTINUE
3   CONTINUE
2   CONTINUE
      IF(SIGN .EQ. 1) THEN
          DO 22 I=1,L*L
              Y(I)=-Y(I)
22  CONTINUE
      ELSE
          END IF
      RETURN
      END

```

```

SUBROUTINE TABLE(L,M,N)
C*****C
C THIS SUBROUTINE RETURNS THE PRIME FACTORS OF L C
C*****C
INTEGER N(*)
INTEGER NF(59,4)
DATA (NF( 1,J),J=1,4) /2,0,0,0/
DATA (NF( 2,J),J=1,4) /3,0,0,0/
DATA (NF( 3,J),J=1,4) /4,0,0,0/
DATA (NF( 4,J),J=1,4) /5,0,0,0/
DATA (NF( 5,J),J=1,4) /2,3,0,0/
DATA (NF( 6,J),J=1,4) /7,0,0,0/
DATA (NF( 7,J),J=1,4) /8,0,0,0/
DATA (NF( 8,J),J=1,4) /9,0,0,0/
DATA (NF( 9,J),J=1,4) /2,5,0,0/
DATA (NF(10,J),J=1,4) /3,4,0,0/
DATA (NF(11,J),J=1,4) /2,7,0,0/
DATA (NF(12,J),J=1,4) /3,5,0,0/
DATA (NF(13,J),J=1,4) /16,0,0,0/
DATA (NF(14,J),J=1,4) /2,9,0,0/
DATA (NF(15,J),J=1,4) /4,5,0,0/
DATA (NF(16,J),J=1,4) /3,7,0,0/
DATA (NF(17,J),J=1,4) /3,8,0,0/
DATA (NF(18,J),J=1,4) /4,7,0,0/
DATA (NF(19,J),J=1,4) /2,3,5,0/
DATA (NF(20,J),J=1,4) /5,7,0,0/
DATA (NF(21,J),J=1,4) /4,9,0,0/
DATA (NF(22,J),J=1,4) /5,8,0,0/
DATA (NF(23,J),J=1,4) /2,3,7,0/
DATA (NF(24,J),J=1,4) /5,9,0,0/
DATA (NF(25,J),J=1,4) /3,16,0,0/
DATA (NF(26,J),J=1,4) /7,8,0,0/
DATA (NF(27,J),J=1,4) /3,4,5,0/
DATA (NF(28,J),J=1,4) /7,9,0,0/
DATA (NF(29,J),J=1,4) /2,5,7,0/
DATA (NF(30,J),J=1,4) /8,9,0,0/
DATA (NF(31,J),J=1,4) /5,16,0,0/
DATA (NF(32,J),J=1,4) /3,4,7,0/
DATA (NF(33,J),J=1,4) /2,5,9,0/
DATA (NF(34,J),J=1,4) /3,5,7,0/
DATA (NF(35,J),J=1,4) /7,16,0,0/
DATA (NF(36,J),J=1,4) /3,5,8,0/
DATA (NF(37,J),J=1,4) /2,7,9,0/
DATA (NF(38,J),J=1,4) /4,5,7,0/
DATA (NF(39,J),J=1,4) /9,16,0,0/
DATA (NF(40,J),J=1,4) /3,7,8,0/
DATA (NF(41,J),J=1,4) /4,5,9,0/
DATA (NF(42,J),J=1,4) /2,3,5,7/
DATA (NF(43,J),J=1,4) /3,5,16,0/
DATA (NF(44,J),J=1,4) /4,7,9,0/
DATA (NF(45,J),J=1,4) /5,7,8,0/
DATA (NF(46,J),J=1,4) /5,7,9,0/
DATA (NF(47,J),J=1,4) /3,7,16,0/
DATA (NF(48,J),J=1,4) /5,8,9,0/
DATA (NF(49,J),J=1,4) /3,4,5,7/
DATA (NF(50,J),J=1,4) /8,7,9,0/
DATA (NF(51,J),J=1,4) /5,7,16,0/
DATA (NF(52,J),J=1,4) /2,5,7,9/
DATA (NF(53,J),J=1,4) /5,9,16,0/
DATA (NF(54,J),J=1,4) /3,5,7,8/

```

```

DATA (NF(55,J),J=1,4) /7,9,16,0/
DATA (NF(56,J),J=1,4) /4,5,7,9/
DATA (NF(57,J),J=1,4) /3,5,7,16/
DATA (NF(58,J),J=1,4) /5,7,8,9/
DATA (NF(59,J),J=1,4) /5,7,9,16/
IF(L .EQ. 2) THEN
  M=1
  K=1
ELSE IF(L .EQ. 3) THEN
  M=1
  K=2
ELSE IF(L .EQ. 4) THEN
  M=1
  K=3
ELSE IF(L .EQ. 5) THEN
  M=1
  K=4
ELSE IF(L .EQ. 6) THEN
  M=2
  K=5
ELSE IF(L .EQ. 7) THEN
  M=2
  K=6
ELSE IF(L .EQ. 8) THEN
  M=1
  K=7
ELSE IF(L .EQ. 9) THEN
  M=1
  K=8
ELSE IF(L .EQ. 10) THEN
  M=2
  K=9
ELSE IF(L .EQ. 12) THEN
  M=2
  K=10
ELSE IF(L .EQ. 14) THEN
  M=2
  K=11
ELSE IF(L .EQ. 15) THEN
  M=2
  K=12
ELSE IF(L .EQ. 16) THEN
  M=1
  K=13
ELSE IF(L .EQ. 18) THEN
  M=2
  K=14
ELSE IF(L .EQ. 20) THEN
  M=2
  K=15
ELSE IF(L .EQ. 21) THEN
  M=2
  K=16
ELSE IF(L .EQ. 24) THEN
  M=2
  K=17
ELSE IF(L .EQ. 28) THEN
  M=2
  K=18
ELSE IF(L .EQ. 30) THEN

```

```
M=3
K=19
ELSE IF(L .EQ. 35) THEN
M=2
K=20
ELSE IF(L .EQ. 36) THEN
M=2
K=21
ELSE IF(L .EQ. 40) THEN
M=2
K=22
ELSE IF(L .EQ. 42) THEN
M=3
K=23
ELSE IF(L .EQ. 45) THEN
M=2
K=24
ELSE IF(L .EQ. 48) THEN
M=2
K=25
ELSE IF(L .EQ. 56) THEN
M=2
K=26
ELSE IF(L .EQ. 60) THEN
M=3
K=27
ELSE IF(L .EQ. 63) THEN
M=2
K=28
ELSE IF(L .EQ. 70) THEN
M=3
K=29
ELSE IF(L .EQ. 72) THEN
M=2
K=30
ELSE IF(L .EQ. 80) THEN
M=2
K=31
ELSE IF(L .EQ. 84) THEN
M=3
K=32
ELSE IF(L .EQ. 90) THEN
M=3
K=33
ELSE IF(L .EQ. 105) THEN
M=3
K=34
ELSE IF(L .EQ. 112) THEN
M=2
K=35
ELSE IF(L .EQ. 120) THEN
M=3
K=36
ELSE IF(L .EQ. 126) THEN
M=3
K=37
ELSE IF(L .EQ. 140) THEN
M=3
K=38
ELSE IF(L .EQ. 144) THEN
```

```
M=2
K=39
ELSE IF(L .EQ. 168) THEN
M=3
K=40
ELSE IF(L .EQ. 180) THEN
M=3
K=41
ELSE IF(L .EQ. 210) THEN
M=4
K=42
ELSE IF(L .EQ. 240) THEN
M=3
K=43
ELSE IF(L .EQ. 252) THEN
M=3
K=44
ELSE IF(L .EQ. 280) THEN
M=3
K=45
ELSE IF(L .EQ. 315) THEN
M=3
K=46
ELSE IF(L .EQ. 336) THEN
M=3
K=47
ELSE IF(L .EQ. 360) THEN
M=3
K=48
ELSE IF(L .EQ. 420) THEN
M=4
K=49
ELSE IF(L .EQ. 504) THEN
M=3
K=50
ELSE IF(L .EQ. 560) THEN
M=3
K=51
ELSE IF(L .EQ. 630) THEN
M=4
K=52
ELSE IF(L .EQ. 720) THEN
M=3
K=53
ELSE IF(L .EQ. 840) THEN
M=4
K=54
ELSE IF(L .EQ. 1008) THEN
M=3
K=55
ELSE IF(L .EQ. 1260) THEN
M=4
K=56
ELSE IF(L .EQ. 1680) THEN
M=4
K=57
ELSE IF(L .EQ. 2520) THEN
M=4
K=58
ELSE IF(L .EQ. 5040) THEN
```

```
      N=4
      K=59
      ELSE
      END IF
      DO 1 J=1,4
        N(J)=NF(K,J)
1      CONTINUE
      RETURN
      END
```


UNIVERSITY OF MICHIGAN



3 9015 03024 4167